

Lattice models that realize \mathbb{Z}_n -1-symmetry protected topological states for even n

Lokman Tsui¹ and Xiao-Gang Wen¹

¹*Department of Physics, Massachusetts Institute of Technology, Cambridge, MA 02139, USA*

Higher symmetries can emerge at low energies in a topologically ordered state with no symmetry, when some topological excitations have very high energy scales while other topological excitations have low energies. The low energy properties of topological orders in this limit, with the emergent higher symmetries, may be described by higher symmetry protected topological order. This motivates us, as a simplest example, to study a lattice model of \mathbb{Z}_n -1-symmetry protected topological (1-SPT) states in 3+1D for even n . We write down an exactly solvable lattice model and study its boundary transformation. On the boundary, we show the existence of anyons with non-trivial self-statistics. For the $n = 2$ case, where the bulk classification is given by an integer $m \bmod 4$, we show that the boundary can be gapped with double semion topological order for $m = 1$ and toric code for $m = 2$. The bulk ground state wavefunction amplitude is given in terms of the linking numbers of loops in the dual lattice. Our construction can be generalized to arbitrary 1-SPT protected by finite unitary symmetry.

CONTENTS

I. Introduction	1	C. Boundary perspective	16
A. Statement of results	2	X. Conclusions	17
B. Notations and conventions	2	A. Space-time complex, cochains, and cocycles	17
C. Overview of paper	2	B. Procedure for deriving Hamiltonian from topological partition function	20
II. A brief review of topological order, SPT states, and higher SPT states	3	1. Zero background gauge field case	21
III. Intuitive argument for boundary transformation string statistics	5	2. Non-zero background gauge field case	22
IV. A 3+1D model to realize a \mathbb{Z}_n -1-SPT phase for even n	6	C. Ground state wavefunction	23
A. The bulk exactly solvable Lagrangian	7	1. Zero background gauge field case	23
V. Exactly solvable Hamiltonian	8	2. Non-zero background gauge field case	24
A. Even m case	8	D. Triangulation of hypercubic lattice	24
B. General m case	9	E. Evaluation of $\int_{I^4} (b^{\mathbb{Z}_n})^2$ in a hypercube	25
VI. Ground state wavefunctions and boundary transformations	9	F. Evaluation of P_{ij} in the m =even case	25
A. Boundary States and their 1-symmetry transformations	9	G. Evaluation of P_{ij} for general m	26
B. Boundary transformation strings	10	H. Calculation details for $\theta_q, \theta_{q_1 q_2}$	27
C. Self and mutual statistics of boundary transformation strings	10	I. Evaluation of $W_{\odot i}$ for $(n, m) = (2, 1)$	27
1. Self-statistics	10	1. DS projection Hamiltonian	28
2. Mutual-statistics	11	J. ω_4, ϕ_3 and ϕ_2	28
VII. Gapped symmetric boundaries	11	K. Generalization of (49) and (51) to G -protected 1-SPT for finite unitary groups	29
A. Engineering boundary gapped Hamiltonian	12	References	30
1. H_∂ is exactly solvable and has 1-symmetry	12		
2. Topological ordered surface states for $n = 2$	13		
3. Connection to Works of Wan and Wang	13		
VIII. Geometric interpretation of ground state wavefunction	13		
A. Even m case	14		
B. Odd m case	14		
IX. Non-zero background gauge field	15		
A. Exactly Solvable Hamiltonian	16		
B. Geometric interpretation of wavefunction	16		

I. INTRODUCTION

In the last few decades, there has been rapid progress in understanding “topological phases” of matter, which despite sharing the same symmetry, must undergo a phase transition to reach one phase from another. Some famous examples are the topological ordered states with no symmetry^{1,2} which have degenerate ground states on topological non-trivial closed manifolds, as well

as symmetry protected topological (SPT) states with symmetry³⁻⁶, which does not have topological order and have a unique gapped ground state in closed manifolds.

A 3+1D topological order can have point-like and string-like topological excitations⁷⁻⁹. For example, a 3+1D topological order described by \mathbb{Z}_n gauge theory has \mathbb{Z}_n charges (the point-like topological excitations) and \mathbb{Z}_n flux-lines (the string-like topological excitations). If the \mathbb{Z}_n charges have very large energy gap, then the theory for low energy \mathbb{Z}_n flux-lines will have an emergent higher symmetry – a \mathbb{Z}_n 1-symmetry¹⁰. In other words the low energy effective Hamiltonian is invariant under the symmetry transformations that act on all closed 2-dimension subspaces of the 3-dimensional space. Thus to understand the topological orders in such a limit, we can study Hamiltonians with a 1-symmetry. This motivates us to study 1-symmetry in this paper, such as the lattice Hamiltonian that realize 1-symmetry and the associated symmetry protected topological order, as well as their boundaries.

We will refer the transformations that act closed 2-dimension subspaces as the transformation membrane. If the 3d space have a boundary, the transformation membrane may intersect with the boundary. Such an intersection will be called transformation string.

A. Statement of results

In this paper, we will study lattice systems with higher symmetries¹¹⁻²⁴. Like the usual symmetry (0-symmetry) that can have SPT order³⁻⁶, higher symmetry can also have higher SPT order^{10,19,21}. In this paper, we will concentrate on 3+1D systems with \mathbb{Z}_n 1-symmetry and the associated associated 3+1D \mathbb{Z}_n 1-SPT states. Those systems can appear as low energy effective theories for 3+1D \mathbb{Z}_n topological order where the \mathbb{Z}_n charges have a large energy gap.

The 3+1D \mathbb{Z}_n 1-SPT states are known to have a \mathbb{Z}_{2n} classification^{25,26}, labeled by $m \in \mathbb{Z}_{2n}$. We study them in the Hamiltonian formalism and write down an exactly solvable bulk Hamiltonian, which has a compact expression when m is even.

The boundary of our system can also have the \mathbb{Z}_n 1-symmetry, but such a \mathbb{Z}_n 1-symmetry is anomalous^{19,21,27}. We find that on the boundary, the transformation strings can carry non-trivial self-statistics, as a reflection of the anomaly. This predicts the gapped boundary of the 1-SPT to have emergent anyons. We also find that it is possible for its surface state to be a gapped topological ordered state. The topological ordered boundary state has degenerate ground states if the surface manifold has non-zero genus. These degenerate states exhibit the spontaneous breaking of 1-symmetry. We also give a geometric interpretation of the ground state wave function, by writing the wave function amplitude in terms of the linking numbers of loops in the dual lattice.

B. Notations and conventions

In some part of this paper, we will use the Lagrangian formalism to describe quantum lattice systems. This allows us to use extensively the notion of cochain, cocycle, and coboundary, as well as their higher cup product \smile_k and Steenrod square Sq^k , to construct exactly solvable Lagrangian that realize topological orders and (higher) SPT orders. The reason to use modern mathematical formalisms is that they allow us to see the features of topological order and (higher) SPT order easily and quickly.

But the modern mathematical formalisms are not widely used in condensed matter theory. So we provide a brief introduction in Appendix A. Also, the Lagrangian formalism does not give us a lattice Hamiltonian explicitly. So in this paper, we present a systematic and direct way to obtain a lattice Hamiltonian from the those exactly solvable Lagrangian.

We will abbreviate the cup product of cochains $a \smile b$ as ab by dropping \smile . We will use $\stackrel{n}{=}$ to mean equal up to a multiple of n , and use $\stackrel{d}{=}$ to mean equal up to df (*i.e.* up to a coboundary). We will use $\langle l, m \rangle$ to denote the greatest common divisor of l and m ($\langle 0, m \rangle \equiv m$). We will also use $[x]$ to denote the integer that is closest to x . (If two integers have the same distance to x , we will choose the smaller one, *eg.* $[\frac{1}{2}] = 0$.)

In this paper, we will deal with \mathbb{Z}_n -value quantities. We will denote them as:

$$a^{\mathbb{Z}_n} := a - n \lfloor \frac{a}{n} \rfloor,$$

so the value of $a^{\mathbb{Z}_n}$ has a range from $-\lfloor \frac{n-1}{2} \rfloor$ to $\lfloor \frac{n}{2} \rfloor$. We will sometimes lift a \mathbb{Z}_n -value to \mathbb{Z} -value, and when we do so we omit the superscript, *eg.* $a^{\mathbb{Z}_n} \rightarrow a^{\mathbb{Z}} = a$, so we can make sense of expressions like $a^{\mathbb{Z}_n} + a'^{\mathbb{Z}}$, which means $a^{\mathbb{Z}} + a'^{\mathbb{Z}}$. Since $(a + nu^{\mathbb{Z}})^{\mathbb{Z}_n} = a^{\mathbb{Z}_n}$, whenever we lift a \mathbb{Z}_n -value to \mathbb{Z} -value we need to take care whether the final result is independent of choice of lifting, *i.e.* choice of $u^{\mathbb{Z}}$.

We will also use D to denote spacetime dimensions and d to denote space dimensions.

C. Overview of paper

The structure of the paper and a road map for reading is presented as follows.

In section II, we review some background information connecting the cohomology models we studied to the standard many-body theory. We explained what are those cohomology models, and some simple examples of those model that realize simple topological orders and (higher) SPT orders.

In section III we present an intuitive, informal argument for one of our major results, the self and mutual statistics of boundary transformation strings, without using the mathematical machinery of cochains and cocycles. The formal argument begins from section IV, where

we cite from the literature that the \mathbb{Z}_{n-1} SPT has \mathbb{Z}_{2n} classification from cohomology, such that each phase is labeled by $m \in \mathbb{Z}_{2n}$. We write down the exactly solvable Lagrangian, the expression for ω_4 in (11). We also show that it changes by a boundary term under gauge transformation via (16)^d(20),

$$\omega_4[\hat{B}^{\mathbb{Z}_n} + da^{\mathbb{Z}_n}] = \omega_4[\hat{B}^{\mathbb{Z}_n}] + d\phi_3[\hat{B}^{\mathbb{Z}_n}, a^{\mathbb{Z}_n}]$$

for some function ϕ_3 . This implies $\omega_4[\hat{B}^{\mathbb{Z}_n} + da^{\mathbb{Z}_n}]$ and $\omega_4[\hat{B}^{\mathbb{Z}_n}]$ gives the same answer when summed over a closed manifold, which is expected from gauge invariance (1).

In section V we specialize to the case $\hat{B}^{\mathbb{Z}_n} = 0$ and give the explicit form of $\phi_3[a^{\mathbb{Z}_n}]$ in (28). In Appendix B and C, we argue that on a closed spatial manifold \mathcal{M}^3 , $e^{2\pi i \int_{\mathcal{M}^3} \phi_3[a^{\mathbb{Z}_n}]}$ is the amplitude of the ground state wavefunction. We achieve this by examining the time-evolution operator $e^{-T\hat{H}_\infty}$ whose matrix elements are given in (B3). We show that it is a projection operator (hence an infinite gap) and has trace 1 (hence a unique ground state). We further argue this transfer matrix can be decomposed into local commuting projection operators P_{ij} (B6). We then build our exactly solvable Hamiltonian with a finite gap by summing over the $-P_{ij}$'s. We then verify that the ground state wavefunction is indeed given in terms of $\phi_3[a^{\mathbb{Z}_n}]$.

To write down the exactly solvable Hamiltonian, we consider a particular triangulation of \mathcal{M}^3 , given in Appendix D. We compute the explicit form for P_{ij} for the even m case in Appendix F and the odd m case in Appendix G. Unfortunately, we are unable to further simplify the expression in the odd m case. The results are summarized and presented in section V.

In section VI we consider the case when \mathcal{M}^3 has a boundary. We introduced the notion of a ‘‘boundary state’’ (36), which is obtained by fixing the degrees of freedom on the boundary and relaxing the bulk degrees of freedom to their ground state. As a result, the originally non-anomalous 1-symmetry transformation from the bulk now transform the boundary states with an additional phase $e^{2\pi i \int_{\partial\mathcal{M}^3} \phi_2[a^{\mathbb{Z}_n}, h^{\mathbb{Z}_n}]}$. This phase captures the ’t Hooft anomaly of 1-symmetry in the boundary. Any boundary Hamiltonian must be symmetric under this anomalous 1-symmetry in order to cancel the ’t Hooft anomaly. We show that $\phi_2[a^{\mathbb{Z}_n}]$ is related to the ground state wavefunction $\phi_3[a^{\mathbb{Z}_n}]$ by (40):

$$\phi_3[(a + dh)^{\mathbb{Z}_n}] - \phi_3[a^{\mathbb{Z}_n}] = -d\phi_2[a^{\mathbb{Z}_n}, h^{\mathbb{Z}_n}]$$

which states that under the 1-symmetry, the ground state wavefunction changes by a boundary term. We write down the explicit form of $\phi_2[a^{\mathbb{Z}_n}, h^{\mathbb{Z}_n}]$ in (41). Using this explicit form, we are able to compute the self(49) and mutual(51) statistics of the transformation strings. Details of the computation are given in H. The boundary transformation strings may be interpreted as hopping operators for anyons residing on the end of the strings. This

predicts the emergence of such anyon on the boundary theory and is the main result of the paper.

In section VII we test our prediction by writing down some gapped boundary Hamiltonians which obeys the anomalous 1-symmetry. We specialize to $n = 2$ and check the cases $m = 2$ and $m = 1$. We show that the gapped boundary is identical to the toric code model (for $m = 2$) and the double semion model (for $m = 1$). We verify in both cases that the boundary indeed contains an anyon with the predicted statistics. Details of the computation for the boundary Hamiltonian are given in I.

In section VIII we return to examine the ground state wavefunction. We present the geometric interpretation of the bulk wave function amplitude as a knot invariant (linking number) of loops dual to $da^{\mathbb{Z}_n}$.

In section IX we extend our study to the case with a non-zero background gauge field. In the even m case, we find a line charge with charge $-m$ is attached to the dual line of the background gauge field. Details are presented in Appendix B 2 and C 2.

In Appendix J we go deeper into the origin of the connections between ω_4 , ϕ_3 , ϕ_2 , and show that they are members of a series of algebraic objects ϕ_k which encodes the same cocycle ω_4 at sub-manifolds of dimension k .

In Appendix K we present the result of generalizing the computation of boundary string statistics to other unitary groups.

II. A BRIEF REVIEW OF TOPOLOGICAL ORDER, SPT STATES, AND HIGHER SPT STATES

A large class of topological orders can be realized by exactly solvable Lagrangian model. To write down the Lagrangian model, we first triangulate the spacetime to obtain a spacetime lattice \mathcal{M}^D , whose vertices are labeled by i, j, \dots . The physical degrees of freedom \mathcal{B}_{ij} live on the link ij , and takes value in a group G , *i.e.* $\mathcal{B}_{ij} \in G$. In this paper, we always assume G to be Abelian. The collection of those values \mathcal{B}_{ij} give us a field \mathcal{B} on spacetime, which, in this case, is also called a gauge configuration. A quantum system in Lagrangian formulation is described by a path integral with an action amplitude. For our model, the action amplitude assigns a $U(1)$ phase $e^{2\pi i S^{\text{top}}[\mathcal{M}^D, \mathcal{B}]}$ to a gauge configuration \mathcal{B} on a D -dimensional spacetime lattice \mathcal{M}^D . The gauge field \mathcal{B} satisfies the ‘‘flatness condition’’ $d\mathcal{B} = 0$ which is enforced by an energy penalty term $U|d\mathcal{B}|^2$ in $U \rightarrow \infty$ limit. The model is exactly solvable if the $U(1)$ phase is a topological invariant, meaning it remains unchanged under ‘‘deformations’’ of the lattice \mathcal{M}^D (change of triangulation), and is also invariant under gauge transformations $\mathcal{B} \rightarrow \mathcal{B} + da$, *i.e.* (in this paper we will assume the underlying group G is an Abelian finite group.)

$$S^{\text{top}}[\mathcal{M}^D, \mathcal{B} + da] \stackrel{1}{=} S^{\text{top}}[\mathcal{M}^D, \mathcal{B}], \quad a \in G \quad (1)$$

Here $\stackrel{\perp}{=}$ means equal up to 1. The partition function, after summing all the degrees of freedom (*i.e.* the G values in all the links), is given by

$$Z(\mathcal{M}^D) = \sum_{\{\mathcal{B}\}} e^{2\pi i S^{\text{top}}[\mathcal{M}^D, \mathcal{B}]}.$$

Up to a volume term,^{7,28} the partition function $Z(\mathcal{M}^D)$ is a topological invariant of manifold \mathcal{M}^D , that characterizes a topological order. When $S^{\text{top}}[\mathcal{M}^D, \mathcal{B}] = 0$, our model realizes a G topological order described by a G -gauge theory. When $S^{\text{top}}[\mathcal{M}^D, \mathcal{B}] \neq 0$, our exactly solvable model realizes a topological order described by a twisted G -gauge theory, which is also known as Dijkgraaf-Witten model²⁹.

The action amplitude $e^{2\pi i S^{\text{top}}[\mathcal{M}^D, \mathcal{B}]}$ of the exactly solvable model can also be viewed as an SPT invariant^{30–32} that characterizes an SPT order protected by symmetry G , if we view \mathcal{B} as the background gauge field \hat{B} that describes the symmetry twist on the space-time \mathcal{M}^D . Such a relation is also referred to as “ungauging” a topological order, which results in a SPT order. The SPT invariant $e^{2\pi i S^{\text{top}}[\mathcal{M}^D, \hat{B}]}$ characterizes a large class of SPT orders.

To realize the SPT states characterized by the above SPT invariant, we write $\mathcal{B} = \hat{B} + da$, fix a background gauge configuration \hat{B} , and treat the different gauge transformations a as distinct physical fields. The partition function, after summing all the degrees of freedom a , reproduces the SPT invariant, up to a space-time volume term:^{7,28}

$$Z[\mathcal{M}^D, \hat{B}] = \int \mathcal{D}a e^{2\pi i S^{\text{top}}[\mathcal{M}^D, \hat{B} + da]} \sim e^{2\pi i S^{\text{top}}[\mathcal{M}^D, \hat{B}]}$$

Note that the action is invariant under the symmetry $a \rightarrow a + \alpha$ for α satisfying $d\alpha = 0$. An SPT is trivial if $e^{2\pi i S^{\text{top}}[\mathcal{M}^D, \hat{B}]} = 1$ for all closed manifolds and background gauge fields \hat{B} . SPTs also form an Abelian group under stacking. The topological action S^{top} for the stacked SPT is the sum of the topological actions of its layers. The trivial SPT is the identity element under stacking and describes a direct product state.

“Group cohomology construction”⁵ is one way to write down $S^{\text{top}}[\mathcal{M}^D, \hat{B}]$. In this construction, we assume that $S^{\text{top}}[\mathcal{M}^D, \hat{B}]$ can be written as a sum over all the D -simplices Δ^D :

$$S^{\text{top}}[\mathcal{M}^D, \hat{B}] = \int_{\mathcal{M}^D} \omega_D[\hat{B}] = \sum_{\Delta^D} \omega_D[\hat{B}] \quad (2)$$

where $\omega_D[\hat{B}]$ assigns a number to each D -simplex. The requirement that $S^{\text{top}}[\mathcal{M}^D, \hat{B}]$ is invariant under triangulation leads to the following constraint on $\omega_D[\hat{B}]$, known as the “cocycle condition”:

$$d\omega_D[\hat{B}] \stackrel{\perp}{=} 0,$$

whose solutions are called cocycles. (The left hand side is evaluated on a $D+1$ -simplex and d is called the coboundary operator analogous to the exterior derivative for differential forms. See Appendix A for further details.) Distinct solutions of the cocycle condition do not necessarily correspond to distinct topological phases, since two solutions ω_D, ω'_D may give the same S^{top} on closed manifolds if $\omega_D = \omega'_D + d\beta_{D-1}$ for some function β_{D-1} . Defining an equivalence relation $\omega_D \sim \omega'_D + d\beta_{D-1}$ on cocycles and solving for the equivalence classes of cocycles, the resulting algebraic object is known as a cohomology group, which also provide a way to classify SPTs.

In the traditional SPT, the gauge field \hat{B} assigns a group element of G to every 1-dimensional simplex (*i.e.* links), and are thus called 1-cochain. (A G -valued m -cochain is an assignment of a group element of G to each m -simplex.) Gauge transformations are parameterized by a 0-cochain a which assigns a group element to every 0-dimensional simplex (*i.e.* vertices). Symmetry is parameterized by 0-cochain α . The condition $d\alpha = 0$ implies α is a constant function on every connected component. Physically this corresponds to a global symmetry acting on a connected component of the spatial slice. An example is the \mathbb{Z}_2 -protected SPT in $D = 2 + 1$.⁴ The \mathbb{Z}_2 symmetric ground state wavefunction can be constructed as the superposition of domain walls in the \mathbb{Z}_2 symmetry breaking state, with $(-1)^{\text{no. of domain walls}}$ as its amplitude³³.

With the above description of usual SPT states, we can now describe higher SPTs. Higher SPT states, or “ k -symmetry protected topological states” (k -SPT)^{10,19,21}, is a generalization of traditional SPTs. They have symmetry acting on closed sub-lattices of codimension k .^{11–24} The 1-cochain (*i.e.* the vector field) \mathcal{B} is promoted to $(k+1)$ -cochain. The gauge transformation is now described by a k -cochain a :

$$\mathcal{B} \rightarrow \mathcal{B} + da. \quad (3)$$

The path integral on spacetime lattice \mathcal{M}^D that realize a higher SPT state is given by

$$Z[\mathcal{M}^D, \hat{B}] = \sum_{\{a\}} e^{2\pi i \int_{\mathcal{M}^D} \omega_D(\hat{B} + da)} \quad (4)$$

where the dynamical field a is now a k -cochain (a field which takes values on the k simplices), and $S^{\text{top}}[\mathcal{M}^D, \mathcal{B}]$ is given by eqn. (2). In such a lattice model, the higher symmetry is generated by a k -cocycle α :

$$a \rightarrow a + \alpha. \quad (5)$$

We see that the symmetry acts on k -simplices where $\alpha \neq 0$. Such k -simplices are dual to a $(D-k)$ -dimensional manifold $\tilde{\alpha}$ on the dual lattice. The condition $d\alpha = 0$ implies $\tilde{\alpha}$ has no boundary within the space-time manifold. $\tilde{\alpha}$ may have a non-empty boundary if it intersects the boundary of the space-time manifold $\partial\mathcal{M}^D$.

When $\omega_D = 0$, eqn. (4) describes a state with trivial k -SPT order. When ω_D is a non-trivial cocycle, eqn. (4)

realizes a state with a non-trivial k -SPT order. The traditional SPT corresponds to $k = 0$ case.

The above Lagrangian is a realization of higher SPT states. In this paper, we show how to convert the above Lagrangian realization into a Hamiltonian realization. In the Hamiltonian formalism, a k -symmetry operator acts on codimension k sub-lattices in the spatial manifold. For example in a 3 space dimensions, a 1-symmetry operator acts on closed membranes. These membranes may intersect the boundary as strings. We show in Section VI that the 1-symmetry membrane operators in the bulk corresponds to 1-symmetry string operators on the boundary.

The hallmark of non-trivial SPT is that its boundary cannot be gapped with a unique ground state on all manifolds. If it were the case, we could start from a trivial SPT, nucleate a small bubble of the non-trivial SPT, and expand the bubble to fill up the entire space. This would have provided a path connecting the trivial and the non-trivial SPTs without closing the energy gap, leading to a contradiction. Generically the boundary of non-trivial SPT is gapless, breaks symmetry spontaneously, or has topological order. The inability for the boundary to achieve a uniquely gapped state on all manifolds is encoded by the 't Hooft anomaly of the k -symmetry on the boundary. Therefore studying such anomaly is a way to probe the non-trivial nature of the topological bulk.

III. INTUITIVE ARGUMENT FOR BOUNDARY TRANSFORMATION STRING STATISTICS

In this section we present an informal argument for the self and mutual statistics of the boundary strings.

The 't Hooft anomaly of the boundary transformation of SPTs may be interpreted via symmetry fractionalization^{34,35}: when the symmetry acts on the entire boundary manifold, and hence can be extended into the bulk, the group representation structure is preserved. But when we attempt to examine the symmetry acting only on a local patch of the boundary manifold, various group representation structures may be spoiled.

Take for example the non-trivial G -protected 1d 0-SPT³⁶, for which the AKLT³⁷ chain with $G = SO(3)$ is a well-known instance. The boundary of a 1d segment are its two endpoints, indexed by L and R respectively. When the bulk is gapped, the low energy effective theory are described in terms of its boundary degrees of freedom, and the Hilbert space may be expressed as a tensor product $\mathcal{H}_L \otimes \mathcal{H}_R$ of the local Hilbert spaces \mathcal{H}_L and \mathcal{H}_R for the two ends. For two group elements g, h acting on the tensor product space, we have

$$\mathcal{R}_{L+R}(g)\mathcal{R}_{L+R}(h) = \mathcal{R}_{L+R}(gh)$$

which says $\mathcal{R}_{L+R}(g) = \mathcal{R}_L(g) \otimes \mathcal{R}_R(g)$ is a linear representation of G . This is because when the same $g \in G$ acts on both boundaries, it may be extended into a symmetry acting globally in the bulk, where the group is

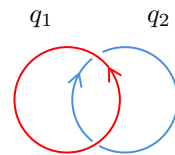
represented linearly. When localizing on the left end, \mathcal{R}_L becomes a projective representations of G :

$$\mathcal{R}_L(g)\mathcal{R}_L(h) = \omega(g, h)\mathcal{R}_L(gh).$$

The 't Hooft anomaly is expressed as the non-trivial phase $\omega(g, h)$, which spoils the linearity of the representation.

In the same spirit, for our case with \mathbb{Z}_n -1-SPT, we may expect 't Hooft anomaly to appear as the spoiling of some group representation structure when localizing to a part of the boundary. If the boundary symmetry can be extended into the bulk, the group representation structure is expected to be preserved.

Consider the case where we have two 1-symmetries, W_1 and W_2 , associated with group elements $q_1^{\mathbb{Z}_n}$ and $q_2^{\mathbb{Z}_n}$ respectively. They act on two contractible loops, as shown below:



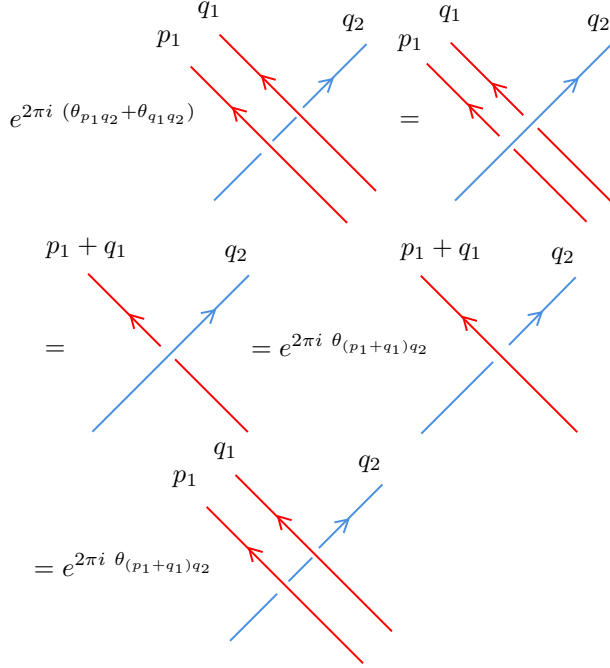
Each loop can be extended into the bulk as a 1-symmetry acting on a hemisphere. In the bulk, the 1-symmetries commute. We therefore expect that on the boundary, the two loop operators also commute. This is represented by the diagrammatic equation:

There are two intersections of the loops. Motivated by the symmetry fractionalization picture, we may guess that when localizing to one of the intersections, the commutativity is spoiled by a $U(1)$ phase $e^{2\pi i \theta_{q_1 q_2}}$:

(6)

If we further assume that two parallel lines associated with group elements $p_1^{\mathbb{Z}_n}$ and $q_1^{\mathbb{Z}_n}$ could stack into a single line $(p_1 + q_1)^{\mathbb{Z}_n}$ without incurring any phase, we can deduce that $\theta_{q_1 q_2}$ is a linear function of q_1 by the following

manipulations:



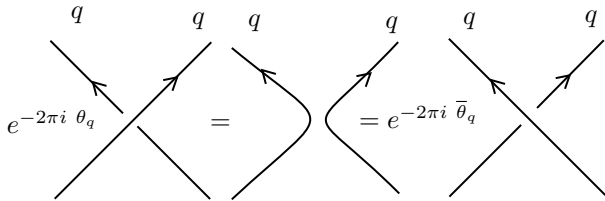
A similar argument shows $\theta_{q_1 q_2}$ is linear in q_2 . We conclude

$$\theta_{q_1 q_2} \propto q_1 q_2$$

Since $q_1^{\mathbb{Z}^n}$, $q_2^{\mathbb{Z}^n}$ are defined up to multiples of n , we expect $e^{2\pi i \theta_{q_1 q_2}}$ to be invariant under $q_1 \rightarrow q_1 + n$. Thus the coefficient should be a fraction $\frac{m}{n}$ for some integer m .

$$\theta_{q_1 q_2} = \frac{m}{n} q_1 q_2 \quad (7)$$

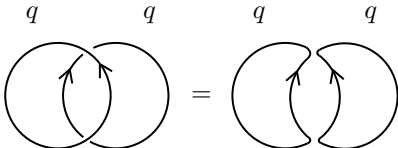
When $q_1 = q_2 = q$, we may also entertain the possibility that at an intersection, the transformation string may “change track” and incur a $U(1)$ phase $e^{2\pi i \theta_q}$ or $e^{2\pi i \bar{\theta}_q}$, depending on the orientation of the crossing:



Comparing to (6) with $q_1 = q_2 = q$, we observe that

$$\theta_q - \bar{\theta}_q \stackrel{\dagger}{=} \theta_{qq}. \quad (8)$$

On the other hand, we also have the equality of these two diagrams:



The reason is as follows, imagine when the left hand side extends into the bulk as two hemispheres which intersect on a line. On the intersection line, the 1-symmetry acts trivially and may be removed by reconnecting the membranes near the line. Thus we may reconnect the two intersecting hemispheres into two non-intersecting membranes which terminates on the surface as shown on the right hand side. This implies

$$\theta_q + \bar{\theta}_q \stackrel{\dagger}{=} 0.$$

Adding this equation to (8), we get $2\theta_q \stackrel{\dagger}{=} \theta_{qq}$. Thus

$$\theta_q \stackrel{1/2}{=} \frac{\theta_{qq}}{2} \stackrel{1/2}{=} \frac{m}{2n} q^2.$$

so

$$\theta_q \stackrel{\dagger}{=} \frac{m}{2n} q^2 + \frac{1}{2} f(q, m, n)$$

For some integer-valued function f . An argument similar to that for the linearity of $\theta_{q_1 q_2}$ implies θ_q is proportional to q^2 . So $f(q, m, n) \propto q^2$ and the coefficient of $\frac{q^2}{2n}$ in θ_q is an integer. Let's redefine m to be this integer coefficient. Thus we have

$$\theta_q = \frac{m}{2n} q^2$$

Upon $q \rightarrow q + n$, the above equation transform as

$$\begin{aligned} \theta_q &= \frac{m}{2n} q^2 \rightarrow \frac{m}{2n} (q^2 + 2qn + n^2) \\ &\stackrel{\dagger}{=} \theta_q + \frac{nm}{2} \end{aligned}$$

so in order for θ_q to be invariant mod 1, nm must be even. In the case n is even, m can be chosen from $0, 1, \dots, 2n-1$. With n odd, m must be an even number chosen from $0, 2, 4, \dots, 2n-2$. Each choice gives a distinct set of θ_q and $\theta_{q_1 q_2}$.

Assuming the set of θ_q and $\theta_{q_1 q_2}$ is bijective to the set of 't Hooft anomalies, which is bijective to the set of 1-SPT phases in the bulk, we would expect the bulk \mathbb{Z}_n -1-SPT to have \mathbb{Z}_{2n} classification for even n , and \mathbb{Z}_n classification for odd n . This agrees with the classification results in Ref.²⁵ derived from cohomology and Ref.²⁶ from cobordism group.

We stress that the odd n case and the even n case differs only in that the odd m 's are forbidden for odd n . In fact, all the results in our paper for even m also applies to odd n case.

In the rest of the paper, we will re-derive the expressions for $\theta_{q_1 q_2}$ and θ_q formally, using the language of group cohomology.

IV. A 3+1D MODEL TO REALIZE A \mathbb{Z}_n -1-SPT PHASE FOR EVEN n

To construct lattice models with higher symmetries, it is convenient to do so in the spacetime Lagrangian

formalism. We construct a spacetime lattice by first triangulating a D -dimensional spacetime manifold M^D . So a spacetime lattice is a D -complex \mathcal{M}^D with vertices labeled by i , links labeled by ij , triangles labeled by ijk , etc (see Fig. 1). The D -complex \mathcal{M}^D also has a dual complex denoted as $\tilde{\mathcal{M}}^D$. The vertices of \mathcal{M}^D correspond to the D -cells in $\tilde{\mathcal{M}}^D$, The links of \mathcal{M}^D correspond to the $(D-1)$ -cells in $\tilde{\mathcal{M}}^D$, etc

Our spacetime lattice model may have a field living on the vertices, g_i . Such a field is called a 0-cochain. The model may also have a field living on the links, a_{ij} . Such a field is called a 1-cochain, etc. To construct spacetime lattice models, in particular, the topological spacetime lattice models,^{19,21,38,39} we will use extensively the mathematical formalism of cochains, coboundaries, and cocycles (see Appendix A).

A. The bulk exactly solvable Lagrangian

We consider a 3+1D bosonic model on a spacetime complex \mathcal{M}^4 , with \mathbb{Z}_n -valued dynamic field $a_{ij}^{\mathbb{Z}_n}$ on the links ij of the complex \mathcal{M}^4 . Here n is even. We also have a \mathbb{Z}_n -valued non-dynamical background field $\hat{B}_{ijk}^{\mathbb{Z}_n}$ on the triangles ijk of the complex \mathcal{M}^4 . $\hat{B}^{\mathbb{Z}_n}$ is a \mathbb{Z}_n -valued 2-cocycle

$$d\hat{B}^{\mathbb{Z}_n} \stackrel{n}{=} 0. \quad (9)$$

The path integral of our bosonic model is given by

$$Z = \sum_{\{a^{\mathbb{Z}_n}\}} e^{2\pi i \int_{\mathcal{M}^4} \omega_4[\mathcal{B}]} \quad (10)$$

$$\omega_4[\mathcal{B}] := \frac{m}{2n} \mathbb{S}q^2 \mathcal{B}^{\mathbb{Z}_n}, \quad (11)$$

$$\mathcal{B} := \hat{B} + da \quad (12)$$

$$\mathcal{B}^{\mathbb{Z}_n} = \hat{B} + da - n \lfloor \frac{\hat{B} + da}{n} \rfloor$$

where $m, n = \text{integers}$, $\sum_{\{a^{\mathbb{Z}_n}\}}$ sums over \mathbb{Z}_n -valued 1-cochains $a^{\mathbb{Z}_n}$. We have lifted the \mathbb{Z}_n -valued quantities $\hat{B}^{\mathbb{Z}_n}$ and $a^{\mathbb{Z}_n}$ to \mathbb{Z} -valued quantities \hat{B} and a . Also $\mathbb{S}q^2$ is the generalized Steenrod square defined by eqn. (A21). We will show that the above model realizes a \mathbb{Z}_n -1-SPT phase.

Since $\omega_4[\mathcal{B}] = \omega_4[\mathcal{B}^{\mathbb{Z}_n}]$ and $\mathcal{B}^{\mathbb{Z}_n}$ is invariant under the transformation

$$\hat{B} \rightarrow \hat{B} + nb^{\mathbb{Z}}, \quad a \rightarrow a + nu^{\mathbb{Z}}, \quad (13)$$

where $b^{\mathbb{Z}}$ and $u^{\mathbb{Z}}$ are any \mathbb{Z} valued 2-cochain and 1-cochain, the action amplitude in eqn. (10) is invariant, even when \mathcal{M}^4 has a boundary. The above result also implies that the model has a \mathbb{Z}_n -1-symmetry generated by

$$a \rightarrow a + \alpha^{\mathbb{Z}_n}, \quad d\alpha^{\mathbb{Z}_n} \stackrel{n}{=} 0, \quad (14)$$

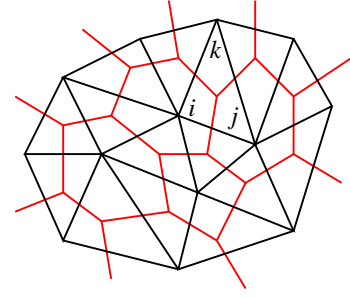


FIG. 1. (Color online) The black lines describe a 2-dimensional spacetime complex \mathcal{M}^2 . The red lines describe the dual complex $\tilde{\mathcal{M}}^2$.

even when \mathcal{M}^4 has a boundary.

Also it can be checked that $e^{2\pi i \omega_4}$ is a $U(1)$ -valued cocycle: Using (A21), (A18) and $d\mathcal{B}^{\mathbb{Z}_n} \stackrel{n}{=} 0$ which follows from (9), and remembering that n is even, we have

$$\begin{aligned} d\omega_4[\mathcal{B}^{\mathbb{Z}_n}] &= \frac{m}{2n} d\mathbb{S}q^2 \mathcal{B}^{\mathbb{Z}_n} \\ &= \frac{m}{2n} d \left(\mathcal{B}^{\mathbb{Z}_n} \mathcal{B}^{\mathbb{Z}_n} + \mathcal{B}^{\mathbb{Z}_n} \underset{1}{\smile} d\mathcal{B}^{\mathbb{Z}_n} \right) \\ &= \frac{m}{2n} \left(d\mathcal{B}^{\mathbb{Z}_n} \mathcal{B}^{\mathbb{Z}_n} + \mathcal{B}^{\mathbb{Z}_n} d\mathcal{B}^{\mathbb{Z}_n} \right. \\ &\quad \left. + d\mathcal{B}^{\mathbb{Z}_n} \underset{1}{\smile} d\mathcal{B}^{\mathbb{Z}_n} + \mathcal{B}^{\mathbb{Z}_n} d\mathcal{B}^{\mathbb{Z}_n} - d\mathcal{B}^{\mathbb{Z}_n} \mathcal{B}^{\mathbb{Z}_n} \right) \\ &= \frac{m}{2n} \left(2\mathcal{B}^{\mathbb{Z}_n} d\mathcal{B}^{\mathbb{Z}_n} + d\mathcal{B}^{\mathbb{Z}_n} \underset{1}{\smile} d\mathcal{B}^{\mathbb{Z}_n} \right) \stackrel{1}{=} 0. \end{aligned}$$

In eqn. (12), $\hat{B}^{\mathbb{Z}_n}$ is the \mathbb{Z}_n background 2-connection to describe the twist of the \mathbb{Z}_n -1-symmetry. The model has a \mathbb{Z}_n gauge symmetry:

$$a \rightarrow a + \hat{a}^{\mathbb{Z}_n}, \quad \hat{B} \rightarrow \hat{B} - d\hat{a}^{\mathbb{Z}_n}. \quad (15)$$

Also, using $d\mathcal{B} \stackrel{n}{=} 0$, (A21) and (A18),

$$\frac{m}{2n} \mathbb{S}q^2 \mathcal{B}^{\mathbb{Z}_n} \quad (16)$$

$$\begin{aligned} &= \frac{m}{2n} \mathbb{S}q^2 \left(\mathcal{B} - n \lfloor \frac{\mathcal{B}}{n} \rfloor \right) \\ &= \frac{m}{2n} \left[\left(\mathcal{B} - n \lfloor \frac{\mathcal{B}}{n} \rfloor \right) \left(\mathcal{B} - n \lfloor \frac{\mathcal{B}}{n} \rfloor \right) \right. \\ &\quad \left. + \left(\mathcal{B} - n \lfloor \frac{\mathcal{B}}{n} \rfloor \right) \underset{1}{\smile} d \left(\mathcal{B} - n \lfloor \frac{\mathcal{B}}{n} \rfloor \right) \right] \\ &\stackrel{1}{=} \frac{m}{2n} \mathbb{S}q^2 \mathcal{B} + \frac{m}{2} \left(\lfloor \frac{\mathcal{B}}{n} \rfloor \mathcal{B} + \mathcal{B} \lfloor \frac{\mathcal{B}}{n} \rfloor + \mathcal{B} \underset{1}{\smile} d \lfloor \frac{\mathcal{B}}{n} \rfloor \right) \\ &\stackrel{1}{=} \frac{m}{2n} \mathbb{S}q^2 \mathcal{B} + \frac{m}{2} d \left(\mathcal{B} \underset{1}{\smile} \lfloor \frac{\mathcal{B}}{n} \rfloor \right) \quad (17) \end{aligned}$$

$$\stackrel{1}{=} \frac{m}{2n} \mathbb{S}q^2 \mathcal{B} = \frac{m}{2n} \mathbb{S}q^2 (\hat{B} + da) \quad (18)$$

$$\begin{aligned} &= \frac{m}{2n} \left[(\hat{B} + da)(\hat{B} + da) + (\hat{B} + da) \underset{1}{\smile} d(\hat{B} + da) \right] \\ &\stackrel{1}{=} \frac{m}{2n} \left[\mathbb{S}q^2 \hat{B} + \hat{B} da + da \hat{B} + da da + da \underset{1}{\smile} d\hat{B} \right] \end{aligned}$$

$$\stackrel{\text{1}}{=} \frac{m}{2n} [\mathbb{S}q^2 \hat{B} + d(a da + da \underset{1}{\smile} \hat{B} + 2a \hat{B})] \quad (19)$$

$$\stackrel{\text{2}}{=} \frac{m}{2n} \mathbb{S}q^2 \hat{B} \stackrel{\text{3}}{=} \frac{m}{2n} \mathbb{S}q^2 \hat{B}^{Z_n}. \quad (20)$$

In the last step we reused (16) $\stackrel{\text{1,d}}{=} (18)$ with \mathcal{B} replaced by \hat{B} . Therefore

$$e^{2\pi i \int_{\mathcal{M}^4} \frac{m}{2n} \mathbb{S}q^2(\hat{B} + da)^{Z_n}} = e^{2\pi i \int_{\mathcal{M}^4} \frac{m}{2n} \mathbb{S}q^2 \hat{B}^{Z_n}} \quad (21)$$

for closed spacetime \mathcal{M}^4 . This is expected from gauge invariance (1). The model is exactly solvable and gapped for closed spacetime \mathcal{M}^4 .

Eqn. (10) has no topological order since on closed spacetime and for $\hat{B}^{Z_n} = 0$

$$Z(\mathcal{M}^4) = \sum_{\{a^{Z_n}\}} e^{2\pi i \int_{\mathcal{M}^4} \frac{m}{2n} \mathbb{S}q^2(da)^{Z_n}} = \sum_{\{a^{Z_n}\}} 1 = n^{N_l}, \quad (22)$$

where N_l is the number of links in the spacetime complex \mathcal{M}^4 . n^{N_l} is the so called the volume term that is linear in the spacetime volume. The topological partition function Z^{top} is given by removing the volume term:^{7,28}

$$Z^{\text{top}}(\mathcal{M}^4) = Z(\mathcal{M}^4)/n^{N_l}, \quad (23)$$

which is equal to 1 for all closed 4-complex \mathcal{M}^4 . Thus the above model has no topological order. After we turn on the flat \mathbb{Z}_n -2-connection \hat{B}^{Z_n} , the topological partition function of the model (10) becomes

$$Z^{\text{top}}(\mathcal{M}^4, \hat{B}) = e^{2\pi i \int_{\mathcal{M}^4} \frac{m}{2n} [\hat{B}^{Z_n} \hat{B}^{Z_n} + \hat{B}^{Z_n} \underset{1}{\smile} d\hat{B}^{Z_n}]}, \quad (24)$$

$$d\hat{B}^{Z_n} \stackrel{\text{2}}{=} 0.$$

In Ref. 25, it was shown that $H^4(\mathcal{B}(\mathbb{Z}_n, 2); \mathbb{R}/\mathbb{Z}) = \mathbb{Z}_{2n}$ for $n = \text{even}$. Furthermore, the classification of higher-SPTs based on a generalized cobordism theory approach also obtains a \mathbb{Z}_{2n} for $n = \text{even}$. See Table 7 of Ref. 26. Thus the above 1-SPT invariant is non-trivial. There are $2n$ distinct \mathbb{Z}_n -1-SPT phases labeled by $m = 0, \dots, 2n - 1$.

V. EXACTLY SOLVABLE HAMILTONIAN

In this section we derive the exactly solvable \mathbb{Z}_n -1-SPT Hamiltonian. For simplicity we focus on the untwisted theory and set the non-dynamical background 2-connection $\hat{B}^{Z_n} = 0$ so Z^{top} depends on a^{Z_n} only. In section IX we will examine the case with non-zero \hat{B}^{Z_n} .

The action (10) is:

$$Z^{\text{top}} = \frac{1}{n^{N_l}} \sum_{\{a^{Z_n}\}} e^{2\pi i \int_{\mathcal{M}^4} \omega_4[da^{Z_n}]}, \quad (25)$$

using (16) $\stackrel{\text{1}}{=} (17)$ and (18) $\stackrel{\text{1}}{=} (19)$ with $\hat{B} = 0$,

$$\omega_4[da^{Z_n}] = \frac{m}{2n} \mathbb{S}q^2(da)^{Z_n}$$

$$\stackrel{\text{1}}{=} \frac{m}{2n} \mathbb{S}q^2 da^{Z_n} + d\left(\frac{m}{2} da^{Z_n} \underset{1}{\smile} \left[\frac{da^{Z_n}}{n}\right]\right)$$

$$= \frac{m}{2n} \mathbb{S}q^2 da^{Z_n} + d\xi_3[a^{Z_n}]$$

$$= d\left(\frac{m}{2n} a^{Z_n} da^{Z_n} + \xi_3[a^{Z_n}]\right)$$

$$= d\phi_3[a], \quad (26)$$

(note that $da^{Z_n} = d(a^{Z_n}) \neq (da)^{Z_n}$) where

$$\xi_3[a] := \frac{m}{2} da \underset{1}{\smile} \left[\frac{da}{n}\right] \quad (27)$$

$$\phi_3[a] := \frac{m}{2n} a^{Z_n} da^{Z_n} + \xi_3[a^{Z_n}]$$

$$\stackrel{\text{1}}{=} \frac{m}{2n} a da + \xi_3[a] + d\xi_2[a] \quad (28)$$

$$\xi_2[a] := \frac{m}{2} \left(a \left[\frac{a}{n}\right] + da \underset{1}{\smile} \left[\frac{a}{n}\right]\right). \quad (29)$$

(28) and (29) are obtained from the previous line by writing out $a^{Z_n} \rightarrow a - n \left[\frac{a}{n}\right]$. By construction we have $\phi_3[a] = \phi_3[a + nu^Z] = \phi_3[a^{Z_n}]$ for any \mathbb{Z} -valued 1-cochain u^Z . However, ξ_3 and ξ_2 do not enjoy this property. (See Appendix J for relationship between ω_4 and ϕ_3 in general.)

We will analyze the cases for even and odd m separately. For each case we write down the Hamiltonian

$$H = - \sum_{ij} P_{ij},$$

which is the sum over links ij of projections P_{ij} , as described in Appendix B. We can compute P_{ij} by assuming a hypercubic lattice for the space-time $\mathcal{M}^4 = \mathbb{R}^4$ triangulated as in Appendix D. The Hilbert space is spanned by $|\{a_{ij}^{Z_n}\}\rangle$ for links ij in the 3D cubic lattice.

A. Even m case

When m is even, (26) and (28) are simplified considerably. The result is

$$\omega_4[da^{Z_n}] \stackrel{\text{1}}{=} \frac{m}{2n} \mathbb{S}q^2(da^{Z_n}) \quad (30)$$

$$\stackrel{\text{1}}{=} d\phi_3[a]$$

$$\phi_3[a] \stackrel{\text{1}}{=} \frac{m}{2n} a da. \quad (31)$$

We will also triangulate \mathbb{R}^3 as described in Appendix D. The variables in our lattice model lives on links. There are three types of links: 1-diagonal, 2-diagonal or 3-diagonal. A link ij is defined to be k -diagonal if the displacement vector from i to j differs by k distinct unit vectors $\in \{\hat{x}_1, \hat{x}_2, \hat{x}_3\}$. In the even m case, as shown in Appendix F, the 2-diagonal and 3-diagonal links form product states and can be ignored.

For the 1-diagonal links, the topological action

$$Z^{\text{top}} = \frac{1}{n^{N_l}} \sum_{\{a^{Z_n}\}} e^{2\pi i \int_{\mathcal{M}^4} \frac{m}{2n} \mathbb{S}q^2(da)^{Z_n}} \quad (32)$$

$$H = -\frac{1}{n} \sum_{ij} \sum_{k=0}^{n-1} \left(\begin{array}{c} \text{Diagram 1} \\ \text{or} \\ \text{Diagram 2} \\ \text{or} \\ \text{Diagram 3} \end{array} \right)^k$$

FIG. 2. (Color online) The lattice Hamiltonian for even m 1-symmetric SPT consists of commuting projections P_{ij} summed over all links in the cubic lattice. The projection consists of an operator \hat{X}_{ij} (depicted in green) which increments the link value $a^{Z_n} \rightarrow (a+1)^{Z_n}$, and the operators $e^{2\pi i \frac{m}{2n} F}$ that multiplies the state by a phase proportional to the fluxes $F = \sum_{\square} da^{Z_n}$ through the two squares (depicted in blue) touching ij .

leads to mutually commuting projections (F2)

$$P_{ij} = \frac{1}{n} \sum_{k=0}^{n-1} \hat{X}_{ij}^k e^{2\pi i \frac{mk}{2n} \frac{\epsilon^{\alpha\beta\gamma}}{2} [F_{\beta\gamma}(\vec{r}_{ij} + \frac{\vec{1}}{2}) + F_{\beta\gamma}(\vec{r}_{ij} - \frac{\vec{1}}{2})]}, \quad (33)$$

where the sum is carried over 1-diagonal links $ij = (\vec{n}, \vec{n} + \hat{\alpha})$, $\hat{X}_{ij}|a_{ij}^{Z_n}\rangle = |(a_{ij} + 1)^{Z_n}\rangle$, $\vec{r}_{ij} = \vec{n} + \frac{\hat{\alpha}}{2}$ is the mid-point of the link. $\frac{\vec{1}}{2} = (\frac{1}{2}, \frac{1}{2}, \frac{1}{2})$ and $F_{\beta\gamma}(\vec{r})$ reads off the ‘‘flux’’ through the square centered at \vec{r} , or more specifically

$$F_{\beta\gamma}(\vec{r}) := \langle da^{Z_n}, (\vec{0}, \hat{\beta}, \hat{\beta} + \hat{\gamma})_{\vec{r} - \frac{\hat{\beta}}{2} - \frac{\hat{\gamma}}{2}} \rangle - (\beta \leftrightarrow \gamma), \quad (34)$$

where $(\vec{a}, \vec{b}, \dots, \vec{c})_{\vec{n}}$ is a shorthand for $(\vec{a} + \vec{n}, \vec{b} + \vec{n}, \dots, \vec{c} + \vec{n})$. The Hamiltonian is illustrated in Fig. 2

B. General m case

In appendix G we show for general m the corresponding projections are given by (G1):

$$P_{ij} = \frac{1}{n} \sum_{k=0}^{n-1} \hat{X}_{ij}^k e^{2\pi i \int_{\mathbb{R}^3} \delta_k \phi_3[a^{Z_n}]}.$$

Here $\delta_k \phi_3[a^{Z_n}]$ is the change in $\phi_3[a^{Z_n}]$ when a single link ij changes as $a_{ij}^{Z_n} \rightarrow (a_{ij} + k)^{Z_n}$. Under our triangulation, it is evaluated for 1-, 2-, 3- diagonal links in Appendix G.

VI. GROUND STATE WAVEFUNCTIONS AND BOUNDARY TRANSFORMATIONS

By Appendix C, the ground state wavefunction in closed space 3-manifold \mathcal{M}^3 is given by

$$|\psi_0\rangle = \sum_{\{a^{Z_n}\}} e^{2\pi i \int_{\mathcal{M}^3} \phi_3[a^{Z_n}]} |\{a^{Z_n}\}\rangle. \quad (35)$$

For physical interpretation of these wavefunctions, see Section VIII.

A. Boundary States and their 1-symmetry transformations

Suppose we are interested in space 3-manifold which has a boundary. We may write down a ‘‘boundary state’’ by separating $\{a^{Z_n}\} = \{a_{bulk}^{Z_n}, a_{\partial}^{Z_n}\}$ into boundary and bulk links, fixing the values of $a_{\partial}^{Z_n}$ at the boundary in (35) and only sum over links $a_{bulk}^{Z_n}$ inside the bulk.

$$|\{a_{\partial}^{Z_n}\}\rangle_{\partial} := \sum_{\{a_{bulk}^{Z_n}\}} e^{2\pi i \int_{\mathcal{M}^3} \phi_3[a_{bulk}^{Z_n}, a_{\partial}^{Z_n}]} |\{a_{bulk}^{Z_n}, a_{\partial}^{Z_n}\}\rangle. \quad (36)$$

Consider a 1-symmetry transformation

$$|a^{Z_n}\rangle \rightarrow |a'^{Z_n}\rangle = |(a + \alpha)^{Z_n}\rangle, \quad (37)$$

where α^{Z_n} is a \mathbb{Z}_n -valued 1-cochain. We have

$$\begin{aligned} & |\{a_{\partial}^{Z_n}\}\rangle_{\partial} \\ & \rightarrow \sum_{\{a_{bulk}^{Z_n}\}} e^{2\pi i \int_{\mathcal{M}^3} \phi_3[a^{Z_n}]} |\{(a + \alpha)^{Z_n}\}\rangle \\ & = \sum_{\{a_{bulk}^{Z_n}\}} e^{2\pi i \int_{\mathcal{M}^3} \phi_3[a'^{Z_n}] - \delta_{\alpha} \phi_3[a^{Z_n}]} |\{a'^{Z_n}\}\rangle \end{aligned} \quad (38)$$

with

$$\delta_{\alpha} \Phi[a] := \Phi[a + \alpha] - \Phi[a].$$

for any function $\Phi[a]$.

For 1-symmetry, we have $da^{Z_n} \stackrel{n}{=} 0$, then

$$\begin{aligned} -\delta_{\alpha} \phi_3[a^{Z_n}] & \stackrel{\perp}{=} -\frac{m}{2n} \alpha^{Z_n} da^{Z_n} + \frac{m}{2} (a^{Z_n} \frac{da^{Z_n}}{n} + \alpha^{Z_n} \frac{d\alpha^{Z_n}}{n}) \\ & + \frac{m}{2} da^{Z_n} \underset{1}{\smile} \frac{da^{Z_n}}{n} + \delta_{\alpha} z_n d\xi_2[a^{Z_n}] \\ & \stackrel{\perp}{=} d\left[\frac{m}{2n} \alpha^{Z_n} a^{Z_n} + \frac{m}{2} (a^{Z_n} \underset{1}{\smile} \frac{da^{Z_n}}{n})\right] \\ & + \delta_{\alpha} z_n \xi_2[a^{Z_n}] + \frac{m}{2} \alpha^{Z_n} \frac{d\alpha^{Z_n}}{n}. \end{aligned} \quad (39)$$

Assuming $\alpha = dh^{Z_n}$ for a \mathbb{Z}_n valued 0-cochain h^{Z_n} , then the last term can be made into a total derivative:

$$\begin{aligned} \frac{m}{2} \alpha^{Z_n} \frac{d\alpha^{Z_n}}{n} & \stackrel{\perp}{=} \frac{m}{2} \left(\alpha \frac{d\alpha}{n} + \alpha d\left[\frac{\alpha}{n}\right] \right) \\ & = \frac{m}{2} dh^{Z_n} d\left[\frac{dh^{Z_n}}{n}\right] \\ & = d\left(\frac{m}{2} h^{Z_n} d\left[\frac{dh^{Z_n}}{n}\right]\right) \\ & \stackrel{\perp}{=} d\left(\frac{m}{2} h d\left[\frac{dh}{n}\right]\right). \end{aligned}$$

So

$$-\delta_{\alpha} \phi_3[a^{Z_n}] = d\phi_2[a, h] \quad (40)$$

$$\begin{aligned}
\phi_2[a, h] &:= \frac{m}{2n} \alpha^{Z_n} a^{Z_n} + \frac{m}{2} (a^{Z_n} \frown_1 \frac{d\alpha^{Z_n}}{n}) \\
&\quad + \delta_{\alpha^{Z_n}} \xi_2[a^{Z_n}] + \frac{m}{2} (h^{Z_n} d[\frac{dh^{Z_n}}{n}]) \quad (41) \\
&\stackrel{\doteq}{=} \frac{m}{2n} \alpha a + \frac{m}{2} (a \frown_1 \frac{d\alpha}{n}) + \delta_{\alpha} \xi_2[a] \\
&\quad + d(\frac{m}{2} [\frac{\alpha}{n}] \frown_1 a) + \frac{m}{2} \alpha [\frac{\alpha}{n}] + \frac{m}{2} (h d[\frac{dh}{n}]) \\
&\stackrel{\doteq}{=} \frac{m}{2n} dha + \delta_{dh} \xi_2[a] + d\xi_1[a, h] \quad (42) \\
\xi_1[a, h] &:= \frac{m}{2} ([\frac{dh}{n}] \frown_1 a + h [\frac{dh}{n}]).
\end{aligned}$$

By construction (41) we have

$$\phi_2[a, h] = \phi_2[a^{Z_n}, h^{Z_n}]. \quad (43)$$

(See Appendix J for relationship between ω_4 , ϕ_3 and ϕ_2 in general.)

We also see that $\int_{\mathcal{M}^3} \delta_{\alpha} \phi_3[\{a^{Z_n}\}]$ is independent of $a_{bulk}^{Z_n}$ or $a'_{bulk}{}^{Z_n}$, so we may take it out of the sum in the last line of (38) and write:

$$\begin{aligned}
&|\{a_{\partial}^{Z_n}\}_{\partial} \\
&\rightarrow e^{-2\pi i \int_{\mathcal{M}^3} \delta_{\alpha} \phi_3[\{a_{\partial}^{Z_n}\}]} |\{a'_{\partial}{}^{Z_n}\}_{\partial} \\
&= e^{2\pi i \int_{\partial\mathcal{M}^3} \phi_2[a_{\partial}^{Z_n}, h^{Z_n}]} |\{a'_{\partial}{}^{Z_n}\}_{\partial}. \quad (44)
\end{aligned}$$

In the even m case, (41) simplifies to

$$\phi_2[a, h] \stackrel{\doteq}{=} \frac{m}{2n} \alpha^{Z_n} a^{Z_n},$$

so the non-onsite phase for the anomalous 1-symmetry is

$$\begin{aligned}
\int_{\partial\mathcal{M}^3} \phi_2[a^{Z_n}, h^{Z_n}] &\stackrel{\doteq}{=} \frac{m}{2n} \int_{\partial\mathcal{M}^3} \alpha^{Z_n} a^{Z_n} \\
&= \frac{m}{2n} \int_{\partial\mathcal{M}^3 \cap \alpha^{Z_n}} a^{Z_n}. \quad (45)
\end{aligned}$$

Here \cap is the cap product⁴⁰, which takes as input a q -cochain ϕ_q and n -chain ($0 \rightarrow n$), and outputs a $(n - q)$ -chain given by:

$$(0 \rightarrow n) \cap \phi_q := \langle \phi_q, (0 \rightarrow q) \rangle (q \rightarrow n). \quad (46)$$

In the more general case, by (41) and (29), the non-onsite phase is:

$$\begin{aligned}
&\int_{\partial\mathcal{M}^3} \phi_2[a^{Z_n}, h^{Z_n}] \\
&\stackrel{\doteq}{=} \int_{\partial\mathcal{M}^3} \frac{m}{2n} \alpha^{Z_n} a^{Z_n} \\
&\quad + \frac{m}{2} (a^{Z_n} \frown_1 \frac{d\alpha^{Z_n}}{n} + (a^{Z_n} + \alpha^{Z_n}) [\frac{a^{Z_n} + \alpha^{Z_n}}{n}]) \\
&\quad + da^{Z_n} \frown_1 [\frac{a^{Z_n} + \alpha^{Z_n}}{n}] + h^{Z_n} d[\frac{dh^{Z_n}}{n}], \quad (47)
\end{aligned}$$

where $\alpha^{Z_n} = (dh^{Z_n})^{Z_n}$

B. Boundary transformation strings

On the boundary $\partial\mathcal{M}^3$, the 1-cocycle α^{Z_n} is Poincaré dual to closed loops $\partial\mathcal{M}^3 \cap \alpha^{Z_n}$. These loops are the boundary of a 2-manifold $-\mathcal{M}^3 \cap \alpha^{Z_n}$ in the bulk. While the 1-symmetry is on-site in the bulk, it is non-onsite on the boundary, accompanied by the phase $\int_{\partial\mathcal{M}^3} \phi_2$. Since the bulk is a non-trivial SPT with 1-symmetry, we expect that its boundary cannot be uniquely gapped without breaking the 1-symmetry.

The 1-symmetry acts on the boundary as string operators. These string operators can be thought of as hopping operators for some emergent flux anyons. We measure the statistics of these anyons in the following subsection.

C. Self and mutual statistics of boundary transformation strings

We triangulate the 2-dimensional boundary $\partial\mathcal{M}^3$ as shown in Fig. 3. We only focus on a yellow central square, whose links are labeled as $a_i^{Z_n}$, $i = 0, 1, 2, 3, 4$. We define string operators: W_i^q , $i = 1, 2, 3, 4$, to be the hopping operator depicted in the bottom of Fig. 3.

Each string operator W_i^q is represented by an oriented red line in the figure. The red line intersects links in the lattice (colored in gray). Every lattice link intersecting the red string is being updated as in (37) with $\alpha = dh^{Z_n}$. $h^{Z_n} = q$ in the pink shaded region and $h^{Z_n} = 0$ in the other unshaded regions. The operator W_i^q acts on the boundary Hilbert space as described in (44), with ϕ_2 given by (45) or (47).

1. Self-statistics

To compute the self statistics for anyon with flux q , we compare the result of hopping an anyon from bottom to top, then another anyon from left to right, versus the result of hopping an anyon from bottom to right, and another anyon from left to top.¹³ As shown in Fig. 4a, the resulting positions of the two final anyons are exchanged in the two processes. More explicitly the self-statistic is given by θ_q , where

$$W_1^q \circ W_2^q = e^{2\pi i \theta_q} W_4^q \circ W_3^q. \quad (48)$$

Using (47) to compute the actions of W_i^q , the result is (derivation details in Appendix H)

$$\theta_q = q^2 \frac{m}{2n}, \quad (49)$$

which is consistent with Ref. 38: The 3+1D bulk state that we have constructed is a \mathbb{Z}_n -1-SPT state labeled by $m \in \{0, 1, \dots, 2n-1\}$, protected by an on-site (anomaly-free) \mathbb{Z}_n -1-symmetry. Its boundary has an anomalous (non-on-site) \mathbb{Z}_n -1-symmetry generated by closed string

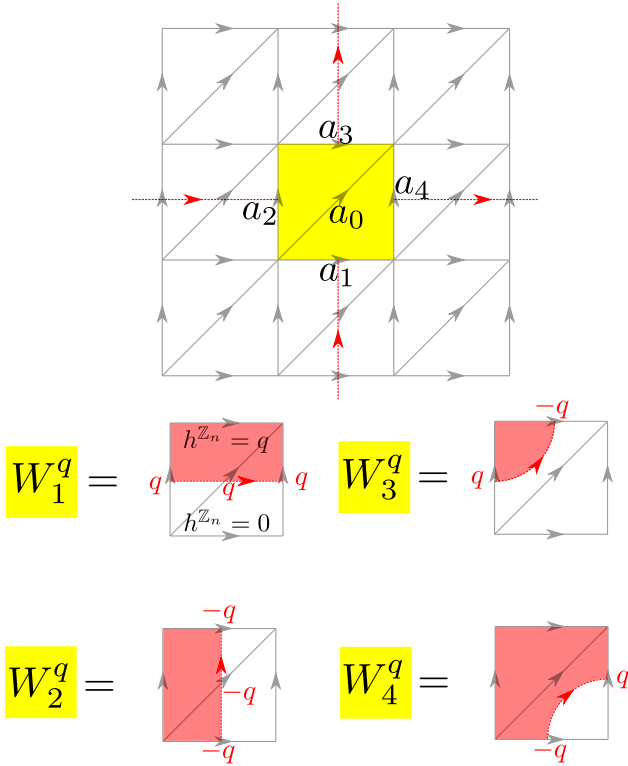


FIG. 3. (Color online) Measurement of self and mutual statistics of flux anyons. Top: A 2D region of $\partial\mathcal{M}^3$ is shown. Here the Hilbert space is spanned by the boundary states given in (36) and the degrees of freedom are a^{zn} living on gray links. Red lines depict the boundary 1-symmetry W_i^q which can be regarded of as an anyon hopping operator. The corresponding α^{zn} is non-zero on the gray links intersecting the red dotted lines, and change these links by $|a^{zn}\rangle_{\partial} \rightarrow \exp(2\pi i \int \phi_2) |(a + \alpha)^{zn}\rangle_{\partial}$, where ϕ_2 is given by (45) or (47). It turns out that, due to $\phi_2[a, h] = 0$ when $dh = 0$, in our calculation for self and mutual statistics it is only necessary to keep track of links a_i^{zn} in the central square, highlighted in yellow. Bottom: the configurations of four different 1-symmetries in the central square. Here $h^{zn} = q$ in the region shaded in pink and $h^{zn} = 0$ in the unshaded regions. The non-zero values of $\alpha = dh^{zn}$ are shown in red on gray links intersected by the red dotted lines.

operators (see eqn. (45) or eqn. (47)). The corresponding open string operators will create topological excitations on the boundary. The anomaly of the boundary 1-symmetry is encoded in the fractional statistics of those topological excitations. For instance if $n = 2$, $q = 1$, then for $m = 2$, the anyon is an emergent fermion. For $m = 1$ the anyon is an emergent semion.

2. Mutual-statistics

Similarly to compute the mutual statistics for two anyons with flux q_1 and q_2 , we compare the result of

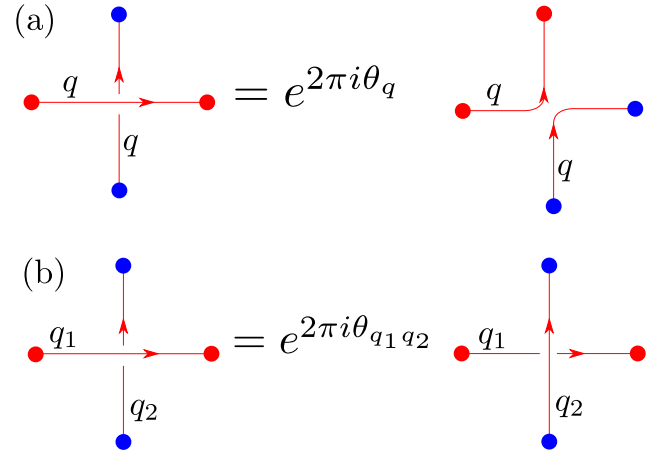


FIG. 4. (Color online) (a) To measure the self statistics, we compare the outcome of two processes. The first hops an anyon (shown in red) from left to right, and then hops an anyon (shown in blue) from bottom to top; the second hops an anyon from left to top and then hops an anyon from bottom to right. The results differ by exchange of two anyons at their final positions. (b) To measure the mutual braiding statistics, we compare the outcome of two processes: the first hops a red anyon (with flux q_1) from left to right, followed by hopping a blue anyon (with flux q_2) from bottom to top; the second process do these two operations in the different order. The results differ by a change of linking number $\Delta Lk(q_1, q_2) = 1$ between the world lines of the two anyons.

hopping a flux q_1 anyon from left to right, then the flux q_2 anyon from bottom to top, versus the result of doing the two processes in a different order, as illustrated in Fig. 4b. The mutual-statistic is given by $\theta_{q_1 q_2}$, where (derivation details in Appendix H)

$$W_1^{q_1} \circ W_2^{q_2} = e^{2\pi i \theta_{q_1 q_2}} W_2^{q_2} \circ W_1^{q_1}, \quad (50)$$

and the result is

$$\theta_{q_1 q_2} = q_1 q_2 \frac{m}{n}. \quad (51)$$

VII. GAPPED SYMMETRIC BOUNDARIES

In this section we attempt to write down boundary Hamiltonians which are symmetric under the non-onsite transformation (44), and contain emergent anyons with self-statistics predicted by (49). We will show that it is possible to gap out the boundary by realizing a topological order, which in the $(n, m) = (2, 1)$ case is the double semion (DS) topological order, which contains an emergent semion. In the $(n, m) = (2, 2)$ case the toric code is realized on the boundary, which contains an emergent fermion. The degenerate ground states for these systems on a manifold with non-trivial cycles spontaneously break the 1-symmetry.

An easy way to see this is as follows. From $\omega_4 =$

$d\phi_3[a]$, if \mathcal{M}^4 has a boundary,

$$\begin{aligned} Z^{\text{top}} &= \frac{1}{n^{N_l}} \sum_{\{a^{Z_n}\}} e^{2\pi i \int_{\mathcal{M}^4} \omega_4[da^{Z_n}]} \\ &= \frac{1}{n^{N_{l\partial}}} \sum_{\{a^{Z_n}\}} e^{2\pi i \int_{\partial\mathcal{M}^4} \phi_3[a^{Z_n}]}, \end{aligned} \quad (52)$$

where $N_{l\partial}$ is the number of links in the space-time triangulation of the boundary.

If we impose the constraint $da^{Z_n} \stackrel{n}{=} 0$ by hand (the constraint doesn't violate 1-symmetry since it is invariant under (14)), then from the expression for ϕ_3 (28), we have

$$\phi_3[a^{Z_n}]|_{da^{Z_n}=0} \stackrel{!}{=} \frac{m}{2n} a^{Z_n} da^{Z_n} = \frac{m}{2} a^{Z_2} \frac{da^{Z_2}}{2},$$

where in the last step we specialized to the case $n = 2$. This can be recognized as the Lagrangian for the surface topological order. To recast it into a more familiar form, we have

$$\frac{da^{Z_2}}{2} = \beta_2 a^{Z_2} \stackrel{2}{=} \text{Sq}^1(a^{Z_2}) \stackrel{2}{=} a^{Z_2} a^{Z_2},$$

where β_2 is the Bockstein homomorphism and the second equality follows from (A33), and the third equality is by definition of Steenrod square (A19) and $da^{Z_2} \stackrel{2}{=} 0$. So, (52) becomes

$$\begin{aligned} Z^{\text{top}}|_{da^{Z_n}=0} &= \frac{1}{n^{N_{l\partial}}} \sum_{\{da^{Z_n}=0\}} e^{2\pi i \int_{\partial\mathcal{M}^4} \frac{m}{2} a^{Z_2} \frac{da^{Z_2}}{2}} \\ &= \frac{1}{n^{N_{l\partial}}} \sum_{\{da^{Z_n}=0\}} e^{2\pi i \int_{\partial\mathcal{M}^4} \frac{m}{2} a^{Z_2} a^{Z_2} a^{Z_2}}, \end{aligned}$$

which for $m = 1$ is (up to a volume term) the partition function for double semion topological order (see for instance Ref. 41). For $m = 2$ the Lagrangian $\stackrel{2}{=} 0$ and describes the \mathbb{Z}_2 gauge theory, *i.e.* toric code.

A. Engineering boundary gapped Hamiltonian

Alternatively, we can explicitly engineer a gapped Hamiltonian consisting of mutually commuting terms on the boundary Hilbert space respecting the anomalous 1-symmetry and realizing the DS topological order.

The following boundary Hamiltonian is proposed:

$$H_{\partial} = - \sum_i H_{s,i} - \sum_{\Delta} H_{p,\Delta} \quad (53)$$

$$H_{s,i} := W_{\odot i}$$

$$H_{p,\Delta} := \delta_{\langle da,\Delta \rangle^{Z_n}, 0}.$$

Here i is summed over all sites and Δ is summed over all 2-simplices (*i.e.* triangles) in the boundary. δ is the Kronecker delta function. $\langle da,\Delta \rangle$ is evaluating the 2-cochain da on the 2-simplex Δ . Hence $H_{p,\Delta}$ enforces the “no flux” constraint $da \stackrel{n}{=} 0$ on every 2-simplices. $W_{\odot i}$ is the 1-symmetry operator corresponding to a tiny loop surrounding site i (see Fig. 5).

1. H_{∂} is exactly solvable and has 1-symmetry

To show that H_{∂} consists of mutually commuting terms, which also commutes with the boundary 1-symmetry operators, it suffices to check the following commutators vanishes:

$$[H_{p,\Delta}, W(h^{Z_n})] = 0 \quad (54)$$

$$[W_{\odot i}, W(h^{Z_n})] = 0 \quad (55)$$

for any \mathbb{Z}_n -valued 0-cochain h^{Z_n} , where $W(h^{Z_n})$ denotes a 1-symmetry operator parameterized by h^{Z_n} , whose action is described by (44) with $a_{\partial}^{Z_n} = (a_{\partial} + dh)^{Z_n}$.

To show (54), notice that

$$\begin{aligned} &W(h^{Z_n})^{-1} H_{p,\Delta} W(h^{Z_n}) \\ &= W(h^{Z_n})^{-1} \delta_{\langle da,\Delta \rangle^{Z_n}, 0} W(h^{Z_n}) \\ &= \delta_{\langle d(a+dh),\Delta \rangle^{Z_n}, 0} = \delta_{\langle da,\Delta \rangle^{Z_n}, 0} = H_{p,\Delta}, \end{aligned}$$

where we used the fact that the non-onsite phases from $W(h^{Z_n})$ and $W(h^{Z_n})^{-1}$ cancels, since $\delta_{\langle da,\Delta \rangle^{Z_n}, 0}$ does not change the value of a^{Z_n} in the ket.

To show (55), notice that for any two \mathbb{Z}_n -valued 0-cochain $h_1^{Z_n}$ and $h_2^{Z_n}$, we have

$$\begin{aligned} &W(h_2^{Z_n})^{-1} W(h_1^{Z_n})^{-1} W(h_2^{Z_n}) W(h_1^{Z_n}) | \{a^{Z_n}\} \rangle_{\partial} \\ &= \exp \left[2\pi i \int_{\partial\mathcal{M}^3} \left(-\phi_2[(a+dh_2)^{Z_n}, h_1^{Z_n}] - \phi_2[a^{Z_n}, h_2^{Z_n}] \right. \right. \\ &\quad \left. \left. + \phi_2[(a+dh_1)^{Z_n}, h_2^{Z_n}] + \phi_2[a^{Z_n}, h_1^{Z_n}] \right) \right] | \{a^{Z_n}\} \rangle_{\partial} \\ &= \exp \left[2\pi i \int_{\partial\mathcal{M}^3} d\phi_1[a^{Z_n}, h_1^{Z_n}, h_2^{Z_n}] \right] | \{a^{Z_n}\} \rangle_{\partial}, \end{aligned} \quad (56)$$

where we applied (43) and (42) in the last step to show that the integrand in the exponent is a total derivative:

$$\begin{aligned} &\phi_2[(a+dh_1)^{Z_n}, h_2^{Z_n}] - \phi_2[a^{Z_n}, h_2^{Z_n}] - (h_1 \leftrightarrow h_2) \\ &= \phi_2[a+dh_1, h_2] - \phi_2[a, h_2] - (h_1 \leftrightarrow h_2) \\ &= \frac{m}{2n} dh_2(a+dh_1) + \delta_{dh_2} \xi_2[a+dh_1] + d\xi_1[a+dh_1, h_2] \\ &\quad - \frac{m}{2n} dh_2 a - \delta_{dh_2} \xi_2[a] - d\xi_1[a, h_2] - (h_1 \leftrightarrow h_2) \\ &= \frac{m}{2n} dh_2 dh_1 + d\delta_{dh_1} \xi_1[a, h_2] - (h_1 \leftrightarrow h_2) \\ &= d\phi_1[a^{Z_n}, h_1^{Z_n}, h_2^{Z_n}] \end{aligned}$$

where

$$\begin{aligned} \phi_1[a, h_1, h_2] &:= \frac{m}{2n} h_2^{Z_n} dh_1^{Z_n} + \xi_1[a^{Z_n} + dh_1^{Z_n}, h_2^{Z_n}] \\ &\quad - \xi_1[a^{Z_n}, h_2^{Z_n}] - (h_1 \leftrightarrow h_2) \quad (57) \\ &\stackrel{!}{=} \frac{m}{2n} h_2 dh_1 + \delta_{dh_1} \xi_1[a, h_2] + d\xi_0[h_1, h_2] \\ &\quad - (h_1 \leftrightarrow h_2) \\ \xi_0[h_1, h_2] &:= \frac{m}{2} \left(\lfloor \frac{h_2}{n} \rfloor \smile_1 dh_1 + h_1 \lfloor \frac{h_2}{n} \rfloor \right). \end{aligned}$$

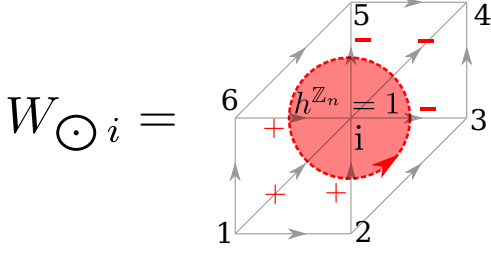


FIG. 5. (Color online) $W_{\odot i}$ is the 1-symmetry operator on the boundary Hilbert space for a tiny loop surrounding site i . Here the pink shaded region has $h^{\mathbb{Z}_n} = 1$. The non-zero values of $\alpha = dh^{\mathbb{Z}_n} = \pm 1$ are drawn in red. The neighboring sites of i are labeled $j = 1, \dots, 6$.

(See Appendix J for relationship between ω_4 , ϕ_3 , ϕ_2 and ϕ_1 in general.)

Thus by Stoke's theorem, (56) implies that when evaluated on the closed manifold $\partial\mathcal{M}^3$, $[W(h_1^{\mathbb{Z}_n}), W(h_2^{\mathbb{Z}_n})] = 0$ for any \mathbb{Z}_n -valued 0-cochains h_1, h_2 . For the case of our interest (55), we may take $h_1^{\mathbb{Z}_n} = h_{\odot i}^{\mathbb{Z}_n}$ where $W_{\odot i} = W(h_{\odot i}^{\mathbb{Z}_n})$ as depicted in Fig. 5, and $h_2^{\mathbb{Z}_n} = h^{\mathbb{Z}_n}$ to be an arbitrary 1-symmetry. Alternatively we can evaluate (56) by integrating the exponent over a patch covering the region where $h_{\odot i}^{\mathbb{Z}_n} \neq 0$ and use $\phi_1[a^{\mathbb{Z}_n}, h_1^{\mathbb{Z}_n} = 0, h_2^{\mathbb{Z}_n}] = 0$.

2. Topological ordered surface states for $n = 2$

We can specialize to the case $(n, m) = (2, 1)$ and evaluate $W_{\odot i}$. Assuming “no flux” constraint is enforced, we have (see Appendix I for details)

$$W_{\odot i}|\{a_{ij}^{\mathbb{Z}_2}, a_{jj'}^{\mathbb{Z}_2}\}\rangle \Big|_{da \stackrel{Z}{=} 0} = \prod_{(j, j')} (-)^{a_{ij} a_{ij'}} |\{(a_{ij} + 1)^{\mathbb{Z}_2}, a_{jj'}^{\mathbb{Z}_2}\}\rangle, \quad (58)$$

where $j, j' \in \{1, \dots, 6\}$ are neighboring sites of i (see Fig. 5). The product is taken over six links with neighboring j, j' . The resulting H_{∂} gives rise to DS topological order.

For the $m = 2$ case, we have

$$W_{\odot i}|\{a_{ij}^{\mathbb{Z}_2}, a_{jj'}^{\mathbb{Z}_2}\}\rangle \Big|_{da \stackrel{Z}{=} 0} = |\{(a_{ij} + 1)^{\mathbb{Z}_2}, a_{jj'}^{\mathbb{Z}_2}\}\rangle$$

So $h_{s,i}$ is the usual star term and $h_{p,\Delta}$ is the usual plaquette term for the toric code model. Thus H_{∂} gives rise to the toric code topological order.

3. Connection to Works of Wan and Wang

A general theory of gapped symmetric boundaries of higher SPT is presented in Section III of Ref. 42, which is

a generalization of Ref. 41. It was then applied in Section IX of Ref. 43, and Section 8 of Ref. 44, which also contains a lattice Hamiltonian description for a 4+1D bulk/3+1D boundary.

We give a rough review of their result in the following. In general, a 1-SPT protected by 1-form finite symmetry Π_2 (which is Abelian) and 0-form finite symmetry G , may be associated with a “2-group” \mathbb{G} , such that its classifying space $B\mathbb{G} = B(G, \Pi_2)$ has $\pi_1 = G$, $\pi_2 = \Pi_2$ and $\pi_0 = \pi_{k>2} = 0$. (In addition, \mathbb{G} also contains the data²⁵ $\alpha_2 : G \rightarrow \text{Aut}(\Pi_2)$ and $\bar{n}_3 \in H^3(BG, \Pi_2^{\alpha_2})$ describing the interplay between G and Π_2 .) A space-time field configuration is a map $\phi : \mathcal{M}^D \rightarrow B\mathbb{G}$, and the cocycle ω_D describing the 1-SPT is the pullback: $\omega_D = \phi^* \bar{\omega}_D$ for a topological term $\bar{\omega}_D$, which can be an element of $H^D(B\mathbb{G}, U(1))$, or a bordism invariant in general. Section III of Ref. 42 claimed that the gapped boundary of 1-SPT corresponds to a fibration:

$$B\mathbb{K} \rightarrow B\mathbb{H} \rightarrow B\mathbb{G}$$

such that the topological invariant $\bar{\omega}_D$ in $B\mathbb{G}$ is pulled back to a trivial topological invariant in $B\mathbb{H}$. Here \mathbb{H} is a 2-group, viewed as an extension of \mathbb{G} . $B\mathbb{K}$ is the total space of a fibration $B^2 K_{[1]} \rightarrow B\mathbb{K} \rightarrow BK_{[0]}$, where $K_{[0]}, K_{[1]}$ are some 0-form and 1-form symmetries respectively. For a finite group G , $B^2 G = K(G, 2)$ is a Eilenberg-MacLane space for which the only non-trivial homotopy group is $\pi_2 = G$. To be precise, the topological invariants of the classifying spaces $B\mathbb{G}$, $B\mathbb{H}$ are bordism invariants of the bordism groups^{45,46} $\Omega_D^{S_G}(B\mathbb{G})$, $\Omega_D^{S_H}(B\mathbb{H})$, computed²⁶ with respect to an “ S -structure”, $S_{G,H} = \text{SO}/\text{O}/\text{Spin}/\text{Pin}^{\pm}$, corresponding to unitary bosonic SPT/time-reversal invariant bosonic SPT/unitary fermionic SPT/time-reversal invariant fermionic SPT with $T^2 = (\mp)^F$, respectively.

In this framework, our \mathbb{Z}_2 -1-SPT has $D = 4$, $(G, \Pi_2) = (0, \mathbb{Z}_2)$ and $S_G = \text{SO}$. Gapping out its 2+1D boundary for $m = 2$ with toric code topological order corresponds to the fibration:

$$B\mathbb{Z}_2 \rightarrow B\text{Spin}(4) \times B^2\mathbb{Z}_2 \rightarrow B\text{SO}(4) \times B^2\mathbb{Z}_2$$

where the pullback of $\bar{\omega}_4$ is trivial because of a relation between \mathbb{Z}_2 -valued 2-cocycle $\mathcal{B}^{\mathbb{Z}_2}$ and the Stiefel-Whitney classes w_1, w_2 (which is derived using Wu formula, *eg.* in Appendix D.5 of Ref. 38):

$$\mathbb{S}_0^2(\mathcal{B}^{\mathbb{Z}_2}) = (w_1^2 + w_2)\mathcal{B}^{\mathbb{Z}_2},$$

where w_1, w_2 vanishes when pulled back to $B\text{Spin}(4) \times B^2\mathbb{Z}_2$, which is a spin manifold. The emergent fermion is due to the emergent spin structure.

VIII. GEOMETRIC INTERPRETATION OF GROUND STATE WAVEFUNCTION

In this section we attempt to provide an intuitive interpretation of the ground state wavefunction (35) on a closed 3-manifold.

Recall from (35) and (28), the ground state wavefunction is

$$|\psi_0\rangle = \sum_{\{a^{\mathbb{Z}^n}\}} e^{2\pi i \int_{\mathcal{M}^3} \phi_3[a^{\mathbb{Z}^n}]} |\{a^{\mathbb{Z}^n}\}\rangle$$

$$\phi_3[a] = \frac{m}{2n} a da + \frac{m}{2} da \frown_1 \lfloor \frac{da}{n} \rfloor + d\xi_2[a].$$

In a closed 3-manifold \mathcal{M}^3 , we can ignore the $d\xi_2$ term. In the dual manifold $\tilde{\mathcal{M}}^3$, a is dual to 2-chains \tilde{a} , and da is dual to $\partial\tilde{a}$, which is a 1-cycle.

If we focus on the term $\frac{m}{2n} a da$, which only depends on 1-diagonal links, we can imagine the dual 2-chains and 1-cycles as living on the dual faces and links of a simple cubic lattice. Geometrically, $\frac{m}{2n} a da$ is contributed from the intersections of \tilde{a} and $\partial\tilde{a}'$, which is $\partial\tilde{a}$ displaced by the framing vector $-\vec{\frac{1}{2}} = (-1/2, -1/2, -1/2)$.

$$\int_{\mathcal{M}^3} \frac{m}{2n} a da = \sum_{p \in \tilde{a} \cap \partial\tilde{a}'} \frac{m}{2n} q_{a,p} q_{\partial a',p},$$

where $q_{a,p}, q_{\partial a',p} \in \mathbb{Z}$ denote the integer coefficients of the 2-chain \tilde{a} and 1-cycle $\partial\tilde{a}'$ at the intersection point p .

If the 1-cycle $\partial\tilde{a}$ can be resolved into non-intersecting loops K_i , then \tilde{a} are the Seifert surfaces S_i for these loops. A Seifert surface of loop K_i is an oriented surface with K_i as its boundary. It is known that the signed intersection number between K_i and a Seifert surface of K_j' is the sum of signed crossings between K_i and K_j' (viewed from the $-\vec{\frac{1}{2}}$ direction), which is the linking number $Lk(K_i, K_j')$ ⁴⁷. Thus

$$\begin{aligned} \int_{\mathcal{M}^3} \frac{m}{2n} a da &= \sum_{i,j} \sum_{S_i \cap K_j'} \frac{m}{2n} q_i q_j \\ &= \frac{m}{2n} \sum_{i,j} q_i q_j Lk(K_i, K_j') \\ &= \frac{m}{2n} \sum_i q_i^2 w(K_i) + \frac{m}{n} \sum_{i < j} q_i q_j Lk(K_i, K_j), \end{aligned} \quad (59)$$

where $w(K_i) = Lk(K_i, K_i')$ is the self-linking number of K_i , and for $i \neq j$, $Lk(K_i, K_j') = Lk(K_i, K_j)$ is the linking number between K_i and K_j . $q_i \in \mathbb{Z}$ denote the “strength” of each loop K_i . Note the result (59) is invariant (mod 1) under $q_i \rightarrow q_i + nu_i$ for any integers $\{u_i\}$ for general m . For example in Figure 6(a), we see that for an unknot with self linking number +1 carrying flux $da = q$, $\int_{\mathcal{M}^3} \frac{m}{2n} a da = \frac{m}{2n} q^2$. In Figure 6(b), for the Hopf link with linking number 1, with two loops carrying flux $da = q_1$ and q_2 , we have $\int_{\mathcal{M}^3} \frac{m}{2n} a da = \frac{m}{n} q_1 q_2$. This could be regarded as an alternative way to derive the self-statistics (49) and mutual-statistics (51) of the boundary transformation strings, from the 3d bulk space perspective instead of the 2+1d boundary spacetime perspective.

However, when multiple lines intersect at a point, we need to carefully resolve the 1-cycle $\partial\tilde{a}$ into non-intersecting loops. We will consider the even m case and the odd m case separately.

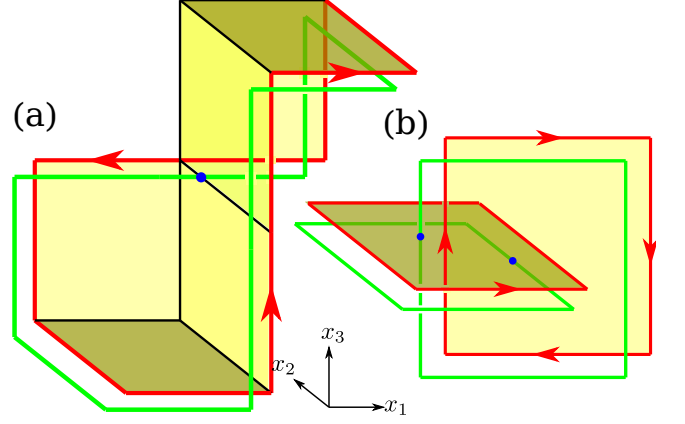


FIG. 6. (Color online) Evaluation of $\int_{\mathcal{M}^3} \frac{m}{2n} a da$ in the dual lattice. Yellow squares, red links and green links represent \tilde{a} , $\partial\tilde{a}$ and $\partial\tilde{a}'$ respectively. Blue dot represents the intersection of green links and yellow square, where $a da \neq 0$. The configuration of $\partial\tilde{a}$ is: (a) an unknot with self-linking number +1, where the coefficient of the 2-chain \tilde{a} on every yellow square is q ; (b) a Hopf link with linking number +1, where the coefficient of the 2-chain \tilde{a} on the two yellow squares are q_1 and q_2 .

A. Even m case

In the case of even m , (28) is

$$\phi_3[a] \stackrel{1}{=} \frac{m}{2n} a da.$$

Each lattice point of the dual cubic lattice has six connecting dual links. Given a dual cycle configuration $\partial\tilde{a}$, we project these six links onto the plane perpendicular to the $-\vec{\frac{1}{2}}$ framing vector. Then we resolve the intersection into disjoint loops with “no-crossing” resolution: requiring that no crossing occurs in this intersection. An example is shown in Fig. 7.

Since all the crossings are contributed away from intersections, the wavefunction amplitude (59) is

$$\int_{\mathcal{M}^3} \phi_3[a] = \frac{m}{2n} \sum_i q_i^2 w(K_i) + \frac{m}{n} \sum_{i < j} q_i q_j Lk(K_i, K_j).$$

with K_i obtained from $\partial\tilde{a}$ by “no-crossing” resolution at each vertex.

B. Odd m case

In the case of odd m , (28) is

$$\phi_3[a] \stackrel{d,1}{=} \frac{m}{2n} a da + \frac{m}{2} da \frown_1 \lfloor \frac{da}{n} \rfloor.$$

As explained previously,

$$\int_{\mathcal{M}^3} \frac{m}{2n} a da = \frac{m}{2n} \times \sum \left(\begin{array}{c} \text{signed crossings} \\ \text{away from intersections} \end{array} \right).$$

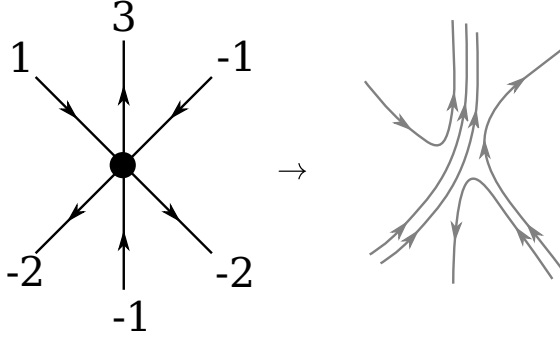


FIG. 7. (Color online) “No-crossing” resolution at an intersection. In the simple cubic dual lattice, every vertex is connected to six oriented links. Each link carries an integer q which is the coefficient of the 1-cycle $\partial\tilde{a}$. The figure on the left shows one such configuration, viewed from $\frac{\vec{1}}{2}$. In the “no-crossing” resolution, each link is resolved into q parallel strands away from the original vertex. Near the vertex the strands are connected such that there is no crossing when viewed from $\frac{\vec{1}}{2}$. Such resolution may not be unique, but can be fixed by choosing some convention.

In the following we will also interpret the second term as $\frac{m}{2n} \times$ the sum of signed crossings under a “quotient-remainder” resolution at intersections.

Since the term $\frac{m}{2} da \smile_1 \lfloor \frac{da}{n} \rfloor \stackrel{!}{=} \frac{m}{2} (da)^{\mathbb{Z}_n} \smile_1 \lfloor \frac{da}{n} \rfloor$ also depends on 2- and 3-diagonal links, we need to use the full triangulation described in Appendix D with six tetrahedrons per unit cubic cell. The dual lattice is a cubic lattice with six sites forming a hexagon in each unit cell, depicted in Fig. 8(a).

The “quotient-remainder” resolution is the following: write $da = (da)^{\mathbb{Z}_n} + n \lfloor \frac{da}{n} \rfloor$. These two terms are called the “remainder” and “quotient” respectively. The 1-cycles dual to da live on the links of the dual lattice. We split each link in the dual lattice into two channels: the “remainder” channel dual to $(da)^{\mathbb{Z}_n}$, and the “quotient” channel dual to $n \lfloor \frac{da}{n} \rfloor$. They are depicted as black and red links respectively in Fig. 8(b). If we detach the ‘quotient’ intersections from the “remainder” intersections by displacing them slightly towards the center of each cube, then $da \smile_1 n \lfloor \frac{da}{n} \rfloor$ is the sum of signed crossings (mod $2n$) between the “remainder” channels and the “quotient” channels, viewed from $\frac{\vec{1}}{2}$, as depicted in Fig. 8(b). All other intersections (black and red dots in Fig. 8(b)) are resolved with the “no-crossing” resolution.

Thus $\frac{m}{2} da \smile_1 \lfloor \frac{da}{n} \rfloor$ is $\frac{m}{2n} \times$ sum of signed crossings between quotient channels and remainder channels at a vertex. As before, the sum of signed crossings is the sum of linking numbers between resolved loops. Hence the wavefunction amplitude (59) is

$$\int_{\mathcal{M}^3} \phi_3[a] = \frac{m}{2n} \sum_i q_i^2 w(K_i) + \frac{m}{n} \sum_{i < j} q_i q_j Lk(K_i, K_j).$$

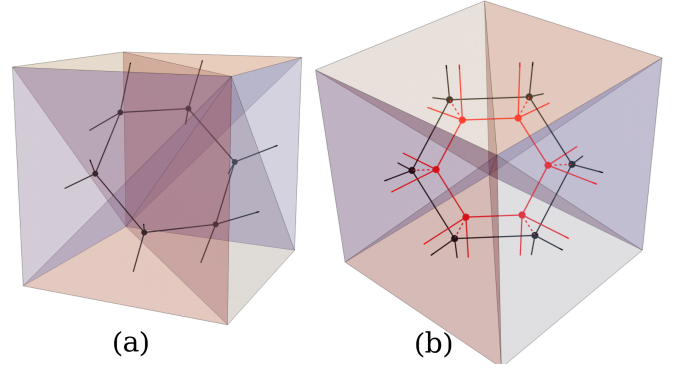


FIG. 8. (Color online) (a) A cubic cell is triangulated with six tetrahedrons. In the dual lattice they corresponds to six vertices (shown in black), which forms a hexagon. There are two external links at each face which connects to vertices of a neighboring cube. (b) Each link is separated into a “remainder” channel (black) dual to $(da)^{\mathbb{Z}_n}$ and a “quotient” channel (red) dual to $n \lfloor \frac{da}{n} \rfloor$. In each tetrahedron, the intersections for “quotient” channels (red dots) were displaced slightly towards the center of the cube, away from intersections for “remainder” channels (black dots). The resulting crossings between “remainder” and “quotient” channels viewed from $\frac{\vec{1}}{2}$ contribute to $da \smile_1 \lfloor \frac{da}{n} \rfloor$. The two channels are coupled within each tetrahedron by a red dashed line, dual to $n d \lfloor \frac{da}{n} \rfloor$.

with K_i obtained from $\partial\tilde{a}$ by “quotient-remainder” resolution at each vertex.

The term $\frac{m}{2} da \smile_1 \lfloor \frac{da}{n} \rfloor$ is necessary to ensure that $\phi_3[a]$ is invariant mod 1 under $a \rightarrow a + nu$ for \mathbb{Z} -valued 1-chain u . Indeed under $a \rightarrow a + nu$, all changes occur only in the quotient channel $n \lfloor \frac{da}{n} \rfloor \rightarrow n \lfloor \frac{da}{n} \rfloor + n du$. The change to $\phi_3[a]$ mod 1 is $\frac{1}{2} \times$ the sum of signed crossings between the dual of $(da)^{\mathbb{Z}_2}$ in remainder channel and the dual of du in the quotient channel. Since both of them are closed loops living in separate channels, the total number of signed crossing is even. Hence $\phi_3[a]$ is invariant mod 1.

IX. NON-ZERO BACKGROUND GAUGE FIELD

We may also extend our derivations to the case where the background gauge field \hat{B} in (12) is non-zero. By keeping track of the coboundary terms in (16)^d(20), it can be shown that (26),(27),(28),(29) become

$$\begin{aligned} \omega_4[(\hat{B} + da)^{\mathbb{Z}_n}] &= \frac{m}{2n} \text{Sq}^2 \hat{B}^{\mathbb{Z}_n} + d\phi_3[a, \hat{B}] \\ &= \omega_4[\hat{B}^{\mathbb{Z}_n}] + d\phi_3[a, \hat{B}] \end{aligned}$$

where

$$\begin{aligned} \phi_3[a, \hat{B}] : &= \frac{m}{2n} (a^{\mathbb{Z}_n} da^{\mathbb{Z}_n} + a^{\mathbb{Z}_n} \hat{B}^{\mathbb{Z}_n} + \hat{B}^{\mathbb{Z}_n} a^{\mathbb{Z}_n}) \\ &+ \xi_3[a^{\mathbb{Z}_n}, \hat{B}^{\mathbb{Z}_n}] \end{aligned} \quad (60)$$

$$\begin{aligned} & \stackrel{\perp}{=} \frac{m}{2n} (a da + a \hat{B} + \hat{B} a) + \xi_3[a, \hat{B}] + d\xi_2[a, \hat{B}] \\ \xi_3[a, \hat{B}] & := \frac{m}{2} \left[(\hat{B} + da) \underset{1}{\smile} \left[\frac{\hat{B} + da}{n} \right] + a \underset{1}{\smile} \frac{d\hat{B}}{n} \right. \\ & \quad \left. + \hat{B} \underset{1}{\smile} \left[\frac{\hat{B}}{n} \right] \right] \end{aligned}$$

$$\xi_2[a, \hat{B}] := \frac{m}{2} \left(a \left[\frac{a}{n} \right] + da \underset{1}{\smile} \left[\frac{a}{n} \right] + a \underset{1}{\smile} \left[\frac{\hat{B}}{n} \right] + \hat{B} \underset{1}{\smile} \left[\frac{a}{n} \right] \right).$$

and (39),(40),(41),(42) become

$$\begin{aligned} -\delta_\alpha \phi_3[a^{\mathbb{Z}_n}, \hat{B}^{\mathbb{Z}_n}] & = d \left[\frac{m}{2n} (\alpha a - \alpha \underset{1}{\smile} \hat{B}) \right. \\ & \quad \left. + \frac{m}{2} \left(a \underset{1}{\smile} \frac{d\alpha}{n} + \delta_\alpha \xi_2[a, \hat{B}] + \hat{B} \underset{2}{\smile} \frac{d\alpha}{n} \right) \right] \\ -\frac{m}{n} \hat{B} \alpha + \frac{m}{2} \alpha \frac{d\alpha}{n} & = d\phi_2[a, h, \hat{B}] \end{aligned} \quad (61)$$

where

$$\begin{aligned} \phi_2[a, h, \hat{B}] & := \frac{m}{2n} (\alpha^{\mathbb{Z}_n} a^{\mathbb{Z}_n} - a^{\mathbb{Z}_n} \underset{1}{\smile} \hat{B}^{\mathbb{Z}_n}) \\ & \quad + \frac{m}{2} \left(a^{\mathbb{Z}_n} \underset{1}{\smile} \frac{d\alpha^{\mathbb{Z}_n}}{n} + \delta_{\alpha^{\mathbb{Z}_n}} \xi_2[a^{\mathbb{Z}_n}, \hat{B}^{\mathbb{Z}_n}] + \hat{B}^{\mathbb{Z}_n} \underset{2}{\smile} \frac{d\alpha^{\mathbb{Z}_n}}{n} \right) \\ & \quad - \frac{m}{n} \hat{B}^{\mathbb{Z}_n} h^{\mathbb{Z}_n} + \frac{m}{2} h^{\mathbb{Z}_n} d \left[\frac{dh^{\mathbb{Z}_n}}{n} \right] \\ & \stackrel{\perp}{=} \frac{m}{2n} (dha - dh \underset{1}{\smile} \hat{B}) - \frac{m}{n} \hat{B} h + \delta_{dh} \xi_2[a, \hat{B}] + d\xi_1[a, h] \end{aligned} \quad (62)$$

$$\xi_1[a, h] := \frac{m}{2} \left(\left[\frac{dh}{n} \right] \underset{1}{\smile} a + h \left[\frac{dh}{n} \right] \right).$$

In Appendix B2, we generalize the construction of an exactly solvable Hamiltonian with a unique ground state to the case of non-zero \hat{B} . Also in Appendix C2 we generalize the expression of the ground state wavefunction (C3) in terms of ϕ_3 :

$$|\psi_0[\hat{B}]\rangle = \frac{1}{N_\psi} \sum_{\{a\}} e^{2\pi i \int_{\mathcal{M}^3} \phi_3[a, \hat{B}] - \phi_3[0, \hat{B}]} |\{a\}\rangle. \quad (63)$$

In the following we consider the case m is even, where (60), (62) simplifies to

$$\phi_3[a, \hat{B}] \stackrel{\perp}{=} \frac{m}{2n} (a da + a \hat{B} + \hat{B} a) \quad (64)$$

$$\phi_2[a, h, \hat{B}] \stackrel{\perp}{=} \frac{m}{2n} (dha - dh \underset{1}{\smile} \hat{B}) - \frac{m}{n} \hat{B} h \quad (65)$$

A. Exactly Solvable Hamiltonian

The bulk Hamiltonian is given by

$$H = - \sum P_{ij}[\hat{B}]$$

By using (C4) to write down matrix elements of $P_{ij}[\hat{B}]$ It can be shown that $P_{ij}[\hat{B}]$ are the same as (33),

$$P_{ij}[\hat{B}] = \frac{1}{n} \sum_{k=0}^n \hat{X}_{ij}^k e^{2\pi i \frac{mk}{2n} \frac{\epsilon \alpha \beta \gamma}{2} [F_{\beta\gamma}(\vec{r}_{ij} + \frac{\vec{1}}{2}) + F_{\beta\gamma}(\vec{r}_{ij} - \frac{\vec{1}}{2})]},$$

except that in the definition (34) of the flux F , da is replaced by $\hat{B} + da$:

$$F_{\beta\gamma}(\vec{r}) := \langle (\hat{B} + da)^{\mathbb{Z}_n}, (\vec{0}, \hat{\beta}, \hat{\beta} + \hat{\gamma})_{\vec{r} - \frac{\hat{B}}{2} - \frac{\vec{1}}{2}} \rangle - (\beta \leftrightarrow \gamma) \quad (66)$$

B. Geometric interpretation of wavefunction

In (64), the background gauge field \hat{B} is coupled to a through the extra terms

$$\frac{m}{2n} (a \hat{B} + \hat{B} a) \quad (67)$$

Geometrically, in 3d space, the 2-cocycle gauge field \hat{B} is dual to a 1d line \tilde{B} . we may shift these lines in the $\pm \frac{\vec{1}}{2}$ directions to obtain \tilde{B}_\pm . Then the extra terms (67) contributes a phase $e^{2\pi i \frac{m}{2n}}$ to every signed intersections between \tilde{B}_\pm and \tilde{a} (Recall \tilde{a} is the surface dual to a).

For simplicity let's pretend \tilde{a} will not fluctuate too wildly near the intersection, and so \tilde{B}_\pm gives the same number of signed intersections as \tilde{B} , then the extra terms contribute a phase $e^{2\pi i \frac{m}{n}}$ for every such intersection.

$$\int_{\mathcal{M}^3} \frac{m}{2n} (a \hat{B} + \hat{B} a) \approx \frac{m}{n} \times \sum \left(\begin{array}{c} \text{signed intersections} \\ \text{between } \tilde{B} \text{ and } \tilde{a} \end{array} \right).$$

We may interpret such phase as a charge attachment to \tilde{B} . In 1-SPT, charged objects are 1-dimensional: a charge k line pick up a phase $e^{2\pi i \frac{k}{n}}$ for every intersection with a unit-shift (*i.e.* acting by the generator of \mathbb{Z}_n) 1-symmetry membrane operator. Charge lines live on the original lattice.

Thus in a \mathbb{Z}_n -1-SPT labeled by m , consider the 1-symmetry transformation $|\{a\}\rangle \rightarrow |\{a + \alpha\}\rangle = |\{a'\}\rangle$, where α is a unit-shift acting on a membrane intersecting \tilde{B} once. We have(as in (38))

$$\begin{aligned} |\psi_0[\hat{B}]\rangle & = \frac{1}{N_\psi} \sum_{\{a\}} e^{2\pi i \int_{\mathcal{M}^3} \phi_3[a, \hat{B}] - \phi_3[0, \hat{B}]} |\{a\}\rangle \\ & \rightarrow \frac{1}{N_\psi} \sum_{\{a'\}} e^{2\pi i \int_{\mathcal{M}^3} \phi_3[a', \hat{B}] - \phi_3[0, \hat{B}] - \delta_\alpha \phi_3[a, \hat{B}]} |\{a'\}\rangle \\ & = e^{2\pi i \int_{\mathcal{M}^3} \frac{-m}{n} \hat{B} \alpha} |\psi_0[\hat{B}]\rangle. \end{aligned}$$

using (61) and assuming $\partial \mathcal{M}^3 = \emptyset$. Hence the ground state wavefunction picks up a phase $e^{-2\pi i \frac{m}{n}}$ due to the background gauge field. Thus the dual of the background gauge fields \tilde{B} (with unit gauge strength) is attached a charge $-m$ line (located at \tilde{B}_+ , to be exact).

C. Boundary perspective

We can alternatively consider the effect of background gauge field from a boundary perspective. Consider the

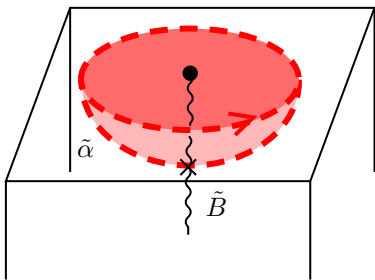


FIG. 9. A non-zero background gauge field \hat{B} , whose dual \tilde{B} is depicted as the wiggly line in the figure, intersects the 1-symmetry membrane α acting in the bulk (whose dual $\tilde{\alpha}$ is depicted as dotted red lines). The intersection in the bulk is denoted by a cross \times . From the boundary, the endpoint of \tilde{B} (depicted as a black dot) is enclosed in a region $h^{\mathbb{Z}_n} = 1$ (shaded in pink), where $\alpha = dh$, and $h = 0$ outside the pink region. The line \tilde{B} with unit gauge strength acquires a phase $e^{-2\pi i \frac{m}{n}}$ under a unit shift 1-symmetry α .

arrangement depicted in Fig. 9. In the bulk, the unit strength background gauge \hat{B} intersects the 1-symmetry α once. On the boundary, the 0d endpoint of background gauge field is enclosed in a region where $h^{\mathbb{Z}_n} = 1$, and the endpoint is far away from the 1-symmetry operator in the boundary (so $dh = 0$ near the end point). From (65), under this 1-symmetry there is an extra term

$$\begin{aligned} & \int_{\partial\mathcal{M}^3} \phi_2[a_\partial, h, \hat{B}] - \int_{\partial\mathcal{M}^3} \phi_2[a_\partial, h, 0] \\ &= \int_{\partial\mathcal{M}^3} -\frac{m}{n} \hat{B}h = -\frac{m}{n} \end{aligned} \quad (68)$$

contributed to the boundary transformation (44), compared to the case without background gauge fields. The boundary state hence acquires a phase $e^{-2\pi i \frac{m}{n}}$ due to the background gauge field. *i.e.* the endpoint of \tilde{B} has charge $-m$ under the boundary 1-symmetry.

We observe that the above boundary argument extends to the odd m case as well. (68) still holds by inspecting (62) and again assuming $dh = 0$ near the end point where $\hat{B} \neq 0$. So we expect the same charge attachment also occurs for odd m .

X. CONCLUSIONS

In this paper we studied the \mathbb{Z}_n -1-symmetry protected topological states in 3+1-dimensions, which is labeled by $m \in \{0, 1, \dots, 2n-1\}$. The \mathbb{Z}_n -1-symmetry is generated by closed membrane operators. We presented an exactly solvable Hamiltonian which commutes with the closed membrane operators, and wrote down the ground state wavefunction. We also studied the effective boundary theory in 2+1-dimensions. The effective boundary theory has an anomalous \mathbb{Z}_n -1-symmetry generated by closed string operators. We showed that those boundary string operators create topological excitations at the

string ends, which may have non-trivial self-statistics. In particular for the $n = 2$ case, they have self-semionic (for $m = 1$) or fermionic statistics (for $m = 2$). In these cases we can gap out the boundary with an engineered boundary Hamiltonian *with the anomalous \mathbb{Z}_n -1-symmetry*, which gives the same ground state as the toric code model (for $m = 2$) and double-semion model (for $m = 1$) on the boundary. We interpreted the wavefunction amplitudes of the bulk ground states as linking numbers of strings in the dual lattice. Finally we extend to the case of non-zero background gauge field and find the lines dual to the background gauge field is attached with line charge $-m$.

In the future, we would like to study the nature of the gapless boundary states. It is also interesting to see whether other knot invariants can be derived from the wavefunction amplitude for other 1-SPT's.

LT thanks Yuan-Ming Lu and Juven Wang for helpful discussions. LT is supported by the Croucher Fellowship for Postdoctoral Research. XGW is partially supported by NSF Grant No. DMS-1664412 and by the Simons Collaboration on Ultra-Quantum Matter, which is a grant from the Simons Foundation (651440)

Appendix A: Space-time complex, cochains, and cocycles

In this paper, we consider models defined on a space-time lattice. A spacetime lattice is a triangulation of the D -dimensional spacetime M^D , which is denoted by \mathcal{M}^D . We will also call the triangulation \mathcal{M}^D as a space-time complex, which is formed by simplices – the vertices, links, triangles, *etc.* We will use i, j, \dots to label vertices of the spacetime complex. The links of the complex (the 1-simplices) will be labeled by $(i, j), (j, k), \dots$. Similarly, the triangles of the complex (the 2-simplices) will be labeled by $(i, j, k), (j, k, l), \dots$.

In order to define a generic lattice theory on the space-time complex \mathcal{M}^D using local Lagrangian term on each simplex, it is important to give the vertices of each simplex a local order. A nice local scheme to order the vertices is given by a branching structure.^{5,48,49} A branching structure is a choice of orientation of each link in the d -dimensional complex so that there is no oriented loop on any triangle (see Fig. 10).

The branching structure induces a *local order* of the vertices on each simplex. The first vertex of a simplex is the vertex with no incoming links, and the second vertex is the vertex with only one incoming link, *etc.* So the simplex in Fig. 10a has the following vertex ordering: 0, 1, 2, 3.

The branching structure also gives the simplex (and its sub-simplices) a canonical orientation. Fig. 10 illustrates two 3-simplices with opposite canonical orientations compared with the 3-dimension space in which they are embedded. The blue arrows indicate the canonical orientations of the 2-simplices. The black arrows indicate the

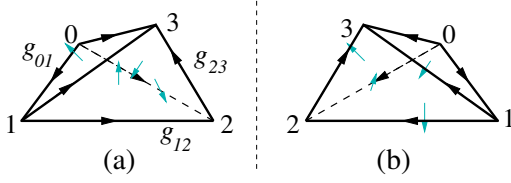


FIG. 10. (Color online) Two branched simplices with opposite orientations. (a) A branched simplex with positive orientation and (b) a branched simplex with negative orientation.

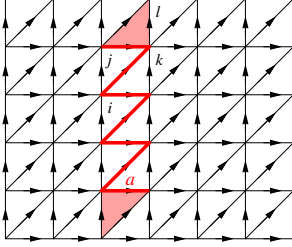


FIG. 11. (Color online) A 1-cochain a has a value 1 on the red links: $a_{ik} = a_{jk} = 1$ and a value 0 on other links: $a_{ij} = a_{kl} = 0$. da is non-zero on the shaded triangles: $(da)_{jkl} = a_{jk} + a_{kl} - a_{jl}$. For such 1-cochain, we also have $a \smile a = 0$. So when viewed as a \mathbb{Z}_2 -valued cochain, $\beta_2 a \neq a \smile a \pmod{2}$.

canonical orientations of the 1-simplices.

Given an Abelian group $(\mathbb{M}, +)$, an n -cochain f_n is an assignment of values in \mathbb{M} to each n -simplex, for example a value $f_{n;i,j,\dots,k} \in \mathbb{M}$ is assigned to n -simplex (i, j, \dots, k) . So a cochain f_n can be viewed as a bosonic field on the spacetime lattice.

\mathbb{M} can also be viewed a \mathbb{Z} -module (*i.e.* a vector space with integer coefficient) that also allows scaling by an integer:

$$\begin{aligned} x + y = z, \quad x * y = z, \quad mx = y, \\ x, y, z \in \mathbb{M}, \quad m \in \mathbb{Z}. \end{aligned} \quad (\text{A1})$$

The direct sum of two modules $\mathbb{M}_1 \oplus \mathbb{M}_2$ (as vector spaces) is equal to the direct product of the two modules (as sets):

$$\mathbb{M}_1 \oplus \mathbb{M}_2 \stackrel{\text{as set}}{=} \mathbb{M}_1 \times \mathbb{M}_2 \quad (\text{A2})$$

We like to remark that a simplex (i, j, \dots, k) can have two different orientations. We can use (i, j, \dots, k) and $(j, i, \dots, k) = -(i, j, \dots, k)$ to denote the same simplex with opposite orientations. The value $f_{n;i,j,\dots,k}$ assigned to the simplex with opposite orientations should differ by a sign: $f_{n;i,j,\dots,k} = -f_{n;j,i,\dots,k}$. So to be more precise f_n is a linear map $f_n : n\text{-simplex} \rightarrow \mathbb{M}$. We can denote the linear map as $\langle f_n, n\text{-simplex} \rangle$, or

$$\langle f_n, (i, j, \dots, k) \rangle = f_{n;i,j,\dots,k} \in \mathbb{M}. \quad (\text{A3})$$

More generally, a cochain f_n is a linear map of n -chains:

$$f_n : n\text{-chains} \rightarrow \mathbb{M}, \quad (\text{A4})$$

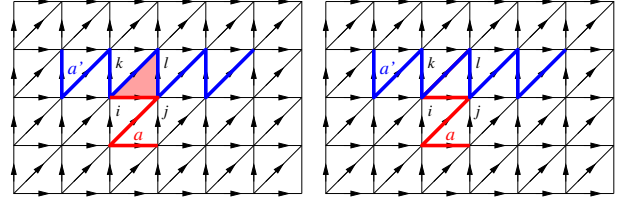


FIG. 12. (Color online) A 1-cochain a has a value 1 on the red links, Another 1-cochain a' has a value 1 on the blue links. On the left, $a \smile a'$ is non-zero on the shade triangles: $(a \smile a')_{ijl} = a_{ij}a'_{jl} = 1$. On the right, $a' \smile a$ is zero on every triangle. Thus $a \smile a' + a' \smile a$ is not a coboundary.

or (see Fig. 11)

$$\langle f_n, n\text{-chain} \rangle \in \mathbb{M}, \quad (\text{A5})$$

where a *chain* is a composition of simplices. For example, a 2-chain can be a 2-simplex: (i, j, k) , a sum of two 2-simplices: $(i, j, k) + (j, k, l)$, a more general composition of 2-simplices: $(i, j, k) - 2(j, k, l)$, etc. The map f_n is linear respect to such a composition. For example, if a chain is m copies of a simplex, then its assigned value will be m times that of the simplex. $m = -1$ correspond to an opposite orientation.

We will use $C^n(\mathcal{M}^D; \mathbb{M})$ to denote the set of all n -cochains on \mathcal{M}^D . $C^n(\mathcal{M}^D; \mathbb{M})$ can also be viewed as a set all \mathbb{M} -valued fields (or paths) on \mathcal{M}^D . Note that $C^n(\mathcal{M}^D; \mathbb{M})$ is an Abelian group under the $+$ -operation.

The total spacetime lattice \mathcal{M}^D correspond to a D -chain. We will use the same \mathcal{M}^D to denote it. Viewing f_D as a linear map of D -chains, we can define an “integral” over \mathcal{M}^D :

$$\begin{aligned} \int_{\mathcal{M}^D} f_D &\equiv \langle f_D, \mathcal{M}^D \rangle \\ &= \sum_{(i_0, i_1, \dots, i_D)} s_{i_0 i_1 \dots i_D} (f_D)_{i_0, i_1, \dots, i_D}. \end{aligned} \quad (\text{A6})$$

Here $s_{i_0 i_1 \dots i_D} = \pm 1$, such that a D -simplex in the D -chain \mathcal{M}^D is given by $s_{i_0 i_1 \dots i_D} (i_0, i_1, \dots, i_D)$.

We can define a derivative operator d acting on an n -cochain f_n , which give us an $(n+1)$ -cochain (see Fig. 11):

$$\begin{aligned} \langle df_n, (i_0 i_1 i_2 \dots i_{n+1}) \rangle \\ = \sum_{m=0}^{n+1} (-)^m \langle f_n, (i_0 i_1 i_2 \dots \hat{i}_m \dots i_{n+1}) \rangle \end{aligned} \quad (\text{A7})$$

where $i_0 i_1 i_2 \dots \hat{i}_m \dots i_{n+1}$ is the sequence $i_0 i_1 i_2 \dots i_{n+1}$ with i_m removed, and $i_0, i_1, i_2 \dots i_{n+1}$ are the ordered vertices of the $(n+1)$ -simplex $(i_0 i_1 i_2 \dots i_{n+1})$.

A cochain $f_n \in C^n(\mathcal{M}^D; \mathbb{M})$ is called a *cocycle* if $df_n = 0$. The set of cocycles is denoted by $Z^n(\mathcal{M}^D; \mathbb{M})$. A cochain f_n is called a *coboundary* if there exist a cochain f_{n-1} such that $df_{n-1} = f_n$. The set of coboundaries is denoted by $B^n(\mathcal{M}^D; \mathbb{M})$. Both $Z^n(\mathcal{M}^D; \mathbb{M})$ and

$B^n(\mathcal{M}^D; \mathbb{M})$ are Abelian groups as well. Since $d^2 = 0$, a coboundary is always a cocycle: $B^n(\mathcal{M}^D; \mathbb{M}) \subset Z^n(\mathcal{M}^D; \mathbb{M})$. We may view two cocycles differ by a coboundary as equivalent. The equivalence classes of cocycles, $[f_n]$, form the so called cohomology group denoted by

$$H^n(\mathcal{M}^D; \mathbb{M}) = Z^n(\mathcal{M}^D; \mathbb{M})/B^n(\mathcal{M}^D; \mathbb{M}), \quad (\text{A8})$$

$H^n(\mathcal{M}^D; \mathbb{M})$, as a group quotient of $Z^n(\mathcal{M}^D; \mathbb{M})$ by $B^n(\mathcal{M}^D; \mathbb{M})$, is also an Abelian group.

For the \mathbb{Z}_N -valued cocycle x_n , $dx_n \stackrel{N}{=} 0$. Thus

$$\beta_N x_n \equiv \frac{1}{N} dx_n \quad (\text{A9})$$

is a \mathbb{Z} -valued cocycle. Here β_N is Bockstein homomorphism.

We notice the above definition for cochains still makes sense if we have a non-Abelian group (G, \cdot) instead of an Abelian group $(\mathbb{M}, +)$, however the differential d defined by eqn. (A7) will not satisfy $d \circ d = 1$, except for the first two d 's. That is, one may still make sense of 0-cocycle and 1-cocycle, but no more further naively by formula eqn. (A7). For us, we only use non-Abelian 1-cocycle in this article. Thus it is ok. Non-Abelian cohomology is then thoroughly studied in mathematics motivating concepts such as gerbes to enter.

From two cochains f_m and h_n , we can construct a third cochain p_{m+n} via the cup product (see Fig. 12):

$$\begin{aligned} p_{m+n} &= f_m \smile_k h_n, \\ \langle p_{m+n}, (0 \rightarrow m+n) \rangle &= \langle f_m, (0 \rightarrow m) \rangle \times \\ &\quad \langle h_n, (m \rightarrow m+n) \rangle, \end{aligned} \quad (\text{A10})$$

where $i \rightarrow j$ is the consecutive sequence from i to j :

$$i \rightarrow j \equiv i, i+1, \dots, j-1, j. \quad (\text{A11})$$

Note that the above definition applies to cochains with global.

The cup product has the following property

$$d(h_n \smile_k f_m) = (dh_n) \smile_k f_m + (-)^n h_n \smile_k (df_m) \quad (\text{A12})$$

for cochains with global or local values. We see that $h_n \smile_k f_m$ is a cocycle if both f_m and h_n are cocycles. If both f_m and h_n are cocycles, then $f_m \smile_k h_n$ is a coboundary if one of f_m and h_n is a coboundary. So the cup product is also an operation on cohomology groups $\smile: H^m(M^D; \mathbb{M}) \times H^n(M^D; \mathbb{M}) \rightarrow H^{m+n}(M^D; \mathbb{M})$. The cup product of two cocycles has the following property (see Fig. 12)

$$f_m \smile_k h_n = (-)^{mn} h_n \smile_k f_m + \text{coboundary} \quad (\text{A13})$$

We can also define higher cup product $f_m \smile_k h_n$ which gives rise to a $(m+n-k)$ -cochain⁵⁰:

$$\langle f_m \smile_k h_n, (0, 1, \dots, m+n-k) \rangle$$

$$\begin{aligned} &= \sum_{0 \leq i_0 < \dots < i_k \leq m+n-k} (-)^p \langle f_m, (0 \rightarrow i_0, i_1 \rightarrow i_2, \dots) \rangle \times \\ &\quad \langle h_n, (i_0 \rightarrow i_1, i_2 \rightarrow i_3, \dots) \rangle, \end{aligned} \quad (\text{A14})$$

and $f_m \smile_k h_n = 0$ for $k < 0$ or for $k > m$ or n . Here $i \rightarrow j$ is the sequence $i, i+1, \dots, j-1, j$, and p is the number of permutations to bring the sequence

$$0 \rightarrow i_0, i_1 \rightarrow i_2, \dots; i_0+1 \rightarrow i_1-1, i_2+1 \rightarrow i_3-1, \dots \quad (\text{A15})$$

to the sequence

$$0 \rightarrow m+n-k. \quad (\text{A16})$$

For example

$$\begin{aligned} \langle f_m \smile_1 h_n, (0 \rightarrow m+n-1) \rangle &= \sum_{i=0}^{m-1} (-)^{(m-i)(n+1)} \times \\ \langle f_m, (0 \rightarrow i, i+n \rightarrow m+n-1) \rangle &\langle h_n, (i \rightarrow i+n) \rangle. \end{aligned} \quad (\text{A17})$$

We can see that $\smile_0 = \smile$. Unlike cup product at $k=0$, the higher cup product of two cocycles may not be a cocycle. For cochains f_m, h_n , we have

$$\begin{aligned} d(f_m \smile_k h_n) &= df_m \smile_k h_n + (-)^m f_m \smile_k dh_n + \\ &(-)^{m+n-k} f_m \smile_{k-1} h_n + (-)^{mn+m+n} h_n \smile_{k-1} f_m \end{aligned} \quad (\text{A18})$$

Let f_m and h_n be cocycles and c_l be a chain, from eqn. (A18) we can obtain

$$\begin{aligned} d(f_m \smile_k h_n) &= (-)^{m+n-k} f_m \smile_{k-1} h_n \\ &+ (-)^{mn+m+n} h_n \smile_{k-1} f_m, \\ d(f_m \smile_k f_m) &= [(-)^k + (-)^m] f_m \smile_{k-1} f_m, \\ d(c_l \smile_{k-1} c_l + c_l \smile_k dc_l) &= dc_l \smile_k dc_l \\ &- [(-)^k - (-)^l] (c_l \smile_{k-2} c_l + c_l \smile_{k-1} dc_l). \end{aligned} \quad (\text{A19})$$

From eqn. (A19), we see that, for \mathbb{Z}_2 -valued cocycles z_n ,

$$\text{Sq}^{n-k}(z_n) \equiv z_n \smile_k z_n \quad (\text{A20})$$

is always a cocycle. Here Sq is called the Steenrod square. More generally $h_n \smile_k h_n$ is a cocycle if $n+k = \text{odd}$ and h_n is a cocycle. Usually, the Steenrod square is defined only for \mathbb{Z}_2 -valued cocycles or cohomology classes. Here, we like to define a generalized Steenrod square for \mathbb{M} -valued cochains c_n :

$$\text{Sq}^{n-k} c_n \equiv c_n \smile_k c_n + c_n \smile_{k+1} dc_n. \quad (\text{A21})$$

From eqn. (A19), we see that

$$d\text{Sq}^k c_n = d(c_n \smile_{n-k} c_n + c_n \smile_{n-k+1} dc_n) \quad (\text{A22})$$

$$= \mathbb{S}q^k dc_n + (-)^n \begin{cases} 0, & k = \text{odd} \\ 2\mathbb{S}q^{k+1}c_n & k = \text{even} \end{cases}.$$

In particular, when c_n is a \mathbb{Z}_2 -valued cochain, we have

$$d\mathbb{S}q^k c_n \stackrel{\cong}{=} \mathbb{S}q^k dc_n. \quad (\text{A23})$$

Next, let us consider the action of $\mathbb{S}q^k$ on the sum of two \mathbb{M} -valued cochains c_n and c'_n :

$$\begin{aligned} \mathbb{S}q^k(c_n + c'_n) &= \mathbb{S}q^k c_n + \mathbb{S}q^k c'_n + \\ & c_n \smile_{n-k} c'_n + c'_n \smile_{n-k} c_n + c_n \smile_{n-k+1} dc'_n + c'_n \smile_{n-k+1} dc_n \\ &= \mathbb{S}q^k c_n + \mathbb{S}q^k c'_n + [1 + (-)^k] c_n \smile_{n-k} c'_n \\ & - (-)^{n-k} [(-)^{n-k} c'_n \smile_{n-k} c_n + (-)^n c_n \smile_{n-k} c'_n] \\ & + c_n \smile_{n-k+1} dc'_n + c'_n \smile_{n-k+1} dc_n \end{aligned} \quad (\text{A24})$$

Notice that (see eqn. (A18))

$$\begin{aligned} & - (-)^{n-k} c'_n \smile_{n-k} c_n + (-)^n c_n \smile_{n-k} c'_n \\ &= d(c'_n \smile_{n-k+1} c_n) - dc'_n \smile_{n-k+1} c_n - (-)^n c'_n \smile_{n-k+1} dc_n, \end{aligned} \quad (\text{A25})$$

we see that

$$\begin{aligned} \mathbb{S}q^k(c_n + c'_n) &= \mathbb{S}q^k c_n + \mathbb{S}q^k c'_n + [1 + (-)^k] c_n \smile_{n-k} c'_n \\ & + (-)^{n-k} [dc'_n \smile_{n-k+1} c_n + (-)^n c'_n \smile_{n-k+1} dc_n] \\ & - (-)^{n-k} d(c'_n \smile_{n-k+1} c_n) + c_n \smile_{n-k+1} dc'_n + c'_n \smile_{n-k+1} dc_n \\ &= \mathbb{S}q^k c_n + \mathbb{S}q^k c'_n + [1 + (-)^k] c_n \smile_{n-k} c'_n \\ & + [1 + (-)^k] c'_n \smile_{n-k+1} dc_n - (-)^{n-k} d(c'_n \smile_{n-k+1} c_n) \\ & - [(-)^{n-k+1} dc'_n \smile_{n-k+1} c_n - c_n \smile_{n-k+1} dc'_n]. \end{aligned} \quad (\text{A26})$$

Notice that (see eqn. (A18))

$$\begin{aligned} & (-)^{n-k+1} dc'_n \smile_{n-k+1} c_n - c_n \smile_{n-k+1} dc'_n \\ &= d(dc'_n \smile_{n-k+2} c_n) + (-)^n dc'_n \smile_{n-k+2} dc_n, \end{aligned} \quad (\text{A27})$$

we find

$$\begin{aligned} \mathbb{S}q^k(c_n + c'_n) &= \mathbb{S}q^k c_n + \mathbb{S}q^k c'_n + [1 + (-)^k] c_n \smile_{n-k} c'_n \\ & + [1 + (-)^k] c'_n \smile_{n-k+1} dc_n - (-)^{n-k} d(c'_n \smile_{n-k+1} c_n) \\ & - d(dc'_n \smile_{n-k+2} c_n) - (-)^n dc'_n \smile_{n-k+2} dc_n \\ &= \mathbb{S}q^k c_n + \mathbb{S}q^k c'_n - (-)^n dc'_n \smile_{n-k+2} dc_n \\ & + [1 + (-)^k] [c_n \smile_{n-k} c'_n + c'_n \smile_{n-k+1} dc_n] \\ & - (-)^{n-k} d(c'_n \smile_{n-k+1} c_n) - d(dc'_n \smile_{n-k+2} c_n). \end{aligned} \quad (\text{A28})$$

We see that, if one of the c_n and c'_n is a cocycle,

$$\mathbb{S}q^k(c_n + c'_n) \stackrel{2, d}{=} \mathbb{S}q^k c_n + \mathbb{S}q^k c'_n. \quad (\text{A29})$$

We also see that

$$\begin{aligned} & \mathbb{S}q^k(c_n + df_{n-1}) \\ &= \mathbb{S}q^k c_n + \mathbb{S}q^k df_{n-1} + [1 + (-)^k] df_{n-1} \smile_{n-k} c_n \\ & - (-)^{n-k} d(c_n \smile_{n-k+1} df_{n-1}) - d(dc_n \smile_{n-k+2} df_{n-1}) \\ &= \mathbb{S}q^k c_n + [1 + (-)^k] [df_{n-1} \smile_{n-k} c_n + (-)^n \mathbb{S}q^{k+1} f_{n-1}] \\ & + d[\mathbb{S}q^k f_{n-1} - (-)^{n-k} c_n \smile_{n-k+1} df_{n-1} - dc_n \smile_{n-k+2} df_{n-1}]. \end{aligned} \quad (\text{A30})$$

Using eqn. (A28), we can also obtain the following result if dc_n is even

$$\begin{aligned} & \mathbb{S}q^k(c_n + 2c'_n) \\ & \stackrel{4}{=} \mathbb{S}q^k c_n + 2d(c_n \smile_{n-k+1} c'_n) + 2dc_n \smile_{n-k+1} c'_n \\ & \stackrel{4}{=} \mathbb{S}q^k c_n + 2d(c_n \smile_{n-k+1} c'_n) \end{aligned} \quad (\text{A31})$$

As another application, we note that, for a \mathbb{Q} -valued cochain m_d and using eqn. (A18),

$$\begin{aligned} \mathbb{S}q^1(m_d) &= m_d \smile_{d-1} m_d + m_d \smile_d dm_d \\ &= \frac{1}{2} (-)^d [d(m_d \smile_d m_d) - dm_d \smile_d m_d] + \frac{1}{2} m_d \smile_d dm_d \\ &= (-)^d \beta_2(m_d \smile_d m_d) - (-)^d \beta_2 m_d \smile_d m_d + m_d \smile_d \beta_2 m_d \\ &= (-)^d \beta_2 \mathbb{S}q^0 m_d - 2(-)^d \beta_2 m_d \smile_{d+1} \beta_2 m_d \\ &= (-)^d \beta_2 \mathbb{S}q^0 m_d - 2(-)^d \mathbb{S}q^0 \beta_2 m_d \end{aligned} \quad (\text{A32})$$

This way, we obtain a relation between Steenrod square and Bockstein homomorphism, when m_d is a \mathbb{Z}_2 -valued cochain

$$\mathbb{S}q^1(m_d) \stackrel{2}{=} \beta_2 m_d, \quad (\text{A33})$$

where we have used $\mathbb{S}q^0 m_d = m_d$ for \mathbb{Z}_2 -valued cochain.

For a k -cochain a_k , $k = \text{odd}$, we find that

$$\begin{aligned} & \mathbb{S}q^k a_k = a_k a_k + a_k \smile_1 da_k \\ &= \frac{1}{2} [da_k \smile_1 a_k - a_k \smile_1 da_k - d(a_k \smile_1 a_k)] + a_k \smile_1 da_k \\ &= \frac{1}{2} [da_k \smile_2 da_k - d(da_k \smile_2 a_k)] - \frac{1}{2} d(a_k \smile_1 a_k) \\ &= \frac{1}{4} d(da_k \smile_3 da_k) - \frac{1}{2} d(a_k \smile_1 a_k + da_k \smile_2 a_k) \end{aligned} \quad (\text{A34})$$

Thus $\mathbb{S}q^k a_k$ is always a \mathbb{Q} -valued coboundary, when k is odd.

Appendix B: Procedure for deriving Hamiltonian from topological partition function

We briefly review the procedure for writing down local commuting projection Hamiltonians from the topological action. The reader may refer to Ref. ^{5,51} for details.

1. Zero background gauge field case

Suppose $\mathcal{M}^4 = \mathcal{M}^3 \times I$ for some closed 3-manifold \mathcal{M}^3 and I is an interval parameterized by $t \in [0, T]$, to be regarded as the time direction. The space-time has boundaries at $t = 0, T$, where the field configurations are given by $\{a_0\}$ and $\{a_T\}$. The transfer matrix is given by

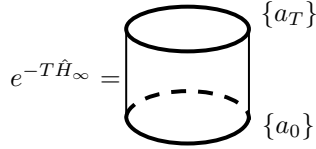
$$\langle \{a_T\} | e^{-T\hat{H}^\infty} | \{a_0\} \rangle = Z^{\text{top}}[\{a_T\}, \{a_0\}] \quad (\text{B1})$$

$$Z_{\mathcal{M}^3 \times I}^{\text{top}}[\{a_T\}, \{a_0\}] \quad (\text{B2})$$

$$= \frac{1}{n^{N_{l,int} + (N_{l,0} + N_{l,T})/2}} \sum_{\{a_{int}\}} e^{2\pi i \int_{\mathcal{M}^3 \times I} \omega_4}, \quad (\text{B3})$$

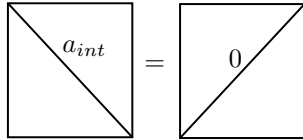
where $\int_{\mathcal{M}^3 \times I} \omega_4$ is evaluated with link configurations at its boundaries fixed to be $\{a_0\}, \{a_T\}$. Links not living on the boundary are called internal links. Their configuration is given by $\{a_{int}\}$. $N_{l,0}, N_{l,T}$ and $N_{l,int}$ are the number of links at the two boundaries and in the space-time bulk respectively. In the following we assume the two boundaries have the same triangulation so $N_{l,0} = N_{l,T} = N_{l,\mathcal{M}^3}$.

We may represent the transfer matrix diagrammatically as a spacetime cylinder



where the top and bottom ellipses represent the spatial closed manifold \mathcal{M}^3 at $t = T, 0$ respectively. They are the boundaries of the space-time cylinder and are drawn as bold lines. Note that although \mathcal{M}^3 is a three-dimensional manifold, we draw it as a one-dimensional ellipse.

Recall from Ref.^{5,51} that under a local spacetime re-triangulation, the topological action $\int_{\mathcal{M}^4} \omega_4$ changes by $d\omega_4$. Hence the cocycle condition $d\omega_4 \stackrel{\pm}{=} 0$ implies the action is invariant under re-triangulation mod 1. Moreover, during a re-triangulation, the boundary degrees of freedom cannot change, thus we can only conclude that the value of $\int_{\mathcal{M}^3 \times I} \omega_4$ is independent of triangulations of the internal bulk, but it could depend on the boundary triangulation. Furthermore, $\int_{\mathcal{M}^3 \times I} \omega_4$ is independent of the values of a_{int} . This is because during a re-triangulation, the internal link values are forgotten, which can be illustrated with the re-triangulation of a square:

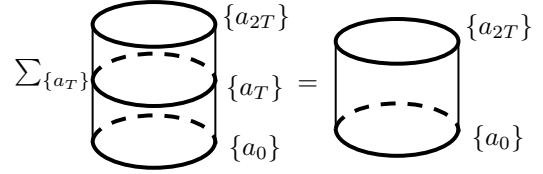


Thus $Z^{\text{top}}[\{a_T\}, \{a_0\}]$ is independent of both the triangulation and field configuration of the internal bulk and only depends on the configuration at its boundaries.

We can show that the transfer matrix is a projection with a computation:

$$\begin{aligned} & \langle \{a_{2T}\} | e^{-T\hat{H}^\infty} e^{-T\hat{H}^\infty} | \{a_0\} \rangle \\ &= \sum_{\{a_T\}} Z^{\text{top}}[\{a_{2T}\}, \{a_T\}] Z^{\text{top}}[\{a_T\}, \{a_0\}] \\ &= \sum_{\{a_T, a_{int}\}} \frac{1}{n^{N_{l,int} + 2N_{l,\mathcal{M}^3}}} e^{2\pi i (\int_{\mathcal{M}^3 \times [0, T]} \omega_4 + \int_{\mathcal{M}^3 \times [T, 2T]} \omega_4)} \\ &= \sum_{\{a_T, a_{int}\}} \frac{1}{n^{N_{l,int} + 2N_{l,\mathcal{M}^3}}} e^{2\pi i \int_{\mathcal{M}^3 \times [0, 2T]} \omega_4} \\ &= \frac{1}{n^{N_{l,int'} + N_{l,\mathcal{M}^3}}} \sum_{\{a_{int'}\}} e^{2\pi i \int_{\mathcal{M}^3 \times [0, 2T]} \omega_4} \\ &= \langle \{a_{2T}\} | e^{-T\hat{H}^\infty} | \{a_0\} \rangle \end{aligned}$$

where the label int includes all the links not on the slices $t = 0, T, 2T$ and the label int' includes all the links not on the slices $t = 0, 2T$. This computation can be expressed diagrammatically as

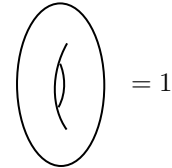


Since the eigenvalues of a projection is 1 or 0, correspondingly \hat{H}_∞ has eigenvalues 0 or ∞ , *i.e.* an infinite energy gap.

Moreover, the transfer matrix has trace 1. This is because $\text{Tr}[e^{-T\hat{H}_\infty}]$ is evaluated by identifying the top and bottom link configurations of the cylinder and summing over them. With the two ends identified, $\mathcal{M}^3 \times I = \mathcal{M}^3 \times S^1$ becomes a closed manifold. As we showed in (22), on a closed manifold without any background gauge fields, $\int_{\mathcal{M}^4} \omega_4 \stackrel{\pm}{=} 0$. Thus we have

$$\text{Tr}[e^{-T\hat{H}_\infty}] = \frac{1}{n^{N_{l,int} + N_{l,\mathcal{M}^3}}} \sum_{\{a_{int}, a_0\}} 1 = 1 \quad (\text{B4})$$

Diagrammatically, this is expressed as



hence the ground state of \hat{H}_∞ is unique.

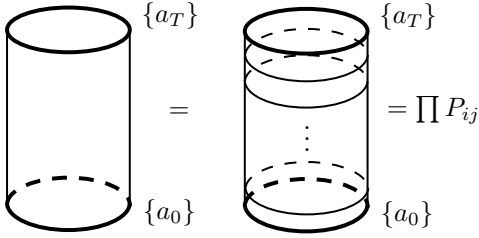
Although the transfer matrix is a non-local operator, it can be decomposed into a product of local operators. Suppose we evaluate $\int_{\mathcal{M}^3 \times I} \omega_4$ with a triangulation of the internal space-time, such that it consists of $N_{l,\mathcal{M}^3} + 1$ infinitesimal spatial slices, each slice having the same triangulation of the spatial slices at $t = 0, T$. Between

two adjacent slices, only a single link ij is updated from $a_{0,ij}$ to $a_{T,ij}$, while all other links remains the same. We have

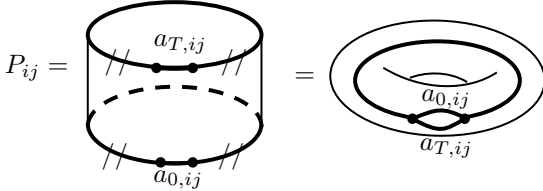
$$e^{-T\hat{H}^\infty} = \prod_{ij} P_{ij} \quad (\text{B5})$$

$$\langle \{a_T\} | P_{ij} | \{a_0\} \rangle = n^{N_{l, \mathcal{M}^3} - 1} \prod_{i'j' \neq ij} \delta_{a_{0,i'j'}, a_{T,i'j'}} \times Z_{\mathcal{M}^3 \times I}^{\text{top}}[\{a_T\}, \{a_0\}], \quad (\text{B6})$$

In diagrams, this means



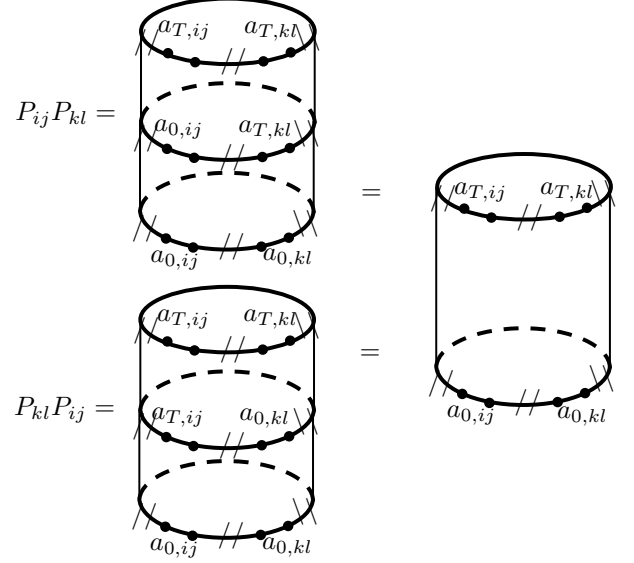
In (B6), it is not very clear that P_{ij} is a local operator. The locality of P_{ij} can be seen by examining the diagrammatic expression for P_{ij} ,



where double slash indicates the region in which field configurations on the top needs to be identified with that on the bottom. On the right hand side we see that P_{ij} is associated with $\mathcal{M}^3 \times S^1$ with a slit at the link ij . This means that in \mathcal{M}^3 , the links far away from ij become internal links in the non-zero matrix elements of P_{ij} , and hence the non-zero matrix elements of P_{ij} are independent of the value of links far away from ij . Thus P_{ij} is a local operator.

Using the same arguments as before, it can be shown that P_{ij} is a projection operator with trace $n^{N_{l, \mathcal{M}^3} - 1}$. So each projection by P_{ij} reduces the dimension of the ground state Hilbert space by a factor of n . Furthermore, in the following we will show that any two such operators P_{ij} , P_{kl} commute. The two orderings $P_{ij}P_{kl}$ or $P_{kl}P_{ij}$

corresponds to triangulations shown below



It is readily seen that the two diagrams only differs for the internal links. Thus $P_{ij}P_{kl} = P_{kl}P_{ij}$.

We note that the computation for P_{ij} can be further simplified by setting $a_{int} = 0$.

$$\langle \{a_T\} | P_{ij} | \{a_0\} \rangle = \prod_{i'j' \neq ij} \delta_{a_{0,i'j'}, a_{T,i'j'}} \frac{1}{n} e^{2\pi i \int_{\mathcal{M}^3 \times I} \omega_4} \Big|_{a_{int}=0} \quad (\text{B7})$$

The ground state of \hat{H}^∞ satisfies $P_{ij}|\psi_0\rangle = |\psi_0\rangle$. We can construct a Hamiltonian with finite gap but the same ground state as \hat{H}^∞ by defining

$$\hat{H} = - \sum_{ij} P_{ij}. \quad (\text{B8})$$

2. Non-zero background gauge field case

Suppose we are given a background gauge field on the spatial manifold \mathcal{M}^3 . In order to define the transfer matrix, we need to specify the background gauge field \hat{B} on the spacetime $\mathcal{M}^3 \times I$. We propose that \hat{B} should be *static*, meaning that it should be invariant under time translation, *i.e.* \hat{B} is the same on every spatial slice. This is sensible because a non-static background gauge field actually correspond to the insertion of a 1-symmetry operator into the transfer matrix.

Such static background gauge field \hat{B} on $\mathcal{M}^3 \times I$ can be constructed from a given flat \hat{B} on \mathcal{M}^3 as follows. We triangulate $\mathcal{M} \times I$ such that any 2-cell (ijk) in $\mathcal{M}^3 \times I$, when projected onto \mathcal{M}^3 , is either also a 2-cell $(i_0j_0k_0)$ in \mathcal{M}^3 , or a lower dimensional cell. Then we define

$$\langle \hat{B}, (ijk) \rangle := \begin{cases} \langle \hat{B}, (i_0j_0k_0) \rangle & \text{if } (ijk) \text{ projects to a 2-cell} \\ 0 & \text{else} \end{cases}$$

it can be checked $\hat{B} = 0$.

We then construct the transfer matrix with such static background gauge field. Diagrammatically, the transfer matrix is represented as follows:

$$e^{-T\hat{H}_\infty[\hat{B}]} = \text{Cylinder}(\{a_T\}, \{a_0\})$$

where the wiggly vertical line represents the static \hat{B} . We may repeat the same analysis as in the previous subsection, except that we include a wiggly vertical line in the diagrams. For example, in showing the transfer matrix is a projection, we have

$$\sum_{\{a_T\}} \text{Cylinder}(\{a_{2T}\}, \{a_0\}) = \text{Cylinder}(\{a_{2T}\}, \{a_0\})$$

We need to be slightly careful about generalizing the argument that trace of transfer matrix is 1. Recall from the previous section at (B4), we used the fact that on a closed manifold $\mathcal{M}^4 = \mathcal{M}^3 \times S^1$, we have

$$\int_{\mathcal{M}^4} \omega_4[da] \stackrel{\perp}{=} \int_{\mathcal{M}^4} \omega_4[0] = 0,$$

which is due to gauge invariance of the topological action (21). In the present case we have

$$\int_{\mathcal{M}^4} \omega_4[\hat{B} + da] \stackrel{\perp}{=} \int_{\mathcal{M}^4} \omega_4[\hat{B}]$$

To complete the argument, note that a ‘‘static’’ background gauge field on $\mathcal{M}^3 \times S^1$ may be extended into a higher dimensional manifold $\mathcal{M}^3 \times D^2$, where $\partial D^2 = S^1$ with the same construction as before.⁵² Thus

$$\begin{aligned} \int_{\mathcal{M}^4} \omega_4[\hat{B}] &= \int_{\partial(\mathcal{M}^3 \times D^2)} \omega_4[\hat{B}] \\ &= \int_{\mathcal{M}^3 \times D^2} d\omega_4[\hat{B}] \stackrel{\perp}{=} 0. \end{aligned} \quad (\text{B9})$$

using Stoke’s theorem and the cocycle condition.

Therefore we have

$$\text{Tr} \left(e^{-T\hat{H}_\infty[\hat{B}]} \right) = \text{Cylinder}(\text{hole}) = 1$$

and the ground state is unique.

All the arguments in the previous section will follow through for the present case. We can construct commuting projections $P_{ij}[\hat{B}]$ which differs from the zero-gauge

projections only when ij is near the non-zero \hat{B} . Its corresponding diagram is

$$P_{ij}[\hat{B}] = \text{Cylinder}(\text{hole}, \text{hole})$$

Appendix C: Ground state wavefunction

1. Zero background gauge field case

Suppose $\omega_4 = d\phi_3$ for some 3-cochain ϕ_3 (which may not have 1-symmetry, so this does not mean ω_4 is a coboundary with 1-symmetry), then ϕ_3 can be interpreted as the phase of a ground state wavefunction. Define $|\psi_0\rangle = \frac{1}{N_\psi} \sum_{\{a\}} e^{2\pi i \int_{\mathcal{M}^3} \phi_3[a]} |\{a\}\rangle$ with normalization $N_\psi = \sqrt{n^{N_i, \mathcal{M}^3}}$. Suppose the spatial manifold $\mathcal{M}^3 = \partial\mathcal{M}_0^4$ is the boundary of some manifold \mathcal{M}_0^4 (such \mathcal{M}_0^4 exists for any closed, oriented 3-manifold⁷). Then the amplitude is

$$\int_{\mathcal{M}^3} \phi_3[a] = \int_{\partial\mathcal{M}_0^4} \phi_3[a] = \int_{\mathcal{M}_0^4} d\phi_3[a] = \int_{\mathcal{M}_0^4} \omega_4[a].$$

So $|\psi_0\rangle$ may be represented diagrammatically as

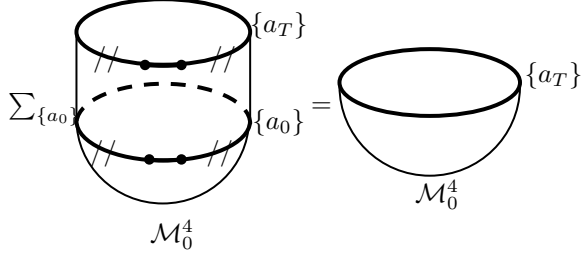
$$|\psi_0\rangle = \text{Bowl}(\mathcal{M}_0^4)$$

We check that $|\psi_0\rangle$ survives the P_{ij} projection:

$$\begin{aligned} \langle \{a_T\} | P_{ij} | \psi_0 \rangle &= \frac{1}{N_\psi n} \sum_{\{a_0\}} \prod_{i'j' \neq ij} \delta_{a_0, i'j', a_T, i'j'} e^{2\pi i [\int_{\mathcal{M}^3 \times I} \omega_4 + \int_{\mathcal{M}^3} \phi_3[a_0]]} \\ &= \frac{1}{N_\psi n} \sum_{\{a_0\}} \prod_{i'j' \neq ij} \delta_{a_0, i'j', a_T, i'j'} e^{2\pi i \int_{\mathcal{M}^3} \phi_3[a_T]} \\ &= \frac{1}{N_\psi} e^{2\pi i \int_{\mathcal{M}^3} \phi_3[a_T]} = \langle \{a_T\} | \psi_0 \rangle, \end{aligned} \quad (\text{C1})$$

where in the second step we used Stoke’s theorem $\int_{\mathcal{M}^3 \times I} \omega_4 = \int_{\mathcal{M}^3} \phi_3|_0^T$. The same result can also be de-

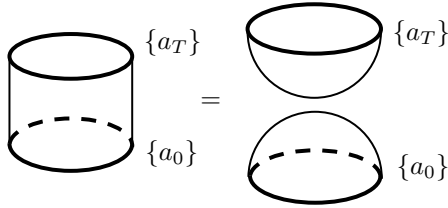
rived diagrammatically as follows:



Therefore, the transfer matrix is

$$e^{-T\hat{H}_\infty} = |\psi_0\rangle\langle\psi_0|,$$

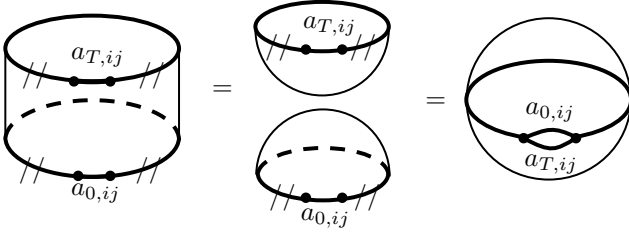
represented diagrammatically by



and the local projections P_{ij} can be expressed in terms of ϕ_3 as

$$\begin{aligned} & \langle\{a_T\}|P_{ij}|\{a_0\}\rangle \\ &= \prod_{i'j' \neq ij} \delta_{a_0, i'j', a_T, i'j'} \frac{1}{n} e^{2\pi i \int_{\mathcal{M}^3} (\phi_3[a_T] - \phi_3[a_0])} \quad (\text{C2}) \end{aligned}$$

which is



2. Non-zero background gauge field case

Suppose $\omega_4[\hat{B} + da] = \omega_4[\hat{B}] + d\phi_3[a, \hat{B}]$. While it is still true that $\mathcal{M}^3 = \partial\mathcal{M}_0^4$ for some manifold \mathcal{M}_0^4 , there may be obstructions in \mathcal{M}_0^4 that forbids the extension of the background gauge field into \mathcal{M}_0^4 , while respecting the flatness constraint $d\hat{B} = 0$.

So we will instead take $\mathcal{M}_0^4 = \mathcal{M}^3 \times I$, where $I = [-1, 0]$ is an interval. The boundary now have two components $\partial\mathcal{M}_0^4 = \mathcal{M}^3 \times \{0\} \amalg \mathcal{M}^3 \times \{-1\}$. We take the first component to be the original spatial manifold and extend the field configurations such that on the other end $\mathcal{M}^3 \times \{-1\}$, we fix $a = 0$. The background gauge field is extended to be “static” as in the previous section.

We define

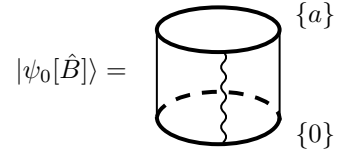
$$|\psi_0[\hat{B}]\rangle = \frac{1}{N_\psi} \sum_{\{a\}} e^{2\pi i \int_{\mathcal{M}^3} \phi_3[a, \hat{B}] - \phi_3[0, \hat{B}]} |\{a\}\rangle. \quad (\text{C3})$$

Thus we have

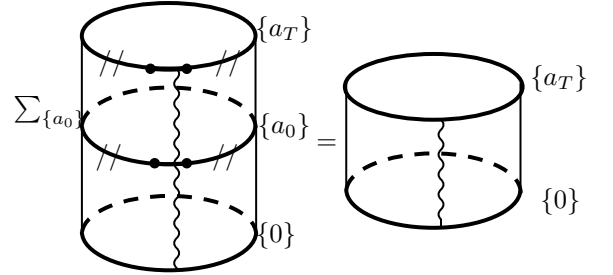
$$\begin{aligned} & \int_{\mathcal{M}^3} \phi_3[a, \hat{B}] - \phi_3[0, \hat{B}] = \int_{\partial\mathcal{M}_0^4} \phi_3[a, \hat{B}] \\ &= \int_{\mathcal{M}_0^4} d\phi_3[a, \hat{B}] = \int_{\mathcal{M}_0^4} \omega_4[\hat{B} + da] - \int_{\mathcal{M}_0^4} \omega_4[\hat{B}] \\ &= \int_{\mathcal{M}_0^4} \omega_4[\hat{B} + da]. \end{aligned}$$

where in the last step the term $\int_{\mathcal{M}_0^4} \omega_4[\hat{B}] \stackrel{\perp}{=} 0$ because its field configuration at $\mathcal{M}^3 \times \{0\}$ and $\mathcal{M}^3 \times \{-1\}$ are the same and the two ends can be glued together to form a closed manifold. The same arguments used in (B9) can be applied.

In diagram, this means



and it is the ground state for the projections $P_{ij}[\hat{B}]$:



and the matrix elements of $P_{ij}[\hat{B}]$ can be expressed in terms of $\phi_3[a, \hat{B}]$:

$$\begin{aligned} & \langle\{a_T\}|P_{ij}[\hat{B}]|\{a_0\}\rangle \\ &= \prod_{i'j' \neq ij} \delta_{a_0, i'j', a_T, i'j'} \frac{1}{n} e^{2\pi i \int_{\mathcal{M}^3} (\phi_3[a_T, \hat{B}] - \phi_3[a_0, \hat{B}])} \quad (\text{C4}) \end{aligned}$$

Appendix D: Triangulation of hypercubic lattice

\mathbb{R}^d may be triangulated by first admitting a hypercubic lattice, and triangulating each hypercube $I^d = \{(x_1, \dots, x_d) : 1 \geq x_i \geq 0 \forall i\}$ into $d!$ simplices Δ_p labeled by p in the permutation group S_d :

$$\Delta_p = \{1 \geq x_{p(1)} \geq \dots \geq x_{p(d)} \geq 0\}.$$

The vertices and branching structure for each Δ_p are given by

$$\begin{aligned} \vec{0} &= (0, \dots, 0) \\ &\rightarrow \widehat{p(1)} \\ &\rightarrow \widehat{p(1)} + \widehat{p(2)} \\ &\dots \\ &\rightarrow \widehat{p(1)} + \dots + \widehat{p(d)} = (1, \dots, 1) = \vec{1}, \end{aligned}$$

where \hat{i} is the unit vector in the x_i direction. The orientation of Δ_p is given by $\sigma(p) = \epsilon^{p(1)\dots p(d)}$.

Appendix E: Evaluation of $\int_{I^4} (b^{\mathbb{Z}^n})^2$ in a hypercube

Let $b^{\mathbb{Z}^n}$ be a 2-cocycle. Under the triangulation in Appendix D for $d = 4$, we have

$$\begin{aligned} &\int_{I^4} (b^{\mathbb{Z}^n})^2 \\ &= \langle (b^{\mathbb{Z}^n})^2, \sum_p \sigma(p) \Delta(p) \rangle = \langle (b^{\mathbb{Z}^n})^2, \epsilon^{\mu\nu\rho\sigma} \Delta_{\{\mu\nu\rho\sigma\}} \rangle \\ &= \epsilon^{\mu\nu\rho\sigma} \langle b^{\mathbb{Z}^n}, (\vec{0}, \hat{\mu}, \hat{\mu} + \hat{\nu}) \rangle \langle b^{\mathbb{Z}^n}, (\hat{\mu} + \hat{\nu}, \hat{\mu} + \hat{\nu} + \hat{\rho}, \vec{1}) \rangle \\ &= \frac{1}{4} \epsilon^{\mu\nu\rho\sigma} \langle b^{\mathbb{Z}^n}, (\vec{0}, \hat{\mu}, \hat{\mu} + \hat{\nu}) - (\nu \leftrightarrow \mu) \rangle \\ &\times \langle b^{\mathbb{Z}^n}, (\hat{\mu} + \hat{\nu}, \hat{\mu} + \hat{\nu} + \hat{\rho}, \vec{1}) - (\rho \leftrightarrow \sigma) \rangle \\ &= \frac{1}{4} \epsilon^{\mu\nu\rho\sigma} F_{\mu\nu} \left(\frac{\hat{\mu}}{2} + \frac{\hat{\nu}}{2} \right) F_{\rho\sigma} \left(\hat{\mu} + \hat{\nu} + \frac{\hat{\rho}}{2} + \frac{\hat{\sigma}}{2} \right), \quad (\text{E1}) \end{aligned}$$

where

$$F_{\mu\nu}(\vec{r}) := \langle b^{\mathbb{Z}^n}, (\vec{0}, \hat{\mu}, \hat{\mu} + \hat{\nu})_{\vec{r} - \frac{\hat{\mu}}{2} - \frac{\hat{\nu}}{2}} - (\mu \leftrightarrow \nu) \rangle.$$

Appendix F: Evaluation of P_{ij} in the m =even case

In this section we follow the procedure described in Appendix B and write down the projections P_{ij} in the m =even case for the topological action (32) with $\mathcal{M}^3 = \mathbb{R}^3$. The matrix elements are given by (B7) and (30):

$$\begin{aligned} \langle \{a_T^{\mathbb{Z}^n}\} | P_{ij} | \{a_0^{\mathbb{Z}^n}\} \rangle &= \prod_{i'j' \neq ij} \delta_{a_{0,i'}^{\mathbb{Z}^n}, a_{T,i'}^{\mathbb{Z}^n}} \\ &\times \frac{1}{n} e^{2\pi i \int_{\mathbb{R}^3 \times I} \frac{m}{2n} \text{Sq}^2(da^{\mathbb{Z}^n})}, \end{aligned}$$

where

$$\begin{aligned} \int_{\mathbb{R}^3 \times I} \text{Sq}^2(da^{\mathbb{Z}^n}) &= \int_{\mathbb{R}^3 \times I} da^{\mathbb{Z}^n} da^{\mathbb{Z}^n} \\ &= \int_{\mathbb{R}^3 \times I} d(a^{\mathbb{Z}^n} da^{\mathbb{Z}^n}) = \int_{\mathbb{R}^3} a^{\mathbb{Z}^n} da^{\mathbb{Z}^n} \Big|_0^T = \delta \left(\int_{\mathbb{R}^3} a^{\mathbb{Z}^n} da^{\mathbb{Z}^n} \right) \\ &= \int_{\mathbb{R}^3} \delta a^{\mathbb{Z}^n} da^{\mathbb{Z}^n} + a^{\mathbb{Z}^n} d\delta a^{\mathbb{Z}^n} + \delta a^{\mathbb{Z}^n} d\delta a^{\mathbb{Z}^n} \end{aligned}$$

$$\stackrel{\text{d}}{=} \int_{\mathbb{R}^3} \delta a^{\mathbb{Z}^n} da^{\mathbb{Z}^n} + da^{\mathbb{Z}^n} \delta a^{\mathbb{Z}^n},$$

where we have defined $\delta(x) := x|_0^T$. In the last step we used integration by part and the fact that $\delta a^{\mathbb{Z}^n} d\delta a^{\mathbb{Z}^n} = 0$ because it is impossible for both factors of the cup product to be non-zero, since $\delta a^{\mathbb{Z}^n}$ is non-zero for only one link ij . So Using the triangulation of Appendix D for $D = 3$ space, we have

$$\begin{aligned} &\int_{\mathbb{R}^3} \delta a^{\mathbb{Z}^n} da^{\mathbb{Z}^n} + da^{\mathbb{Z}^n} \delta a^{\mathbb{Z}^n} \\ &= \sum_{\vec{n} \in \mathbb{Z}^3} \epsilon^{\alpha\beta\gamma} \langle \delta a^{\mathbb{Z}^n} da^{\mathbb{Z}^n} + da^{\mathbb{Z}^n} \delta a^{\mathbb{Z}^n}, (\vec{0}, \hat{\alpha}, \hat{\alpha} + \hat{\beta}, \vec{1})_{\vec{n}} \rangle \\ &= \sum_{\vec{n} \in \mathbb{Z}^3} \epsilon^{\alpha\beta\gamma} \delta a^{\mathbb{Z}^n} (\vec{0}, \hat{\alpha})_{\vec{n}} da^{\mathbb{Z}^n} (\hat{\alpha}, \hat{\alpha} + \hat{\beta}, \vec{1})_{\vec{n}} \\ &+ da^{\mathbb{Z}^n} (\vec{0}, \hat{\alpha}, \hat{\alpha} + \hat{\beta})_{\vec{n}} \delta a^{\mathbb{Z}^n} (\hat{\alpha} + \hat{\beta}, \vec{1})_{\vec{n}} \\ &= \sum_{\vec{n} \in \mathbb{Z}^3} \epsilon^{\alpha\beta\gamma} \delta a^{\mathbb{Z}^n} (\vec{0}, \hat{\alpha})_{\vec{n}} da^{\mathbb{Z}^n} (\hat{\alpha}, \hat{\alpha} + \hat{\beta}, \vec{1})_{\vec{n}} \\ &+ da^{\mathbb{Z}^n} (\vec{0}, \hat{\beta}, \hat{\beta} + \hat{\gamma})_{\vec{n} - \hat{\beta} - \hat{\gamma}} \delta a^{\mathbb{Z}^n} (\vec{0}, \hat{\alpha})_{\vec{n}} \\ &= \sum_{\vec{n} \in \mathbb{Z}^3} \frac{\epsilon^{\alpha\beta\gamma}}{2} \delta a^{\mathbb{Z}^n} (\vec{0}, \hat{\alpha})_{\vec{n}} \\ &\times [F_{\beta\gamma} \left(\frac{\hat{\beta}}{2} + \frac{\hat{\gamma}}{2} \right)_{\vec{n} + \hat{\alpha}} + F_{\beta\gamma} \left(\frac{\hat{\beta}}{2} + \frac{\hat{\gamma}}{2} \right)_{\vec{n} - \hat{\beta} - \hat{\gamma}}] \\ &= \sum_{\vec{n} \in \mathbb{Z}^3} \frac{\epsilon^{\alpha\beta\gamma}}{2} \delta a^{\mathbb{Z}^n} (\vec{0}, \hat{\alpha})_{\vec{n}} [F_{\beta\gamma}(\vec{r}_{ij} + \frac{\vec{1}}{2}) + F_{\beta\gamma}(\vec{r}_{ij} - \frac{\vec{1}}{2})], \quad (\text{F1}) \end{aligned}$$

where $(\vec{a}, \vec{b}, \dots, \vec{c})_{\vec{n}}$ is a shorthand for $(\vec{a} + \vec{n}, \vec{b} + \vec{n}, \dots, \vec{c} + \vec{n})$, and we have dropped the $\langle \rangle$ brackets for pairing cochains and chains. $\vec{r}_{ij} = \vec{n} + \frac{\hat{\alpha}}{2}$ denote the mid-point of $ij = (\vec{0}, \hat{\alpha})_{\vec{n}}$, $\frac{\vec{1}}{2} := (\frac{1}{2}, \frac{1}{2}, \frac{1}{2})$, and

$$F_{\beta\gamma}(\vec{r}) := da^{\mathbb{Z}^n} (\vec{0}, \hat{\beta}, \hat{\beta} + \hat{\gamma})_{\vec{r} - \frac{\hat{\beta}}{2} - \frac{\hat{\gamma}}{2}} - (\beta \leftrightarrow \gamma).$$

Note that the final expression F1 only depends on links which are 1-diagonal. So the 2-diagonal and 3-diagonal links simply form decoupled product states. We may henceforth neglect all these links for the current analysis.

We may now write down the expression for P_{ij}

$$P_{ij} = \frac{1}{n} \sum_{k=0}^n \widehat{X}_{ij}^k e^{2\pi i \frac{mk}{2n} \frac{\epsilon^{\alpha\beta\gamma}}{2} [F_{\beta\gamma}(\vec{r}_{ij} + \frac{\vec{1}}{2}) + F_{\beta\gamma}(\vec{r}_{ij} - \frac{\vec{1}}{2})]}, \quad (\text{F2})$$

summed only over 1-diagonal links $ij = (\vec{n}, \vec{n} + \hat{\alpha})$, \widehat{X}_{ij} increments $a_{ij}^{\mathbb{Z}^n}$ by 1. It can be checked that $[P_{ij}, P_{i'j'}] = 0$ for distinct 1-diagonal links ij and $i'j'$.

Appendix G: Evaluation of P_{ij} for general m

As in the m -even case, the matrix elements of the projections P_{ij} are given by (B7):

$$\langle \{a_T^{Z^n}\} | P_{ij} | \{a_0^{Z^n}\} \rangle = \prod_{i'j' \neq ij} \delta_{a_{0,i'j'}, a_{T,i'j'}^{Z^n}} \times \frac{1}{n} e^{2\pi i \int_{\mathbb{R}^3 \times I} \frac{m}{2n} \mathbb{S}q^2(da^{Z^n}) + d\xi_3[a^{Z^n}]},$$

where the exponent is

$$\begin{aligned} & \int_{\mathbb{R}^3 \times I} \frac{m}{2n} \mathbb{S}q^2 da^{Z^n} + d\xi_3[a^{Z^n}] \\ &= \int_{\mathbb{R}^3 \times I} d\phi_3(a^{Z^n}) = \int_{\mathbb{R}^3} \delta\phi_3[a^{Z^n}], \end{aligned}$$

where ϕ_3 is given in (28). Again $\delta a^{Z^n} d\delta a^{Z^n} = 0$ since we only change by one link.

$$\begin{aligned} \delta\phi_3[a^{Z^n}] &\stackrel{d}{=} \frac{m}{2n} (\delta a^{Z^n} da^{Z^n} + da^{Z^n} \delta a^{Z^n}) \\ &+ \frac{m}{2} \left[(da^{Z^n} + d\delta a^{Z^n}) \underset{1}{\smile} \left[\frac{da^{Z^n} + d\delta a^{Z^n}}{n} \right] \right] \\ &- \frac{m}{2} \left[da^{Z^n} \underset{1}{\smile} \left[\frac{da^{Z^n}}{n} \right] \right] \\ &\stackrel{d,1}{=} \frac{m}{2n} (\delta a^{Z^n} (da)^{Z^n} + (da)^{Z^n} \delta a^{Z^n}) \\ &+ \frac{m}{2} \left[da^{Z^n} \underset{1}{\smile} \delta \left[\frac{da^{Z^n}}{n} \right] \right] \\ &+ \frac{m}{2} \left[\delta a^{Z^n} \underset{1}{\smile} d \left[\frac{da^{Z^n} + d\delta a^{Z^n}}{n} \right] \right]. \end{aligned}$$

Where we integrated by part in the last step and used $\delta a^{Z^n} \delta \left[\frac{da^{Z^n}}{n} \right] = \delta \left[\frac{da^{Z^n}}{n} \right] \delta a^{Z^n} = 0$. Evaluating on the $d=3$ lattice triangulation described in Appendix D, we have

$$\begin{aligned} & \delta\phi_3(\vec{0}, \hat{\alpha}, \hat{\alpha} + \hat{\beta}, \vec{1}) \\ &= \frac{m}{2n} [\delta a^{Z^n}(\vec{0}, \hat{\alpha})(da)^{Z^n}(\hat{\alpha}, \hat{\alpha} + \hat{\beta}, \vec{1}) \\ &+ (da)^{Z^n}(\vec{0}, \hat{\alpha}, \hat{\alpha} + \hat{\beta})\delta a^{Z^n}(\hat{\alpha} + \hat{\beta}, \vec{1})] \\ &+ \frac{m}{2} [da^{Z^n}(\vec{0}, \hat{\alpha} + \hat{\beta}, \vec{1})\delta \left[\frac{da^{Z^n}}{n} \right](\vec{0}, \hat{\alpha}, \hat{\alpha} + \hat{\beta}) \\ &+ da^{Z^n}(\vec{0}, \hat{\alpha}, \vec{1})\delta \left[\frac{da^{Z^n}}{n} \right](\hat{\alpha}, \hat{\alpha} + \hat{\beta}, \vec{1}) \\ &+ \delta a^{Z^n}(\vec{0}, \vec{1})d \left[\frac{da^{Z^n} + d\delta a^{Z^n}}{n} \right](\vec{0}, \hat{\alpha}, \hat{\alpha} + \hat{\beta}, \vec{1})]. \end{aligned}$$

The projections can be written as

$$P_{ij} = \frac{1}{n} \sum_{k=0}^n \hat{X}_{ij}^k e^{2\pi i \int_{\mathbb{R}^3} \delta_k \phi_3[a^{Z^n}]}, \quad (\text{G1})$$

where $\delta_k a^{Z^n} = (a_{ij} + k)^{Z^n} - a_{ij}^{Z^n}$ is non-zero for only one link ij .

There are three cases to consider: ij can be 1-, 2- or 3-diagonal, as defined in subsection V A of the main text.

For the 3-diagonal links $ij = (\vec{n}, \vec{n} + \vec{1})$,

$$\begin{aligned} \int_{\mathbb{R}^3} \delta_k \phi_3[a^{Z^n}] &= \sum_{\vec{n} \in \mathbb{Z}^3} \epsilon^{\alpha\beta\gamma} \delta_k \phi_3(\vec{0}, \hat{\alpha}, \hat{\alpha} + \hat{\beta}, \vec{1})_{\vec{n}} \\ &= \sum_{\alpha, \beta, \gamma} \epsilon^{\alpha\beta\gamma} \frac{m}{2} \delta_k a^{Z^n}(\vec{0}, \vec{1})_{\vec{n}} \\ &\quad \times d \left[\frac{da^{Z^n} + d\delta_k a^{Z^n}}{n} \right](\vec{0}, \hat{\alpha}, \hat{\alpha} + \hat{\beta}, \vec{1})_{\vec{n}} \\ &\stackrel{1}{=} \frac{m}{2} \delta_k a^{Z^n}(\vec{0}, \vec{1})_{\vec{n}} \\ &\quad \times \sum_{\alpha, \beta, \gamma} \epsilon^{\alpha\beta\gamma} \left[\frac{da^{Z^n}}{n} \right](\hat{\alpha}, \hat{\alpha} + \hat{\beta}, \vec{1})_{\vec{n}} + (\vec{0}, \hat{\alpha}, \hat{\alpha} + \hat{\beta})_{\vec{n}}, \end{aligned}$$

where $(\vec{a}, \vec{b}, \vec{c})_{\vec{n}}$ is a shorthand for $(\vec{a} + \vec{n}, \vec{b} + \vec{n}, \vec{c} + \vec{n})$. We see that the 3-diagonal link ij is coupled to $\left[\frac{da^{Z^n}}{n} \right]$ on twelve triangles making up the six faces of the cube whose diagonal is ij .

For the 2-diagonal links $ij = (\vec{n}, \vec{n} + \hat{\alpha} + \hat{\beta})$,

$$\begin{aligned} \int_{\mathbb{R}^3} \delta_k \phi_3[a^{Z^n}] &= \sum_{\vec{n} \in \mathbb{Z}^3} \epsilon^{\alpha\beta\gamma} \delta_k \phi_3(\vec{0}, \hat{\alpha}, \hat{\alpha} + \hat{\beta}, \vec{1})_{\vec{n}} \\ &= \sum_{\gamma} \epsilon^{\alpha\beta\gamma} \frac{m}{2} \left\{ da^{Z^n}(\vec{0}, \hat{\alpha} + \hat{\beta}, \vec{1})_{\vec{n}} \right. \\ &\quad \times \delta_k \left[\frac{da^{Z^n}}{n} \right](\vec{0}, \hat{\alpha}, \hat{\alpha} + \hat{\beta})_{\vec{n}} - (\vec{0}, \hat{\beta}, \hat{\alpha} + \hat{\beta})_{\vec{n}} \\ &\quad \left. + da^{Z^n}(\vec{0}, \hat{\gamma}, \vec{1})_{\vec{n}-\hat{\gamma}} \right. \\ &\quad \left. \times \delta_k \left[\frac{da^{Z^n}}{n} \right](\hat{\gamma}, \hat{\gamma} + \hat{\alpha}, \vec{1})_{\vec{n}-\hat{\gamma}} - (\hat{\gamma}, \hat{\gamma} + \hat{\beta}, \vec{1})_{\vec{n}-\hat{\gamma}} \right\} \\ &= \frac{m}{2} \delta_k \left[\frac{da^{Z^n}}{n} \right](\vec{0}, \hat{\alpha}, \hat{\alpha} + \hat{\beta})_{\vec{n}} - (\vec{0}, \hat{\beta}, \hat{\alpha} + \hat{\beta})_{\vec{n}} \\ &\quad \times \sum_{\gamma} \epsilon^{\alpha\beta\gamma} da^{Z^n} [(\vec{0}, \hat{\alpha} + \hat{\beta}, \vec{1})_{\vec{n}} - (-\hat{\gamma}, \vec{0}, \hat{\alpha} + \hat{\beta})_{\vec{n}}]. \end{aligned}$$

For instance, if $\alpha, \beta = x_1, x_2$, the link ij is involved as $\delta_k \left[\frac{da^{Z^n}}{n} \right]$ in two triangles making up the square in x_1 - x_2 plane enclosing ij . Each of the triangles is coupled to da^{Z^n} on two other faces in the $(x_1 + x_2)$ - x_3 plane. All four triangles intersect at ij .

For the 1-diagonal links $ij = (\vec{n}, \vec{n} + \hat{\alpha})$,

$$\begin{aligned} \int_{\mathbb{R}^3} \delta_k \phi_3[a^{Z^n}] &= \sum_{\vec{n} \in \mathbb{Z}^3} \epsilon^{\alpha\beta\gamma} \delta_k \phi_3(\vec{0}, \hat{\alpha}, \hat{\alpha} + \hat{\beta}, \vec{1})_{\vec{n}} \\ &= \sum_{\beta, \gamma} \epsilon^{\alpha\beta\gamma} \frac{m}{2n} \left(\delta a^{Z^n}(\vec{0}, \hat{\alpha})_{\vec{n}} (da)^{Z^n}(\hat{\alpha}, \hat{\alpha} + \hat{\beta}, \vec{1})_{\vec{n}} \right. \\ &\quad \left. + (da)^{Z^n}(\vec{0}, \hat{\beta}, \hat{\beta} + \hat{\gamma})_{\vec{n}-\hat{\beta}-\hat{\gamma}} \delta a^{Z^n}(\hat{\beta} + \hat{\gamma}, \vec{1})_{\vec{n}-\hat{\beta}-\hat{\gamma}} \right) \\ &\quad + \frac{m}{2} \left(da^{Z^n}(\vec{0}, \hat{\alpha} + \hat{\beta}, \vec{1})_{\vec{n}} \delta \left[\frac{da^{Z^n}}{n} \right](\vec{0}, \hat{\alpha}, \hat{\alpha} + \hat{\beta})_{\vec{n}} \right. \\ &\quad \left. + da^{Z^n}(\vec{0}, \hat{\gamma} + \hat{\alpha}, \vec{1})_{\vec{n}-\hat{\gamma}} \delta \left[\frac{da^{Z^n}}{n} \right](\vec{0}, \hat{\gamma}, \hat{\gamma} + \hat{\alpha})_{\vec{n}-\hat{\gamma}} \right) \end{aligned}$$

$$\begin{aligned}
& + da^{\mathbb{Z}_n}(\vec{0}, \hat{\gamma}, \vec{1})_{\vec{n}-\hat{\gamma}} \delta \left[\frac{da^{\mathbb{Z}_n}}{n} \right] (\hat{\gamma}, \hat{\gamma} + \hat{\alpha}, \vec{1})_{\vec{n}-\hat{\gamma}} \\
& + da^{\mathbb{Z}_n}(\vec{0}, \hat{\beta}, \vec{1})_{\vec{n}-\hat{\beta}-\hat{\gamma}} \delta \left[\frac{da^{\mathbb{Z}_n}}{n} \right] (\hat{\beta}, \hat{\beta} + \hat{\gamma}, \vec{1})_{\vec{n}-\hat{\beta}-\hat{\gamma}} \\
& = \sum_{\beta, \gamma} \epsilon^{\alpha\beta\gamma} \left\{ \frac{m}{2n} \delta a^{\mathbb{Z}_n}(\vec{0}, \hat{\alpha})_{\vec{n}} \right. \\
& \quad \times (da)^{\mathbb{Z}_n} [(\hat{\alpha}, \hat{\alpha} + \hat{\beta}, \vec{1})_{\vec{n}} + (-\hat{\beta} - \hat{\gamma}, -\hat{\gamma}, \vec{0})_{\vec{n}}] \\
& \quad + \frac{m}{2} \left(\delta \left[\frac{da^{\mathbb{Z}_n}}{n} \right] (\vec{0}, \hat{\alpha}, \hat{\alpha} + \hat{\beta})_{\vec{n}} \right. \\
& \quad \times da^{\mathbb{Z}_n} [(\vec{0}, \hat{\alpha} + \hat{\beta}, \vec{1})_{\vec{n}} + (-\hat{\gamma}, \vec{0}, \hat{\alpha} + \hat{\beta})_{\vec{n}}] \\
& \quad + \delta \left[\frac{da^{\mathbb{Z}_n}}{n} \right] (-\hat{\gamma}, \vec{0}, \hat{\alpha})_{\vec{n}} \\
& \quad \left. \times da^{\mathbb{Z}_n} [(-\hat{\gamma}, \hat{\alpha}, \hat{\alpha} + \hat{\beta})_{\vec{n}} + (-\hat{\beta} - \hat{\gamma}, -\hat{\gamma}, \hat{\alpha})_{\vec{n}}] \right\}.
\end{aligned}$$

In the case $n = 2$, $\lfloor \frac{da^{\mathbb{Z}_2}}{2} \rfloor \stackrel{\cong}{=} \mathbb{S}q^1(a^{\mathbb{Z}_2})$.

Appendix H: Calculation details for $\theta_q, \theta_{q_1 q_2}$

It turns out we only need to keep track of the two triangles and five links in the central square, shown in Fig. 3. This is slightly non-trivial, essentially due to $\phi_2[a, h] = 0$ when $dh = 0$. In this section we assume $a_i = a_i^{\mathbb{Z}_n}$ and $q = q^{\mathbb{Z}_n}$. Applying (44), we have

$$\begin{aligned}
W_i^q | \{a^{\mathbb{Z}_n}\} \rangle &= e^{2\pi i [\phi_2(\{a_1, a_4, a_0\}, h(W_i^q)) - \phi_2(\{a_2, a_3, a_0\}, h(W_i^q))]} \\
&\times | \{[a + dh(W_i^q)]^{\mathbb{Z}_n}\} \rangle,
\end{aligned}$$

with $h(W_i^q)$ depicted in the bottom of Fig. 3.

Evaluating ϕ_2 using (47), we have

$$\begin{aligned}
\phi_2(\{a_1, a_4, a_0\}, h(W_1^q)) &\stackrel{\cong}{=} \frac{m}{2} (a_4 - a_0) \lfloor \frac{a_4 + q}{n} \rfloor \\
\phi_2(\{a_2, a_3, a_0\}, h(W_1^q)) &\stackrel{\cong}{=} \frac{m}{2n} q a_3 + \frac{m}{2} (a_2 + a_3 - a_0) \lfloor \frac{a_2 + q}{n} \rfloor \\
\phi_2(\{a_1, a_4, a_0\}, h(W_2^q)) &\stackrel{\cong}{=} \frac{m}{2n} (-q)^{\mathbb{Z}_n} a_4 + \frac{m}{2} (a_1 + a_4 - a_0) \lfloor \frac{a_1 + (-q)^{\mathbb{Z}_n}}{n} \rfloor \\
\phi_2(\{a_2, a_3, a_0\}, h(W_2^q)) &\stackrel{\cong}{=} \frac{m}{2} (a_3 - a_0) \lfloor \frac{a_3 + (-q)^{\mathbb{Z}_n}}{n} \rfloor \\
\phi_2(\{a_1, a_4, a_0\}, h(W_3^q)) &= 0 \\
\phi_2(\{a_2, a_3, a_0\}, h(W_3^q)) &\stackrel{\cong}{=} \frac{m}{2n} q a_3 \\
&+ \frac{m}{2} \left(a_0 \left(\frac{q + (-q)^{\mathbb{Z}_n}}{n} \right) + (a_2 + q) \lfloor \frac{a_3 + (-q)^{\mathbb{Z}_n}}{n} \rfloor \right. \\
&+ (a_2 + a_3 - a_0) \left(\lfloor \frac{a_2 + q}{n} \rfloor + \lfloor \frac{a_3 + (-q)^{\mathbb{Z}_n}}{n} \rfloor \right) \Big) \\
\phi_2(\{a_1, a_4, a_0\}, h(W_4^q)) &\stackrel{\cong}{=} \frac{m}{2n} (-q)^{\mathbb{Z}_n} a_4 \\
&+ \frac{m}{2} \left(a_0 \left(\frac{q + (-q)^{\mathbb{Z}_n}}{n} \right) + (a_1 + (-q)^{\mathbb{Z}_n}) \lfloor \frac{a_4 + q}{n} \rfloor \right.
\end{aligned}$$

$$\begin{aligned}
& + (a_1 + a_4 - a_0) \left(\lfloor \frac{a_1 + (-q)^{\mathbb{Z}_n}}{n} \rfloor + \lfloor \frac{a_4 + q}{n} \rfloor \right) + q \lfloor \frac{-q}{n} \rfloor \Big) \\
\phi_2(\{a_2, a_3, a_0\}, h(W_4^q)) &= 0.
\end{aligned}$$

So for self-statistics (48), after some algebra, we are left with

$$\begin{aligned}
\theta_q &\stackrel{\cong}{=} \phi_2(\{a_1, a_4, a_0\}, h(W_2^q)) - \phi_2(\{a_2, a_3, a_0\}, h(W_2^q)) \\
&+ \phi_2(\{(a_1 - q)^{\mathbb{Z}_n}, a_4, (a_0 - q)^{\mathbb{Z}_n}\}, h(W_1^q)) \\
&- \phi_2(\{a_2, (a_3 - q)^{\mathbb{Z}_n}, (a_0 - q)^{\mathbb{Z}_n}\}, h(W_1^q)) \\
&- \phi_2(\{a_1, a_4, a_0\}, h(W_3^q)) + \phi_2(\{a_2, a_3, a_0\}, h(W_3^q)) \\
&- \phi_2(\{a_1, a_4, a_0\}, h(W_4^q)) \\
&+ \phi_2(\{(a_2 + q)^{\mathbb{Z}_n}, (a_3 - q)^{\mathbb{Z}_n}, a_0\}, h(W_4^q)) \\
&\stackrel{\cong}{=} q^2 \frac{m}{2n}.
\end{aligned}$$

Whereas for mutual-statistics (50), we have

$$\begin{aligned}
\theta_{q_1 q_2} &\stackrel{\cong}{=} \phi_2(\{a_1, a_4, a_0\}, h(W_2^{q_2})) - \phi_2(\{a_2, a_3, a_0\}, h(W_2^{q_2})) \\
&+ \phi_2(\{(a_1 - q_2)^{\mathbb{Z}_n}, a_4, (a_0 - q_2)^{\mathbb{Z}_n}\}, h(W_1^{q_1})) \\
&- \phi_2(\{a_2, (a_3 - q_2)^{\mathbb{Z}_n}, (a_0 - q_2)^{\mathbb{Z}_n}\}, h(W_1^{q_1})) \\
&- \phi_2(\{a_1, a_4, a_0\}, h(W_1^{q_1})) + \phi_2(\{a_2, a_3, a_0\}, h(W_1^{q_1})) \\
&- \phi_2(\{a_1, (a_4 + q_1)^{\mathbb{Z}_n}, (a_0 + q_1)^{\mathbb{Z}_n}\}, h(W_2^{q_2})) \\
&+ \phi_2(\{(a_2 + q_1)^{\mathbb{Z}_n}, a_3, a_0\}, h(W_2^{q_2})) \\
&\stackrel{\cong}{=} q_1 q_2 \frac{m}{n}.
\end{aligned}$$

Appendix I: Evaluation of $W_{\odot i}$ for $(n, m) = (2, 1)$

In this section we derive (58). We also assume $a = a^{\mathbb{Z}_n}$ for all initial link values in this section. Restricting to $(n, m) = (2, 1)$ and enforcing “no flux” rule $da \stackrel{\cong}{=} 0$, (47) is

$$\begin{aligned}
\phi_2[a, h^{\mathbb{Z}_2}] &\stackrel{\cong}{=} \frac{1}{4} \alpha^{\mathbb{Z}_2} a + \frac{1}{2} \left(a \underset{1}{\smile} \frac{da^{\mathbb{Z}_2}}{2} \right. \\
&+ (a + \alpha^{\mathbb{Z}_2}) \lfloor \frac{a + \alpha^{\mathbb{Z}_2}}{2} \rfloor + h^{\mathbb{Z}_2} d \lfloor \frac{dh^{\mathbb{Z}_2}}{2} \rfloor \Big). \quad (I1)
\end{aligned}$$

Applying (44), we have

$$\begin{aligned}
W_{\odot i} | \{a_{ij}, a_{jj'}\} \rangle &\Big|_{da^{\mathbb{Z}_2} \stackrel{\cong}{=} 0} \\
&= e^{2\pi i \Phi[a]} | \{(a_{ij} + 1)^{\mathbb{Z}_2}, a_{jj'}\} \rangle,
\end{aligned}$$

where

$$\begin{aligned}
\Phi[a] &= \langle \phi_2, (1, 2, i) \rangle - \langle \phi_2, (2, i, 3) \rangle + \langle \phi_2, (i, 3, 4) \rangle \\
&- \langle \phi_2, (i, 5, 4) \rangle + \langle \phi_2, (6, i, 5) \rangle - \langle \phi_2, (1, 6, i) \rangle.
\end{aligned}$$

Applying (I1) for each 2-simplex in Fig. 5, we get

$$\begin{aligned}
\langle \phi_2, (1, 2, i) \rangle &= \frac{1}{2} (a_{12} \lfloor \frac{a_{2i} + 1}{2} \rfloor) \\
\langle \phi_2, (2, i, 3) \rangle &= \frac{1}{4} a_{i3} + \frac{1}{2} (a_{23} + (a_{2i} + 1) \lfloor \frac{a_{i3} + 1}{2} \rfloor)
\end{aligned}$$

$$\begin{aligned}
\langle \phi_2, (i, 3, 4) \rangle &= \frac{1}{4} a_{34} \\
\langle \phi_2, (i, 5, 4) \rangle &= \frac{1}{4} a_{54} \\
\langle \phi_2, (6, i, 5) \rangle &= \frac{1}{4} a_{i5} + \frac{1}{2} (a_{65} + (a_{6i} + 1) \lfloor \frac{a_{i5} + 1}{2} \rfloor) \\
\langle \phi_2, (1, 6, i) \rangle &= \frac{1}{2} (a_{16} \lfloor \frac{a_{6i} + 1}{2} \rfloor).
\end{aligned}$$

Note for $a = a^{\mathbb{Z}_2}$ and $a' = a'^{\mathbb{Z}_2}$, we have $\lfloor \frac{a+a'}{2} \rfloor = aa'$. Also for any simplex (i, j, k) , the “no flux” constraint means

$$\begin{aligned}
a_{jk} &= (a_{ij} + a_{ik})^{\mathbb{Z}_2} = a_{ij} + a_{ik} - 2 \lfloor \frac{a_{ij} + a_{ik}}{2} \rfloor \\
&= a_{ij} + a_{ik} - 2a_{ij}a_{ik}.
\end{aligned}$$

After a bit of algebra, simplifying using the above identities, we finally arrive at

$$\Phi[a] \stackrel{\dagger}{=} \frac{1}{2} \sum_{\langle jj' \rangle} a_{ij} a_{ij'}.$$

1. DS projection Hamiltonian

For completeness, we supplement this section by briefly explaining the projection Hamiltonian for DS topological order from the action (up to a volume term)

$$Z_{DS} = \sum_{da \stackrel{\dagger}{=} 0} e^{2\pi i \int_{M^3} \frac{1}{2} a a a}.$$

The construction was well-studied in the literature, see *eg.* Ref. 51. It is similar to that described in Appendix B, except that six links connecting to the same site is updated. We have

$$\hat{H} = - \sum_i P_i \prod_{\Delta_i} \delta_{\langle da, \Delta \rangle, 0} - \sum_{\Delta} \delta_{\langle da, \Delta \rangle, 0},$$

where Δ is summed over all 2-simplices, Δ_i are product over all 2-simplices having i as a vertex.

$$P_i \{a_{ij}, a_{jj'}\} = e^{2\pi i \Phi_{DS}[a]} \{(a_{ij} + 1)^{\mathbb{Z}_2}, a_{jj'}\},$$

and $\Phi_{DS}[a]$ is evaluating the cocycles on the six tetrahedrons involved when a site is updated. Using Fig. 5 and updating i to i' with i' out of paper, where $a_{ij} = (a_{ij} + 1)^{\mathbb{Z}_2}$ and $a_{ii'} = 1$, the result is

$$\begin{aligned}
\Phi_{DS}[a] &\stackrel{\dagger}{=} \frac{1}{2} [a_{12}a_{2i} + a_{2i}(a_{i3} + 1) + (a_{i3} + 1)a_{34} \\
&\quad + (a_{i5} + 1)a_{54} + a_{6i}(a_{i5} + 1) + a_{16}a_{6i}] \\
&\stackrel{\dagger}{=} \frac{1}{2} \sum_{\langle jj' \rangle} a_{ij} a_{ij'}.
\end{aligned}$$

We see it describes the same phase as H_{∂} in (53).

Appendix J: ω_4 , ϕ_3 and ϕ_2

In the main text, we find that for \mathbb{Z}_n -1-SPT, the 4-cocycle ω_4 , the ground state wavefunction amplitude ϕ_3 , and the boundary transform anomalous phase ϕ_2 are related via (26) and (40):

$$\begin{aligned}
\omega_4[da^{\mathbb{Z}_n}] &= d\phi_3[a] \\
-\delta_{\alpha} \phi_3[a^{\mathbb{Z}_n}] &= d\phi_2[a, h].
\end{aligned}$$

In general, given ω_4 satisfying $d\omega_4 = 0$. We can define the 3-cochain ϕ_3^{\dagger} as follows:

$$\langle \phi_3^{\dagger}, (1234) \rangle := \langle \omega_4, (01234) \rangle,$$

where we have introduced an extra “reference” vertex $\overset{*}{0}$. A heuristic way to interpret $\overset{*}{0}$ is that it is located at $t = -\infty$ whereas the other vertices $i = 1, 2, 3, 4$ are located at a spatial slice at $t = 0$. So $a_{ii'}$ are “spatial” links and $a_{\overset{*}{0}i}$ are “temporal” links. We may choose the links $a_{\overset{*}{0}i} = 0$, $i = 1, 2, 3, 4$ as a convention. The dependence of ϕ_3^{\dagger} on $\overset{*}{0}$ is the choice of such convention. For arbitrary 4-chain (01234) , we have

$$\begin{aligned}
\langle d\phi_3^{\dagger}, (01234) \rangle &= \sum_{m=0}^4 (-)^m \langle \phi_3^{\dagger}, (0 \dots \hat{m} \dots 4) \rangle \\
&= \sum_{m=0}^4 (-)^m \langle \omega_4, (\overset{*}{00} \dots \hat{m} \dots 4) \rangle \\
&= \langle \omega_4, (01234) \rangle - \langle d\omega_4, (\overset{*}{00}1234) \rangle \\
&= \langle \omega_4, (01234) \rangle,
\end{aligned}$$

so $\omega_4 = d\phi_3^{\dagger}$.

To generalize (40), note that if we have a 1-symmetry $\alpha = dh$ only on the spatial links, then we can use the invariance of ω_4 under space-time 1-symmetry to undo h from the spatial links and act $(-h)$ on the temporal links instead, *i.e.*

$$\begin{aligned}
\langle \phi_3^{\dagger}[a + \alpha], (1234) \rangle &= \langle \phi_3^{\dagger}[a + dh], (1234) \rangle \\
&= \langle \omega_4[a + (dh)_{\text{spatial}}], (\overset{*}{0}1234) \rangle \\
&= \langle \omega_4[a], (\overset{*}{1}1234) \rangle \\
&= \langle \phi_3^{\dagger}[a], (1234) \rangle.
\end{aligned}$$

So $\delta_{\alpha} \phi_3^{\dagger} = \phi_3^{\dagger} - \phi_3^{\dagger}$. Here $(dh)_{\text{spatial}}$ means it only exists on spatial links $a_{ii'}$, and we have introduced a new vertex $\overset{*}{1}$ where

$$a_{\overset{*}{1}i} := a_{\overset{*}{0}i} - h_i = -h_i.$$

If we define

$$\langle \phi_2^{01}, (234) \rangle := \langle \omega_4, (\hat{0}1234) \rangle,$$

it can then be checked that for arbitrary 3-chain (1234), we have

$$\begin{aligned} & \langle d\phi_2^{01}, (1234) \rangle \\ &= \sum_{m=1}^4 -(-)^m \langle \phi_2^{01}, (1 \dots \hat{m} \dots 4) \rangle \\ &= \sum_{m=1}^4 -(-)^m \langle \omega_4, (\hat{0}11 \dots \hat{m} \dots 4) \rangle \\ &= \sum_{\hat{m}=0}^1 -(-)^{\hat{m}} \langle \omega_4, (\hat{0} \dots \hat{m} \dots \hat{1}1234) \rangle + \langle d\omega_4, (\hat{0}\hat{1}1234) \rangle \\ &= -\langle \omega_4, (\hat{1}1234) \rangle + \langle \omega_4, (\hat{0}1234) \rangle \\ &= -\langle \phi_3^1, (1234) \rangle + \langle \phi_3^0, (1234) \rangle. \end{aligned}$$

So $\delta_\alpha \phi_3^0 = -d\phi_2^{01}$.

In general we may define

$$\langle \phi_k^{\hat{0} \dots (4-\hat{k}-1)}, (01234) \rangle := \langle \omega, (\hat{0} \dots (4-\hat{k}-1)(4-k) \dots 4) \rangle$$

for $k = 3, 2, 1, 0, -1$. They represent the anomaly in the boundary transformation in k -dimensional sub-manifolds in the boundary. $k = -1$ means dimension 0 in the bulk. They satisfy

$$d\phi_k = (-)^k d\phi_{k-1},$$

where

$$(\hat{0} d\phi_k)^{\hat{0} \dots (4-\hat{k})} := \sum_{\hat{m}=0}^{4-k} (-)^{\hat{m}} \phi_k^{\hat{0} \dots \hat{m} \dots (4-\hat{k})}.$$

Appendix K: Generalization of (49) and (51) to G -protected 1-SPT for finite unitary groups

In general, we can carry through the calculations for self-statistics and mutual-statistics for transformation strings, for a G -protected 1-SPT in 3+1D as well, where G is any unitary group. Note G is Abelian since it is a 1-symmetry. In this section we will only present the final results.

Following similar strategies for deriving self- and mutual-statistics in the \mathbb{Z}_n case, it can be shown that for general unitary group G , the self- and mutual- statistics of transformation strings are given by

$$\begin{aligned} \theta_q &= -\omega_4(-q, -q, 0, -q, 0, q) + \omega_4(-q, -q, -q, -q, 0, 0) \\ &\quad - \omega_4(0, -q, 0, -q, -q, 0) + \omega_4(0, 0, 0, 0, -q, 0) \end{aligned}$$

$$+ \omega_4(0, 0, q, 0, 0, 0) - \omega_4(0, 0, -q, 0, -q, -q) \quad (\text{K1})$$

$$\begin{aligned} \theta_{q_1 q_2} &= \left\{ \left[\omega_4(-q_1, 0, -q_1, q_1, 0, -q_1 - q_2) \right. \right. \\ &\quad + \omega_4(0, 0, -q_1, -q_2, -q_1 - q_2, -q_1) \\ &\quad - \omega_4(q_1, 0, 0, -q_1, -q_1 - q_2, -q_2) \\ &\quad \left. \left. - (q_1 \rightarrow 0) \right] - (q_2 \rightarrow 0) \right\} + (q_1 \leftrightarrow q_2), \quad (\text{K2}) \end{aligned}$$

where $q, q_1, q_2 \in G$ labels the group element associated with the transformation string, $\omega_4[\mathcal{B}] = \omega_4(\mathcal{B}_{012}, \mathcal{B}_{013}, \mathcal{B}_{014}, \mathcal{B}_{023}, \mathcal{B}_{024}, \mathcal{B}_{034})$ where $d\mathcal{B} = 0$. It can be checked (K1) and (K2) are topological invariants, namely, they are unchanged under $\omega_4 \rightarrow \omega_4 + d\beta_3$ for any 1-symmetric 3-cochain β_3 .

We will check that (K1) and (K2) recovers (49) and (51) in the case $G = \mathbb{Z}_n$. The \mathbb{Z}_n 4-cocycle (11) is

$$\begin{aligned} \omega_4[\mathcal{B}] &= \frac{m}{2n} \mathbb{S}q^2 \mathcal{B}^{\mathbb{Z}_n} \\ &= \frac{m}{2n} (\mathcal{B}_{012}^{\mathbb{Z}_n} \mathcal{B}_{234}^{\mathbb{Z}_n} + \mathcal{B}_{034}^{\mathbb{Z}_n} (d\mathcal{B}^{\mathbb{Z}_n})_{0123} + \mathcal{B}_{014}^{\mathbb{Z}_n} (d\mathcal{B}^{\mathbb{Z}_n})_{1234}), \quad (\text{K3}) \end{aligned}$$

where

$$\begin{aligned} (d\mathcal{B}^{\mathbb{Z}_n})_{0123} &= \mathcal{B}_{123}^{\mathbb{Z}_n} - \mathcal{B}_{023}^{\mathbb{Z}_n} + \mathcal{B}_{013}^{\mathbb{Z}_n} - \mathcal{B}_{012}^{\mathbb{Z}_n} \\ (d\mathcal{B}^{\mathbb{Z}_n})_{1234} &= \mathcal{B}_{234}^{\mathbb{Z}_n} - \mathcal{B}_{134}^{\mathbb{Z}_n} + \mathcal{B}_{124}^{\mathbb{Z}_n} - \mathcal{B}_{123}^{\mathbb{Z}_n} \\ \mathcal{B}_{ijk}^{\mathbb{Z}_n} &= (\mathcal{B}_{0jk}^{\mathbb{Z}_n} - \mathcal{B}_{0ik}^{\mathbb{Z}_n} + \mathcal{B}_{0ij}^{\mathbb{Z}_n})^{\mathbb{Z}_n} \text{ for } i \neq 0, \end{aligned}$$

so (K1) and (K2) are

$$\begin{aligned} \theta_q &= -\omega_4(-q, -q, 0, -q, 0, q) + \omega_4(-q, -q, -q, -q, 0, 0) \\ &\quad - \omega_4(0, -q, 0, -q, -q, 0) + \omega_4(0, 0, 0, 0, -q, 0) \\ &\quad + \omega_4(0, 0, q, 0, 0, 0) - \omega_4(0, 0, -q, 0, -q, -q) \\ &\stackrel{\dagger}{=} -0 + \left(\frac{m}{2n} q^2\right) - 0 + 0 + 0 - 0 = \frac{m}{2n} q^2. \end{aligned}$$

$$\begin{aligned} \theta_{q_1 q_2} &= \left\{ \left[\omega_4(-q_1, 0, -q_1, q_1, 0, -q_1 - q_2) \right. \right. \\ &\quad + \omega_4(0, 0, -q_1, -q_2, -q_1 - q_2, -q_1) \\ &\quad - \omega_4(q_1, 0, 0, -q_1, -q_1 - q_2, -q_2) \\ &\quad \left. \left. - (q_1 \rightarrow 0) \right] - (q_2 \rightarrow 0) \right\} + (q_1 \leftrightarrow q_2) \\ &= \left\{ \left[\left(\frac{m}{2n} (-q_1)^{\mathbb{Z}_n} (-q_2)^{\mathbb{Z}_n} \right. \right. \right. \\ &\quad + \frac{m}{2} (-q_1 - q_2)^{\mathbb{Z}_n} \frac{-q_1^{\mathbb{Z}_n} - (-q_1)^{\mathbb{Z}_n}}{n} \\ &\quad - \frac{m}{2} (-q_2)^{\mathbb{Z}_n} \frac{-(-q_1)^{\mathbb{Z}_n} - q_1^{\mathbb{Z}_n}}{n} \\ &\quad \left. \left. \left. - (q_1 \rightarrow 0) \right] - (q_2 \rightarrow 0) \right\} + (q_1 \leftrightarrow q_2) \end{aligned}$$

$$\begin{aligned} &\stackrel{\dagger}{=} \left\{ \left[\left(\frac{m}{2n} q_1 q_2 + \frac{m}{2} [q_1 \lfloor \frac{-q_2}{n} \rfloor + q_2 \lfloor \frac{-q_1}{n} \rfloor] \right. \right. \right. \\ &\quad \left. \left. + (q_1 + q_2) (\lfloor \frac{q_1}{n} \rfloor + \lfloor \frac{-q_1}{n} \rfloor) \right] \right\} \end{aligned}$$

$$\begin{aligned}
& -\frac{m}{2}q_2([\frac{q_1}{n}] + [\frac{-q_1}{n}]) \\
& - (q_1 \rightarrow 0)] - (q_2 \rightarrow 0)] \} + (q_1 \leftrightarrow q_2) \\
\stackrel{\pm}{=} & \left\{ \left[\left(\frac{m}{2n}q_1q_2 + \frac{m}{2}[q_1[\frac{-q_2}{n}] + q_2[\frac{-q_1}{n}]] \right. \right. \right. \\
& \left. \left. \left. + q_1([\frac{q_1}{n}] + [\frac{-q_1}{n}]) \right) \right] - (q_2 \rightarrow 0) \right\} + (q_1 \leftrightarrow q_2) \\
\stackrel{\pm}{=} & \left(\frac{m}{2n}q_1q_2 + \frac{m}{2}[q_1[\frac{-q_2}{n}] + q_2[\frac{-q_1}{n}]] \right) + (q_1 \leftrightarrow q_2) \\
\stackrel{\pm}{=} & \frac{m}{n}q_1q_2.
\end{aligned}$$

Thus (49) and (51) are recovered.

-
- ¹ X. G. Wen, *Phys. Rev. B* **40**, 7387 (1989).
² X. G. Wen, *Int. J. Mod. Phys. B* **04**, 239 (1990).
³ Z.-C. Gu and X.-G. Wen, *Phys. Rev. B* **80**, 155131 (2009), [arXiv:0903.1069](#).
⁴ X. Chen, Z.-X. Liu, and X.-G. Wen, *Phys. Rev. B* **84**, 235141 (2011), [arXiv:1106.4752](#).
⁵ X. Chen, Z.-C. Gu, Z.-X. Liu, and X.-G. Wen, *Phys. Rev. B* **87**, 155114 (2013), [arXiv:1106.4772](#).
⁶ X. Chen, Z.-C. Gu, and X.-G. Wen, *Phys. Rev. B* **82**, 155138 (2010), [arXiv:1004.3835](#).
⁷ L. Kong and X.-G. Wen, (2014), [arXiv:1405.5858](#).
⁸ T. Lan, L. Kong, and X.-G. Wen, *Phys. Rev. X* **8**, 021074 (2018), [arXiv:1704.04221](#).
⁹ T. Lan and X.-G. Wen, *Phys. Rev. X* **9**, 021005 (2019), [arXiv:1801.08530](#).
¹⁰ X.-G. Wen, *Phys. Rev. B* **99** (2019), 10.1103/physrevb.99.205139, [arXiv:1812.02517](#).
¹¹ A. Kitaev, *Ann. Phys.* **303**, 2 (2003).
¹² X.-G. Wen, *Phys. Rev. Lett.* **90**, 016803 (2003), [quant-ph/0205004](#).
¹³ M. Levin and X.-G. Wen, *Phys. Rev. B* **67**, 245316 (2003), [cond-mat/0302460](#).
¹⁴ M. B. Hastings and X.-G. Wen, *Phys. Rev. B* **72**, 045141 (2005), [cond-mat/0503554](#).
¹⁵ Z. Nussinov and G. Ortiz, *Proceedings of the National Academy of Sciences* **106**, 16944 (2009), [arXiv:cond-mat/0605316](#).
¹⁶ Z. Nussinov and G. Ortiz, *Ann. Phys.* **324**, 977 (2009), [arXiv:cond-mat/0702377](#).
¹⁷ B. Yoshida, *Ann. Phys.* **326**, 15 (2011), [arXiv:1007.4601](#).
¹⁸ H. Bombín, *Commun. Math. Phys.* **327**, 387 (2014), [arXiv:1107.2707](#).
¹⁹ A. Kapustin and R. Thorngren, (2013), [arXiv:1309.4721](#).
²⁰ D. Gaiotto, A. Kapustin, N. Seiberg, and B. Willett, *J. High Energ. Phys.* **2015**, 172 (2015), [arXiv:1412.5148](#).
²¹ R. Thorngren and C. von Keyserlingk, (2015), [arXiv:1511.02929](#).
²² A. Bullivant, M. Calcada, Z. Kádár, P. Martin, and J. F. Martins, *Phys. Rev. B* **95** (2017), 10.1103/physrevb.95.155118, [arXiv:1702.00868](#).
²³ R. Kobayashi, K. Shiozaki, Y. Kikuchi, and S. Ryu, *Phys. Rev. B* **99** (2019), 10.1103/physrevb.99.014402, [arXiv:1805.05367](#).
²⁴ B. Yoshida, *Physical Review B* **93**, 155131 (2016).
²⁵ C. Zhu, T. Lan, and X.-G. Wen, *Phys. Rev. B* **100**, 045105 (2019), [arXiv:1808.09394](#).
²⁶ Z. Wan and J. Wang, (2018), [arXiv:1812.11967](#).
²⁷ X.-G. Wen, *Phys. Rev. D* **88**, 045013 (2013), [arXiv:1303.1803](#).
²⁸ X.-G. Wen and Z. Wang, (2018), [arXiv:1801.09938](#).
²⁹ R. Dijkgraaf and E. Witten, *Commun. Math. Phys.* **129**, 393 (1990).
³⁰ X.-G. Wen, *Phys. Rev. B* **89**, 035147 (2014), [arXiv:1301.7675](#).
³¹ L.-Y. Hung and X.-G. Wen, *Phys. Rev. B* **89**, 075121 (2014), [arXiv:1311.5539](#).
³² A. Kapustin, (2014), [arXiv:1404.6659](#).
³³ M. Levin and Z.-C. Gu, *Physical Review B* **86**, 115109 (2012).
³⁴ M. Barkeshli, P. Bonderson, M. Cheng, and Z. Wang, *Physical Review B* **100** (2019), 10.1103/physrevb.100.115147.
³⁵ X. Chen, *Reviews in Physics* **2**, 318 (2017).
³⁶ X. Chen, Z.-C. Gu, and X.-G. Wen, *Physical Review B* **83** (2011), 10.1103/physrevb.83.035107.
³⁷ I. Affleck, T. Kennedy, E. H. Lieb, and H. Tasaki, *Phys. Rev. Lett.* **59**, 799 (1987).
³⁸ X.-G. Wen, *Phys. Rev. B* **95**, 205142 (2017), [arXiv:1612.01418](#).
³⁹ T. Lan, C. Zhu, and X.-G. Wen, (2018), [arXiv:1809.01112](#).
⁴⁰ A. Hatcher, *Algebraic Topology* (Cambridge University Press, 2002).
⁴¹ J. Wang, X.-G. Wen, and E. Witten, *Physical Review X* **8**, 031048 (2018), [arXiv:1705.06728](#).
⁴² Z. Wan and J. Wang, *Phys. Rev. D* **99** (2019), 10.1103/physrevd.99.065013, [arXiv:1812.11955](#).
⁴³ Z. Wan and J. Wang, (2018), [arXiv:1812.11968](#).
⁴⁴ Z. Wan, J. Wang, and Y. Zheng, [arXiv:1904.00994](#) (2019).
⁴⁵ A. Kapustin, [arXiv:1403.1467](#) [cond-mat, physics:hep-th] (2014), [arXiv:1403.1467](#).
⁴⁶ A. Kapustin, R. Thorngren, A. Turzillo, and Z. Wang, *Journal of High Energy Physics* **2015**, 1 (2015). <https://www.math.ias.edu/files/wam/LicataLecture3.pdf>.
⁴⁷ F. Costantino, *Math. Z.* **251**, 427 (2005), [math/0403014](#).
⁴⁸ X. Chen, Z.-C. Gu, Z.-X. Liu, and X.-G. Wen, *Science* **338**, 1604 (2012), [arXiv:1301.0861](#).
⁴⁹ N. E. Steenrod, *The Annals of Mathematics* **48**, 290 (1947).
⁵⁰ A. Meszaros and Y. Ran, *Physical Review B* **87**, 155115 (2013).
⁵¹ The intuition is that the obstruction for such extension is due a “symmetry twist” in the time direction. For example, when the line dual to \hat{B} sweeps through a non-contractible surface in 3d, which is equivalent to insertion of a 1-symmetry operator acting on the non-contractible surface.
⁵² V. A. Rohlin, in *Doklady Akad. Nauk. SSSR*, Vol. 81 (1951) p. 355.